Control of cAMP signalling in the cellular migration of pancreatic ductal adenocarcinoma

Thesis submitted in accordance with the requirements of The University of Liverpool for the degree of Doctor in Philosophy

by

Alex T Burdyga

February, 2013

ABSTRACT

Pancreatic ductal adenocarcinoma (PDAC) is characterised by a very high mortality rate and is the 4th most common cause of cancer death (Siegel *et al.*, 2012). The disease initially develops asymptomatically, and at the time of diagnosis patients usually have multiple metastases (Rhim *et al.*, 2012). It would therefore be highly desirable to develop treatments which specifically impede the ability of PDAC cells to metastasise by interfering with the cellular processes responsible for efficient cellular migration. Intracellular signalling cascades, which utilise various signalling proteins, ultimately lead to the appropriate cell coordination and enable efficient cellular motility. One such signalling pathway that participates in the regulation of migration is controlled by the second messenger cyclic adenosine monophosphate (cAMP) (Howe, 2004). Several effectors of cAMP have been found which include protein kinase A (PKA) (Tasken & Aandahl, 2004), exchange factors activated by cAMP (EPAC) (Bos, 2006), and cyclic nucleotide-regulated cation channels (Biel, 2009). PKA has been intimately linked with several cellular processes which contribute towards cell motility. In most cases, the various specific effects of PKA signalling require selective targeting of the kinase into microdomains through interaction with A-kinase-anchoring proteins (AKAPs) (Pidoux & Tasken, 2010). Other cAMP effectors such as EPAC have defined roles in controlling various aspects of migration, such as cellular adhesion to the extracellular matrix (Bos, 2005). The effect of modulating cAMP signalling on the rate of migration has been investigated in several cancer types. Interestingly the results obtained were rather varied; both inhibition and stimulation of migration was observed (Chen *et al.*, 2008; Baljinnyam *et al.*, 2009; Grandoch *et al.*, 2009; Shaikh *et al.*, 2012). However, the effect of cAMP, and its effectors, on the rate of migration has not been investigated in PDAC; this was the main aim of this study. Classical cAMP elevating agents such as forskolin and 3-Isobutyl-1-methylxanthine (IBMX), as well as the cAMP analogue 8-Bromoadenosine 3’5’-cyclic monophosphate (8Br-cAMP), were found to inhibit migration of the PANC-1 cells. The role of cAMP signalling was further supported by the results of experiments utilising cAMP FRET sensors, which were imaged in live single cells. Further characterisation of cAMP effects in 4 other diverse PDAC cell lines yielded similar results, indicating that the mechanism of inhibition was common to all PDAC cell types tested. PANC-1 cell invasion was also inhibited by cAMP elevation. I went on to investigate events such as cell ruffling and focal adhesion assembly, which are processes closely associated with cellular motility. Dual transfection with a cAMP sensor and GFP tagged paxillin revealed a relationship between cAMP elevation and the loss of paxillin from focal adhesions, which was quickly reversible upon cAMP returning back to basal levels. Using a similar approach, peripheral cell ruffling was found to be inhibited by intracellular cAMP elevation. These results indicated that the inhibition of migration upon cAMP elevation was likely to occur as a result of immediate signalling events (and not due to cAMP-dependent changes in gene expression). The final part of the project concentrated on the individual contribution of the downstream effectors of cAMP, with particular emphasis on selective PKA and EPAC modulation. Utilising both PKA and EPAC sensors, I determined the appropriate concentrations of N6-benzoyl-cAMP (6Bnz) and 8-pCPT-2’OMe-cAMP (8pCPT) required to achieve selective PKA and EPAC activation respectively. Interestingly, I found that the two effectors had opposing actions; EPAC activation was found to induce migration, while PKA was found to suppress migration. Further investigation utilised a potent and selective PKA inhibitor peptide (PKI), which upon expression was found to prevent inhibition of ruffling, paxillin loss from focal adhesions, and inhibition of migration in response to cAMP elevation. Furthermore, it was found that suppression of basal PKA activity had a tendency to induce migration. I also utilised a cell permeable peptide (st-Ht31) which inhibits PKA interaction with AKAPs, thus effectively reducing its function by uncoupling the kinase from its specific signalling microdomains. The resulting effect was found to be a large potentiation of PANC-1 migration, which further highlighted the importance of PKA activity in the control of migration.

ACKNOWLEDGEMENTS

I would like to greatly thank Alexei Tepikin for the continuous support throughout this PhD project and during my time at the University. I greatly appreciated the flexibility and experimental freedom that he provided in his laboratory. This has accelerated my development as a scientist, whilst at the same time has made the whole experience very enjoyable and unforgettable.

Further I would like to thank Eithne Costello, Robert Sutton and David Criddle for their advice that has contributed and helped shape this project.

I would also like to thank Svetlana Voronina, Lee Haynes, Misha Chvanov and Gyorgy Lur for passing on their various expertises in microscopy and molecular cloning techniques.

I am very grateful to the external collaborators (Jalink Kees, Jin Zhang, Manuela Zaccolo and Mark Ginsberg) for their generous supply of DNA constructs encoding the cAMP sensors used in this project, as well as genetic inhibitors of PKA.

Great thanks to Hayley Dingsdale for helping with proof reading my thesis.

I would also like to thank Mark Houghton for the large amount of daily help with administration in the laboratory.

Finally, a great thank you to all of the members of Blue Block, who have all been very friendly and helpful of the years. I would also like to thank Red Block were my first rotation project during the MRes year began, which was supervised by Alan Morgan. Also a great thank you to Michele Riesen with whom I spent most of the time in the lab during that rotation, as well as her continuous support throughout the length of my PhD.

This project was funded by the MRC.

ABBREVIATIONS

6Bnz	N6-benzoyl-cAMP
8Br-cAMP	8-Bromoadenosine 3’5’-cyclic monophosphate
8Cl-cAMP	8-Chloroadenosine 3’5’-cyclic monophosphate
8pCPT	8-pCPT-2’OMe-cAMP
AC	adenylyl cyclase
ADP	adenosine diphosphate
AKAP	A-kinase-anchoring proteins
AKAR4	PKA FRET sensor; with backbone comprised of a substrate for PKA
AOBS	acousto-optical beam splitter
aPKC	atypical PKC
Arp2/3	actin-related proteins 2 and 3
ATP	adenosine triphosphate
cAMP	cyclic adenosine monophosphate
CAT	PKA catalytic subunit
CDKN2A	cyclin-dependent kinase inhibitor 2A
CFP	cyan fluorescent protein
cGMP	cyclic guanine monophosphate
CNB	cyclic-nucleotide-binding
CNG	cyclic nucleotide-gated
D/D	PKA’s dimerisation and docking domain
DAG	diacylglycerol
DEP	Dishevelled, Egl-10, Pleckstrin
DMEM	Dulbecco’s modified Eagle medium
DMSO	dimethyl sulfoxide
dnPKA	dominant negative PKA
EHS	Engelberth-Holm-Swarm
EMT	epithelial to mesenchymal transition
EPAC	exchange protein activated by cAMP
ERK	extracellular signal-regulated kinase
ERK5	extracellular signal-regulated kinase 5
FAK	focal adhesion kinase
FAT	C-terminal focal-adhesion targeting
FBS	foetal bovine serum
FRET	Förster electron resonance energy transfer
GDP	guanosine diphosphate
GEF	guanine-exchange factor
GFP	green fluorescent protein
GIT1	G-protein-coupled receptor kinase interacting protein 1
GPCR	G-protein-coupled receptor
GTP	guanosine triphosphate
GAP	GTPase activating protein
HCN	hyperpolarisation-activated cyclic nucleotide-gated
IBMX	3-Isobutyl-1-methylxanthine
IP_3	inositol trisphosphate
KRAS	v-Ki-ras2 Kirsten rat sarcoma viral oncogenes homolog
LSCM	laser scanning confocal microscope
MEF	mouse embryonic fibroblast
MEK	MAPK/ERK kinase
MEKK	MAPK/ERK kinase kinase

MLC	myosin light chain
Myr-PKI	myristoylated PKI
PAK	p21-activated kinase
PanIN	pancreatic intraepithelial neoplasia
PAR3	protease activated receptor 3
PAR6	protease activated receptor 6
PBS	phosphate buffered saline
PDAC	pancreatic ductal adenocarcinoma
PDE	phosphodiesterase
PDGF	platelet derived growth factor
PET	polyethylene terephthalate
PI3K	phosphoinositide 3-kinase
PIX	PAK-interacting exchange factor
PKA	protein kinase A
PKC	protein kinase C
PKG	protein kinase G
PKI	protein kinase A inhibitor
PLC	phospholipase C
PLCγ	phospholipase Cγ
PSmOrange	photo-switchable mOrange
PTB1B	protein tyrosine phosphatase 1B
RFP	red fluorescent protein
RhoGDI	Rho GDP-dissociation inhibitor
ROCK	Rho-associated kinase
sAC	soluble adenylyl cyclase
WASP	Wiskot-Aldrich syndrome protein
WAVE	verprolin homology protein-1
YFP	yellow fluorescent protein

CONTENTS

TITLE PAGE.....1

ABSTRACT.....2

ACKNOWLEDGEMENTS.....3

ABBREVIATIONS.....4

CONTENTS.....6

CHAPTER 1 – INTRODUCTION.....8

1.1. Pancreatic ductal adenocarcinoma.....9
1.2. Cellular motility.....10
1.3. The cAMP signalling pathway.....16
1.3.1. Protein Kinase A.....18
1.3.2. Exchange proteins activated by cAMP.....21
1.3.3. Cyclic nucleotide-regulated cation channels.....24
1.4. The aims of this study.....26

CHAPTER 2 – MATERIALS AND METHODS.....28

2.1. Cell culture.....29
2.2. Exogenous gene expression.....29
2.2.1. Plasmids and constructs.....30
2.3. Microscopy - Perfusion system.....31
2.3.1. Microscopy - Confocal imaging.....32
2.3.2. Microscopy - Fluorochrome excitation and emission.....32
2.3.3. Microscopy - XYT mode of imaging.....33
2.4. FRET measurement and analysis.....33
2.4.1. Image processing and data analysis.....35
2.5. Ruffling analysis.....36
2.6. Chemicals and other reagents.....36
2.7. Migration and Invasion assays.....37
2.8. Scratch assay.....38

CHAPTER 3 –cAMP ELEVATION INHIBITS PANCREATIC DUCTAL ADENOCARCINOMA MIGRATION.....40

3.1. Elevation of intracellular cAMP inhibits migration in pancreatic cancer cell lines 41
3.1.1. Analogue of cAMP inhibits PANC-1 migration.....55
3.2. cAMP elevation inhibits migration in a diverse range of PDAC cell lines.....61
3.3. Cell migration is inhibited when migration is induced by asymmetric FBS gradient.....66
3.4. Cell invasion is inhibited by cAMP elevation in PANC-1 cells.....68
3.5. Directional invasion induced by asymmetric FBS gradient is suppressed by cAMP.....70
3.6. Summary of key results in Chapter 3.....72

CHAPTER 4 – RAPID AFFECT OF CAMP INCREASE ON RUFFLING, STRESS FIBRES, ACTIN DYNAMICS, AND FOCAL ADHESIONS 73
4.1. cAMP elevation inhibits cell ruffling.....74
4.2. Key focal adhesion protein paxillin dissociates from focal adhesions in response to cAMP elevation 81
4.3. cAMP elevation reversibly inhibits actin stress fibre formation.....87
4.4. Summary of key results in Chapter 4.....93

CHAPTER 5 – DOWNSTREAM EFFECTORS OF cAMP SIGNALLING HAVE OPPOSING ROLES IN MODULATING MIGRATION.....94
5.1. Selective EPAC activation potentiates migration.....95
5.2. Selective PKA activation inhibits cell migration.....100
5.3. PKA activity correlates with ruffling.....104
5.3.1. Selective PKA activation using 6Bnz induces paxillin translocation out of focal adhesions.....106
5.4. Testing PKA inhibitors.....111
5.5. PKI-mCherry prevents the effect of cAMP induced inhibition of ruffling 121
5.6. Selective PKA inhibition prevents the loss of paxillin from focal adhesions in response to cAMP elevation.....128
5.7. Selective PKA inhibition prevents the induced inhibition of migration 134
5.7.1. PKA inhibition induces cell migration.....136
5.7.2. Uncoupling PKA from signalling microdomains by disrupting its binding to AKAPs enhances cellular migration rate.....138
5.8. Summary of key results in Chapter 5.....140

CHAPTER 6 – DISCUSSION.....141
6.1. cAMP inhibits migration in 5 diverse PDAC cell lines.....142
6.2. cAMP inhibits migration and invasion in different modes of migration.....145
6.3. Elevation of cAMP inhibits ruffling.....147
6.4. cAMP elevation causes paxillin to dissociate from focal adhesions.....148
6.5. cAMP elevation causes the breakdown of actin stress fibres.....153
6.6. PKA and EPAC have opposing roles in PANC-1 migration.....155
6.7. Concluding remarks.....161

REFERENCES.....162

CHAPTER 1 – INTRODUCTION

1.1. Pancreatic ductal adenocarcinoma

Pancreatic ductal adenocarcinoma (PDAC) is one of the deadliest human malignancies and is the 4th most common cause of cancer death in America (Ferlay *et al.*, 2010; Siegel *et al.*, 2012). Due to a lack of early detection methods and despite great efforts in studying the disease, the 5-year survival rate following diagnosis has remained below 5%. PDAC is a heterogeneous disease, in that the development of PDAC can arise as result of a convergence of several genetic alterations (Campbell *et al.*, 2010). There is significant genomic instability leading to the eventual development of metastatic pancreatic cancer (Iacobuzio-Donahue *et al.*, 2012). However, some key mutations are common to most cases of PDAC development. One of the initial common alterations, which occurs early in the development of PDAC, result in the activating mutation of KRAS oncogene. This occurs during the early stage of pancreatic intraepithelial neoplasia (PanIN); the earliest onset of this is termed PanIN-1 (Iacobuzio-Donahue *et al.*, 2012). Subsequent progression leads to the stage PanIN-2, often during which cyclin-dependent kinase inhibitor 2A alpha (CDKN2Aα, also known as p16) tumour suppressor, is mutated (Iacobuzio-Donahue *et al.*, 2012). Further progression to PanIN-3 stage accumulates mutation in p53 and SMAD4 tumour suppressors (Iacobuzio-Donahue *et al.*, 2012). Further accumulation of genetic alterations eventually can lead to cell dissemination from the primary tumour and invasion of the local tissues, leading to metastasis of the cancer (Iacobuzio-Donahue *et al.*, 2012). Pancreatic cancer effectively forms both local and distant cell metastases (Kamisawa *et al.*, 1995; Marchesi *et al.*, 2004; Yachida *et al.*, 2010). Majority of patient mortality is caused by metastasis of the cancer cells into other tissues, which form secondary tumour sites (Farrell *et al.*, 1997). Hence it is would be very important to understand the mechanism which controls cell migration and invasion, and develop therapeutic interventions which are able to prevent metastasis of pancreatic cancer.

1.2. Cellular motility

Cell motility is a process in which a cell translocates from one location to another. This process is important in many physiological and pathological processes. For example, cellular migration is key process in embryonic development which is responsible for the correct localisation of differentiated cells to form tissues and organs (Kurosaka & Kashina, 2008). In a developed organism, cell motility is required for processes such as wound healing and immune responses (Luster *et al.*, 2005). Conversely, dysregulation of cellular migration can also contribute towards development of diseases, such as cell dissemination from a primary tumour leading to metastasis (Wang *et al.*, 2005). Single or groups of cells can migrate away from the tumour mass and enter the blood or lymph vessels, in a process known as intravasation. Cells can then spread throughout the organism and exit the vasculature (extravasation) and spread to secondary sites to form secondary tumour masses (Wang *et al.*, 2005). The basic mechanism of cell motility that is common to both physiological and pathological processes have been well characterised (Lauffenburger & Horwitz, 1996; Ridley *et al.*, 2003), and consist of initial cell polarisation which enables asymmetric cell morphology with defined leading and trailing edges. The leading edge of the cell possesses protrusive ability to further extend the membrane forward. Adhesion to the extracellular matrix is mediated via a family of integrin proteins and is usually established under the protrusive leading edge. Cell contraction takes place to enable the cell to move in the direction of the leading edge. Finally, trailing edge retraction has to take place in order to ensure that efficient cell motility takes place (Lauffenburger & Horwitz, 1996; Ridley *et al.*, 2003).

Cellular polarity develops upon the initiation of migration. Extracellular cues are among the deciding factors that can induce polarisation and migration. In the case of directed

migration, gradients of soluble factors can induce cell polarisation leading to chemotaxis. Protrusive leading edge is found to establish towards the higher concentration of the gradient, while the trailing edge is situated towards the lower concentration of the gradient (Iglesias & Devreotes, 2008; Swaney *et al.*, 2010). Although in some cases, spontaneous cell polarisation can take place in the absence of any asymmetric cues (Wedlich-Soldner & Li, 2003). Application of chemoattractants in a homogenous non-gradient manner can induce cell polarisation and migration, which indicates that a gradient is not always necessary to induce cell polarisation, and highlights that cells have the ability to self polarise (Verkhovsky *et al.*, 1999). In other situations, adhesion alone to the extracellular matrix can be sufficient to induce cell polarisation and migration (Parsons *et al.*, 2010).

Cell stimulation by soluble factors can activate specific surface receptors which often belong to the G-protein-coupled receptor (GPCR) family (Cotton & Claing, 2009). The main effectors which have been found to be activated downstream of the receptors are phospholipase C (PLC) and protein kinase C (PKC). This leads to the subsequent formation of the second messengers inositol trisphosphate (IP_3) and diacylglycerol (DAG), as well as phosphorylation of target proteins by PKC (Van Haastert & Devreotes, 2004). GPCR mediated activation of phosphoinositide 3-kinase (PI3K) can lead to the production of phosphatidylinositol-3,4,5-trisphosphate (PIP_3). PIP_3 production is confined mainly to the front of the cell and is responsible for asymmetric activation of Rho GTPases, of which the most famous members are the Rac1, RhoA, and Cdc42, via recruitment of guanine-exchange factors (GEFs) (Kolsch *et al.*, 2008; Cain & Ridley, 2009). The GTPase Cdc42 has been shown to be important in the initiation of cell polarity, and it achieves this through recruitment of actin polymerisation machinery as well as atypical PKCs (aPKCs), PAR3 and PAR6 to the leading edge of migrating cells (Etienne-Manneville & Hall, 2003). The activity

Cdc42 has been shown to be absolutely crucial for efficient migration in most cells (Etienne-Manneville, 2004).

Following establishment of cell polarity, the next step of migration is the formation of membrane protrusion at the leading edge. This process requires careful coordination of multiple signalling molecules, which ultimately control the arrangement of actin cytoskeleton to produce the protrusive forces required for the extension of the leading edge of the cell. The actin cytoskeleton comprises of monomeric globular (G) - actin which polymerises to form actin filaments. ATP bound to G-actin is hydrolysed to ADP as two actin monomers are joined together. Further release of the phosphate group destabilises the structure and promotes filament depolymerisation (Korn *et al.*, 1987; Pollard & Borisy, 2003; Pollard & Cooper, 2009). Polymerised actin filaments can be assembled into various structures via several actin binding proteins such as α-actinin, myosin, and filamin.

Filopodia projections are long and thin actin projections composed of unbranched parallel actin bundles. The function of filopodia appears to be exploratory, in that they are able to physically sense the local environment within the cell proximity (Mejillano *et al.*, 2004; Mattila & Lappalainen, 2008). The key membrane protrusive event which is associated with cell motility is the formation of lamellipodia, which are comprised of branched network of thin and short actin filaments (Cramer *et al.*, 1997; Svitkina & Borisy, 1999). Rac1 GTPase was initially considered to be the most important mediator of lamellipodia formation. However more recent findings have demonstrated that all three GTPases (Rac1, RhoA, and Cdc42) play a role in the membrane protrusion/retraction cycle (Machacek *et al.*, 2009). Furthermore, studies have found that the lamellipodial protrusion/retraction cycle is mediated by protein kinase A (PKA) which phosphorylates RhoA, resulting in its inhibition

by increased association with Rho GDP-dissociation inhibitor (RhoGDI) (Tkachenko *et al.*, 2011). Downstream of the Rho GTPases are the effectors which control actin polymerisation to form the membrane protrusions. Some of the main mediators which have been found to be involved in these processes are the Wiskot-Aldrich syndrome protein (WASP) and the verprolin homology protein-1 (WAVE/Scar) complex (Suetsugu *et al.*, 2003; Pollitt & Insall, 2009). Cdc42 has been found to regulate WASP, while Rac1 regulates WAVE/Scar proteins (Eden *et al.*, 2002). Together, they can regulate the activity of actin-related proteins 2 and 3 (Arp2/3) complex (Schweiger, 1991; Suetsugu *et al.*, 2003; Svitkina, 2007; Pollitt & Insall, 2009; Campellone & Welch, 2010). Arp2/3 is a heteroheptameric protein structure which is able to promote actin branching by binding to the side of an actin filament and promote actin polymerisation at approximately 70^{o} angle to the original filament direction (Mullins *et al.*, 1998). The branching of the actin network is an essential process associated with lamellipodia formation (Svitkina, 2007).

Following cell protrusion at the leading edge of the cell, new adhesions can form between the cell and the extracellular matrix. Cellular adhesions were first observed in cultured cells which were seen as sites of overlap between the extracellular fibrils and the actin cytoskeleton (Curtis, 1964). Further investigation into fibroblast migration using electron microscopy, found electron-dense regions at the plasma membrane that made direct contact with extracellular substrate (Abercrombie *et al.*, 1971). Over the years the cell-matrix adhesion sites have been characterised into different groups. Following the immediate formation of an adhesive structure, it is termed a nascent adhesion (Alexandrova *et al.*, 2008). These structures typically have fast turnover time and are smaller in size, and as a result are more rarely observed. Next are the focal complexes; they are bigger than the nascent adhesions and are myosin II dependent structures. They

typically localise at the border where the initiation of lamellipodia formation takes place (Rottner *et al.*, 1999; Giannone *et al.*, 2007). Similarly to nascent adhesions however, the focal complexes also have a more transient nature and either quickly disassemble or mature into full focal adhesions. Finally, a fully matured focal complex is termed a focal adhesion and has the longest turnover lifetime (Zaidel-Bar *et al.*, 2004). Due to the longer lifetime of these structures, they are the most commonly observed cellular adhesions. In the text of this thesis I will be referring to all cellular adhesions as 'focal adhesion' unless otherwise stated.

Within the specific regions of adhesion, there are various associated proteins (Zamir & Geiger, 2001b). There is a considerable overlap, with many proteins localising within different adhesion structures. Of great importance are the integrin family of proteins. They are heterodimeric proteins consisting of α and β subunits. Integrins are transmembrane proteins which have both cytosolic and extracellular components; they can bind many types of extracellular matrix compositions, and this depends on the integrin type (Jockusch *et al.*, 1995; Hynes, 2002; Humphries *et al.*, 2006). Intracellular binding of other focal adhesion associated proteins to integrins can enhance integrin binding to the extracellular matrix. Focal adhesion associated protein, talin, can bind to the cytosolic part of the integrin, which induces a conformational change within the integrin structure, causing increased extracellular binding affinity to the substrate (Shattil *et al.*, 2010). Integrins are also bi-directional in nature, in that they are able to serve as receptors and report the extracellular cues to the intracellular cytoplasmic signalling domains.

In order to generate tractional forces, so that the cell can pull itself forward, the integrin proteins are coupled to the actomyosin cytoskeleton. However, this interaction is not direct

and requires other focal adhesion associated proteins. Talin for example is able to directly bind to both integrins and actin (Critchley, 2009). Other examples of proteins which can crosslink integrins with the cytoskeleton are α-actinin and filamin (Otey *et al.*, 1990; Pfaff *et al.*, 1998). Proteins associated with adhesion sites are not only important in establishing tractional forces, but are also very important in integrating extracellular events and passing on this information through various intracellular signalling networks. For example, proteins such as focal adhesion kinase (FAK) have been implemented in the downstream control of RhoA signalling by interaction with RhoGEFs (Tomar & Schlaepfer, 2009). Another such protein is paxillin, which serves as a very important signalling hub. Although paxillin lacks any kinase activity, its regulatory functions come from many interactions with other signalling proteins. Both direct and indirect binding of GEFs and/or GTPase activating proteins (GAPs) for Rac1, RhoA and Cdc42 helps regulate their activity and subsequently cellular motility (Brown & Turner, 2004; Deakin & Turner, 2008).

Following cellular leading edge protrusion, the cell can advance forward by actomyosin based cytoskeletal contraction. As a result this process is dependent on the protein myosin II, which can generate the tractional forces required (Svitkina *et al.*, 1997; Small *et al.*, 1998). At the same time, cell retraction must take place at the rear of the cell in order to allow net cell movement in a defined direction. Interestingly, RhoA has a different role at the trailing edge of the cell, where through its effector Rho-associated kinase (ROCK) it regulates myosin IIA isoform activity, to promote adhesive contact disassembly (Worthylake *et al.*, 2001). Several processes help the disassembly of cellular adhesion at the trailing edge of the cell. Microtubule targeting appears to play an important role in the initiation of focal adhesion dismantling. It has been found that microtubules preferentially target focal adhesions located at the trailing edge which initiates their disassembly

(Kaverina *et al.*, 1999; Efimov & Kaverina, 2009). Furthermore, proteolytic cleavage of focal adhesion associated proteins such as FAK and talin, is mediated by Ca^{2+} dependent enzyme calpain, which further helps cell detachment at the trailing edge (Franco *et al.*, 2004; Chan *et al.*, 2010). All of these processes are coordinated to enable efficient cellular migration.

1.3. The cAMP signalling pathway

Cyclic adenosine monophosphate (cAMP) signalling cascade is activated through the binding of ligands to GPCRs. Attached to the GPCR is the heterotrimeric G protein which is comprised of the Gα,G β, and Gγ subunits. In a non activated state, the Gα subunit is attached to the Gβγ subunits and is bound to GDP. Activation of the GPCR via ligand binding causes increased GDP-GTP exchange on the Gα subunit. GTP-bound Gα subunit then dissociates from the heterotrimer complex and activates its downstream effectors. The Gβγ stay bound together and also activate their respective downstream effectors. Several subtypes of the Gα subunits exist which include $G_s\alpha$, $G_i\alpha$, $G_q\alpha$, $G_t\alpha$ (transducin), and $G\alpha_{12/13}$. Of importance to cAMP production, $G_s\alpha$ causes activation of adenylyl cyclases (ACs) and thus increase in cAMP production, while $G_i\alpha$ inhibits AC activity (Birnbaumer, 1990; Gilman, 1990). Gβγ subunits can also activate or inhibit ACs which depends on their isoform type (Cooper, 2003).

A total of 9 membrane-bound isoforms of ACs have been identified (AC1-AC9), as well as one soluble form (sAC) (Hanoune & Defer, 2001). Membrane-bound AC1-AC9 isoforms all consist of approximately 130kDa glycoprotein with considerable sequence homology (Sunahara *et al.*, 1996). The structure of AC comprises of two hydrophobic transmembrane domains (Tm1 and Tm2), one small N-terminus cytoplasmic domain (Nt), and two larger

cytoplasmic C-terminus domains (C1 and C2) (Sunahara *et al.*, 1996). The C1 and C2 domains contain the catalytic site of the enzyme (Sunahara *et al.*, 1996). The C1 and C2 domains are further subdivided into the highly conserved catalytic regions (C1a and C2a), and the less conserved non catalytic part of the domains (C1b and C2b) (Sunahara *et al.*, 1996; Cooper, 2003). The distribution of the different isoforms of ACs is quite varied throughout the organism, and are reviewed in (Hanoune & Defer, 2001; Cooper, 2003). From the reviews I can see that AC1 localises mainly in the brain . AC2 is found in both lung and the brain. AC3 localises in the olfactory epithelia and the pancreas. AC4 isoform is ubiquitously expressed and is widespread through the organism. AC5 is located mainly in the heart and striatum. AC6 mostly widespread, but is seen at slightly higher expression levels in the heart and kidney. AC7 is another isoform that is widespread throughout the organism. AC8 is mainly in the brain and pancreas. AC9 is another widespread isoform with some preferential expression in the pituitary tissues. Finally sAC is widely expressed, with particular prominent expression in the testis. Furthermore, AC3-5 have been reported to be localised within membrane lipid rafts and caveolae, suggesting that ACs can form microdomains complexes within the cells (Schwencke *et al.*, 1999). To add to the complexity, AC1 and AC8 can also be activated by Ca^{2+} (Fagan *et al.*, 1996), whereas AC5 and AC6 are inhibited (Cooper *et al.*, 1995).

cAMP that is produced by ACs is broken down by another class of cyclic nucleotide enzymes termed phosphodiesterases (PDEs), and consists of 11 separate families (PDE1-11) (Soderling & Beavo, 2000; Mehats *et al.*, 2002). Some PDEs (PDE4, PDE7, PDE8) are selective for cAMP nucleotide hydrolysis, while other PDEs (PDE5, PDE6, PDE9) are selective for cyclic guanosine monophosphate (cGMP). The remaining PDEs (PDE1, PDE2, PDE3, PDE10 and PDE11) have dual specificity and are able to hydrolyse both cAMP and cGMP (Mehats *et al.*, 2002). Some of the PDE families have subclasses: PDE1 (A, B, and C), PDE3

(A, and B), PDE4 (A, B, C, and D), PDE6 (A, B, C, D, and G), PDE7 (A, and B), and PDE8 (A, and B) (Savai *et al.*, 2010). Furthermore, due to alternative splicing and promoter sequences used, there is likely to be over 40 different PDEs capable of cAMP degradation (Baillie *et al.*, 2005; Lugnier, 2006). The different families of PDEs can respond differently to the same signalling molecules, for example PDE3 is inhibited by cGMP, while PDE2 is activated (Lugnier, 2006; Conti & Beavo, 2007). The structure of different PDEs varies, however they all have a highly conserved catalytic core region which enables them to perform their hydrolytic function (Mehats *et al.*, 2002). Like with ACs, PDEs have differential expression amongst the different tissues within the organism (Savai *et al.*, 2010).

1.3.1. Protein Kinase A

Downstream of cAMP production are the effectors which are directly activated by the cyclic nucleotide. PKA is one such effector and is one of the most studied classical kinase proteins. In the inactive state the PKA holoenzyme consists of a regulatory (R) subunit dimer which is associated noncovalently with two catalytic (C) subunits (Corbin *et al.*, 1973; Corbin & Keely, 1977). There are two sites on each R subunit, termed A and B, to which cAMP can bind. Thus a complete PKA structure can bind 4 cAMP nucleotides. However in the inactive state, only site B is open to allow cAMP biding. Following occupation of site B however, site A becomes more accessible and allows further cAMP binding. After 4 molecules of cAMP bind to the R subunit dimer, a conformation change occurs within PKA and the C subunits can dissociate as two monomers. The dissociation from the R subunits exposes the catalytic site within the C subunits, thus enabling catalytic activity which phosphorylates downstream target proteins on serine and threonine residues, for review of these processes see (Kopperud *et al.*, 2002). PKA has a broad substrate specificity and phosphorylates the amino acids serine/threonine in the following sequences: Arg-Arg-X-Ser/Thr, Arg/Lys-X-X-Ser/Thr, and finally Arg/Lys-X-Ser/Thr (Shabb, 2001).

Two different types of PKA were originally identified based on their elution by ion-exchange chromatography. The classification of these kinases was based on their regulatory subunits. They were termed PKA type I which contained the RI subunits, and PKA type II which contained the RII subunits (Reimann *et al.*, 1971; Corbin *et al.*, 1975). Further analysis has revealed that multiple isoforms of each PKA subunit exist. The R subunits were termed RIα, RIβ, RIIα, and RIIβ, while four isoforms of the C subunits were found and termed Cα, Cβ, Cγ, and PRKX (human X chromosome-encoded protein kinase X) (Skalhegg & Tasken, 2000). PRKX differs from Cα, Cβ, and Cγ subunits in that it does not possess the ability to bind RII subunits in physiological conditions (Zimmermann *et al.*, 1999). Structurally PKA consists of two C subunits bound to RI homodimers / heterodimers, or RII homodimers (Scott, 1991; Tasken *et al.*, 1993). Type I and II PKA also possesses different sensitivities towards cAMP. Type I PKA has a cAMP activation constant of 50-100nM. Type II PKA is less sensitive towards cAMP and has a cAMP activation constant of 200-400nM (Cadd *et al.*, 1990; Dostmann & Taylor, 1991; Gamm *et al.*, 1996).

Despite the different isoforms of R subunits, they all have common features which enable them to perform similar function. All R subunits posses an N-terminal dimerisation and docking domain (D/D). This allows R subunit monomers to form the homo- and/or hetero-dimers. Each R subunit also contains an inhibitor site (pseudosubstrate in RI and a substrate site for RII subunits), and two of the previously mentioned cAMP-binding domains (Heller *et al.*, 2004). Connecting the D/D domain and the cAMP-binding site, is a highly variable linker which contains the autoinhibitory residues required to inhibit the catalytic activity of the bound C subunits (Vigil *et al.*, 2004). Unlike the highly variable linker however, the D/D domain is highly conserved amongst the different R subunit isoforms. The cAMP-binding domains also show high sequence homology (Canaves & Taylor, 2002).

Different forms of PKA are expressed differentially within the tissues which further adds to the specificity of PKA signalling. For example, RIIβ is more expressed in the reproductive, endocrine, fat, and brain tissues, while RIβ subunit is found primarily in the brain (Jahnsen *et al.*, 1986; Clegg *et al.*, 1988; Cadd & McKnight, 1989). On the other hand, both the RIα and RIIα subunits are fairly ubiquitously expressed throughout the organism (Lee *et al.*, 1983; Scott *et al.*, 1987). In addition to providing the capability for R subunit dimerisation, the D/D domain also facilitates docking to A-kinase-anchoring proteins (AKAPs). This intensively investigated interaction provides a means by which differential intracellular targeting of PKA is achieved. Interestingly, the original experiments that found AKAPs had assumed that they were contaminants of purified PKA (Theurkauf & Vallee, 1982; Lohmann *et al.*, 1984; Sarkar *et al.*, 1984). However it was soon found that they can bind PKA, and through a unique targeting sequence can localise PKA to different subcellular compartments. Typically PKA type I was found to be soluble and assumed to be localised within the cytosol. PKA type II however was found to be differentially distributed within subcellular compartments and this was later shown to be as a result of interaction with AKAPs (Colledge & Scott, 1999; Dodge & Scott, 2000; Diviani & Scott, 2001; Michel & Scott, 2002). Later experimental results suggest that PKA type I can also be targeted by dual-specificity AKAPs which anchor type I and II PKA (Huang *et al.*, 1997; Reinton *et al.*, 2000; Hamuro *et al.*, 2002). There are also specific AKAPs which have been found to only bind PKA type I (Angelo & Rubin, 1998; Lim *et al.*, 2007). Thus it is likely that the targeting of PKA to specific signalling networks is more complicated than originally anticipated. Significant volume of experimental data supports the idea that PKA can control various discrete signalling pathways despite having broad substrate specificity.

AKAPs are a broad family of proteins which, if including splice variants, includes over 50 different proteins (Pidoux & Tasken, 2010). They achieve the interaction with R subunits

through a 14-18 amino acid amphipathic helix stretch (Carr *et al.*, 1991). This helix is common to almost all AKAPs characterised so far and is hydrophobic on one side of the helix, while the other side is hydrophilic. The residues within the helix form a total of 5 complete turns, structure of which is important for the interaction with the PKA's D/D domain. The interaction between type II PKA and AKAPs has been shown to occur with high affinity in the low nanomolar range of the participating proteins. (Herberg *et al.*, 2000). However, it has been shown that in order for AKAP binding to occur and the PKA-AKAP complex to form, the N-terminus of RII must first dimerise (Newlon *et al.*, 1999; Gold *et al.*, 2006). Each AKAP also contains a unique domain which enables selective targeting to subcellular regions of the cells. It is also important to note that some AKAPs have been found to not only bind and target PKA, but also are responsible for binding many other diverse proteins such as kinases, phosphodiesterases, and phosphoprotein phosphatases (Coghlan *et al.*, 1995; Schillace & Scott, 1999; Feliciello *et al.*, 2001; Tasken *et al.*, 2001).

1.3.2. Exchange proteins activated by cAMP

Another downstream effector of cAMP that has been recently discovered, is the exchange protein activated by cAMP (EPAC). In the earlier days of the cAMP field development, it was thought that the effects of cAMP were mostly due to PKA activation. However, there were certain effects induced by cAMP that appeared to be independent of PKA activity. One such example was the activation of the small GTPase Rap1 in the presence of PKA inhibitors (de Rooij *et al.*, 1998; Kawasaki *et al.*, 1998; de Rooij *et al.*, 2000). Subsequently, after a search for other cAMP effectors, two separate isoforms of EPAC were discovered and named EPAC1 and EPAC2. Both proteins act as a GEF for Rap1 and Rap2 GTPases. Both EPAC proteins have a similar structure which consists of a catalytic region towards the C-terminal, while the N-terminal contains the regulatory domains. One key difference between EPAC1

and EPAC2 is that the latter has an additional cyclic-nucleotide-binding (CNB) domain located at the end of the N-terminus (Bos, 2006).

Functional studies found that fragments of EPAC containing the catalytic domains displayed full catalytic activity. This suggested that the regulatory domains can suppress the catalytic activity of the protein. Later studies utilised X-ray crystallography and found that the regulatory domains indeed cover the catalytic site when EPAC is not bound to cAMP (Rehmann *et al.*, 2003; Rehmann *et al.*, 2006). This suggested that EPAC is an auto-inhibitory protein, which upon binding of cAMP, undergoes a conformational change and relieves the inhibition at the catalytic site. The mechanism by which this is achieved has been found due to two key features of the protein. Firstly, there is a pseudo β-sheet hinge connecting the regulatory and catalytic domains, around which the protein unfolds. The second feature is an 'ionic latch', which is in the form of an ionic interaction between one of the catalytic domains (CDC25-homology domain) and a CNB that is common to both EPAC 1 and EPAC2. As mentioned previously, EPAC 2 has an extra CNB domain whose function is not very clear. Firstly, this domain binds cAMP with considerably lower affinity then the other CNB that it posses. Secondly, deletion of this extra CNB does not appear to affect the binding of cAMP to the remaining CNB, nor does it affect the auto-inhibitory function of the protein (de Rooij *et al.*, 2000); thus its function is unclear. EPAC activation by cAMP occurs in the low micromolar range, which is considerably higher than that required for PKA, which is in the high nanomolar range (Walsh *et al.*, 1968). This raises the interesting possibility that PKA can be activated at lower level of physiological stimulation than EPAC. The same observation have been made when experiments have been conducted with cAMP sensors based on either PKA or EPAC (Ponsioen *et al.*, 2004). However, this is quite subjective as the localisation of EPAC could greatly influence its exposure to local cAMP flux, and thus its activation. As was discussed above, due to selective targeting with AKAPs, PKA can be

recruited to subcellular microdomains which have the potential to expose PKA to much higher localised fluxes of cAMP. Similarly, EPAC has a targeting domain located in the regulatory region of the protein. The Dishevelled, Egl-10, Pleckstrin (DEP) domain has been found to regulate localisation of EPAC to membranes. Upon deletion of DEP, the localisation of EPAC becomes more cytosolic, although the function and regulation of EPAC by cAMP remains unchanged (de Rooij *et al.*, 2000; Ponsioen *et al.*, 2004). Thus selective targeting of EPAC to specific regions of the cell could potentially counter the lower sensitivity of EPAC by exposing it to a higher localised concentration of cAMP, and thus enable sufficient activation and function of the protein.

Classical tools typically used to study cAMP signalling such as forskolin (AC activator) and 3-Isobutyl-1-methylxanthine (IBMX) (PDE inhibitor) raise intracellular cAMP concentrations. Following the discovery of EPAC however, one needs to consider that raising global cAMP would activate both PKA and EPAC simultaneously. It therefore became crucial develop selective activators of each effector. Subtle differences in the molecular structure of PKA and EPAC proteins has been found to alter cAMP binding sites in such a way that could be exploited for producing selective cAMP analogues. PKA contains a glutamate residue that interacts with 2'OH of a ribose and has been shown to be important in cAMP binding to PKA; this arrangement is not however present in either EPAC 1 or EPAC2 proteins (Yagura & Miller, 1981; Enserink *et al.*, 2002). This led to the development of cAMP analogues which could selectively activate EPAC. One such cAMP analogue was created and termed 8-pCPT-2'OMe-cAMP (8pCPT); it was found to activate both EPAC1 and EPAC2 without causing any substantial activation of PKA (Enserink *et al.*, 2002; Kang *et al.*, 2006). The selective activation of PKA is also desirable. For this reason another cAMP analogue, N6-benzoyl-cAMP (6Bnz), was developed (Christensen *et al.*, 2003). This molecule effectively activates

PKA but not EPAC. Thus, these selective cAMP analogues can be used to study the individual biological effects elicited by each type of effector proteins.

It is important to note that Rap1 activation has been linked with controlling integrin mediated adhesion, and thus could play potentially important role in the control of cell motility (Bos, 2005). Rap1 GTPase can be activated by various signalling systems which are controlled by second messengers such as diacylglycerol, cAMP, and Ca^{2+} (Bos, 2006). The second messengers can modulate activation of several specific GEFs leading to Rap1 activation, which includes both EPAC proteins. Many effectors of Rap1 appear to be in control of important cellular processes. These include cell-cell junction formation regulated by Rap1 effector AF6 (Boettner *et al.*, 2003). Cell adhesion complex formation is controlled by Rap1 effectors RapL and Riam (Katagiri *et al.*, 2003; Lafuente *et al.*, 2004). Actin remodelling has been found to be controlled through the Rap1 effectors Vav2 and Tiam1 which are Rac1 associated GEFs (Arthur *et al.*, 2004). RhoA GAP, Arap3, is also one of the effectors of Rap1 GTPase (Krugmann *et al.*, 2004). However, Rap GTPases are not the only effectors of EPAC proteins which have been noted to play a role in cell signalling. EPAC1 has been shown to directly interact and activate Ras-related GTPase, R-Ras, leading to the downstream stimulation of phospholipase D (Lopez De Jesus *et al.*, 2006). This in turn leads to integrin activation and subsequent adhesion of cells. R-Ras has also been implicated in the control of cell migration through the spatio-temporal regulation of RhoA and Rac1 GTPases (Bezuidenhout, 1992; Holly *et al.*, 2005; Jeong *et al.*, 2005; Wozniak *et al.*, 2005).

1.3.3. Cyclic nucleotide-regulated cation channels

Another class of protein which has been found to directly bind cAMP and cGMP are the cyclic nucleotide-regulated cation channels. Two families of channels have so far been identified which are the cyclic nucleotide-gated (CNG) channels, and the hyperpolarisation-

activated cyclic nucleotide-gated (HCN) channels (Kaupp & Seifert, 2002; Craven & Zagotta, 2006; Biel, 2009). Although both families of channels bind cAMP/cGMP, they differ in their relative sensitivities towards these cyclic nucleotides. CNG channels are preferentially activated by cGMP, whereas HCN channels display approximately 10-fold higher affinity for cAMP (Kaupp & Seifert, 2002). The key differences that determine the selectivity of the nucleotides have been attributed due to several key amino acids changes. Studies in CNG channels have provided evidence that the threonine residue in a β-roll (Altenhofen *et al.*, 1991) and aspartate in the C-helix (Varnum *et al.*, 1995), help stabilise cGMP binding by forming an extra hydrogen bond with the guanine ring of cGMP which is lacking in the adenine ring of cAMP. The corresponding residues are also present on HCN channels which are the threonine 591, but the aspartate is replaced by isoleucine at position 636 (Zhou & Siegelbaum, 2007). Replacement of I636 with aspartate residue converts the HCN into cGMP-selective channels. Other adjacent residues also play a role in cAMP selectivity of HCN channels which are the R632, R635, and the K638 (Zhou & Siegelbaum, 2007).

The basic structure of both CNG and HCN channels is quite similar, and seen in many voltage-gated cation channels (Yu *et al.*, 2005). The general structure of the whole channel consists of a tetrameric complex. Each of the channel's transmembrane cores consists of six α-helixes (S1-S6). There is also an ion conducting pore loop situated between helices S5 and S6 (Biel, 2009). Both the N- and C-terminus are located within the cytoplasm of the cell. Both families of cyclic nucleotide-regulated channels contain positively charged arginine or lysine residues within the S4 helix; these amino acids function as a voltage sensor in the HCN channels and help control the channel activity in combination with cyclic nucleotide binding (Biel, 2009). Although cyclic nucleotide binding is not required for HCN channel activation, the binding of nucleotides shifts the voltage sensitivity of these channels. CNG channels on the other hand are not controlled by membrane potential, but rather only by

direct activation with cyclic nucleotides, thus the role of S4 helix in these channels is unknown. CNG channels are expressed in olfactory neurons as well as in the retinal photoreceptors and play a key role in visual and olfactory signal transduction systems (Kaupp & Seifert, 2002; Hofmann *et al.*, 2005; Biel & Michalakis, 2007). These channels are also found at lower density in other tissues such as the testis, kidney, and in the brain. HCN channels are associated with excitable tissues in the heart, brain and in the photoreceptors (Pape, 1996). For example, the cation current, mediated by an HCN channel, that is activated by the membrane hyperpolarisation (I_h) controls the heart rate rhythm by acting as the pacemaker current in the heart's SA node (Baruscotti *et al.*, 2005). Sympathetic nervous stimulation raises cAMP production in the SA node which causes a positive shift in the I_h current activation, causing an acceleration of the heart rate.

1.4. The aims of this study

The effects of cAMP signalling have been characterised in several cancers, and interestingly was found to modulate the rate of migration and invasion of cancer cells both positively and negatively (Chen *et al.*, 2008; Baljinnyam *et al.*, 2009; Grandoch *et al.*, 2009; Baljinnyam *et al.*, 2010; Shaikh *et al.*, 2012). This was both agonists and cell type dependent. However, so far there has not been any clear investigation of the role played by cAMP signalling and its downstream effectors in pancreatic cancer; this was the reason for initiating my project.

Our first aim was to characterise the cAMP effects on migration of PDAC cells. I utilised five cell lines which covered a range of genetic variations and patient origin; this was to ensure the effects of cAMP were not specific to a particular cell line. To confirm that the effect on the rate of migration was due to cAMP elevation, I used various cAMP elevating agents. Importantly, I planned to correlate migration assay experiments with results

obtained using cAMP sensors. I also planned to characterise the effect of cAMP elevation on the process of invasion and directional migration.

Our second aim of the study was to characterise the effect of cAMP elevation on membrane ruffle formation and trafficking of focal adhesion associated proteins, which are processes associated with cellular migration. The key interest was to determine whether the effect of cAMP elevation was rapid, or took a longer period of time to develop. The migration assays in our study required a period of 6 hours; it would therefore be difficult to determine using these experiments whether the effect of cAMP on migration was due to direct signalling event(s) or mediated by changes of gene expression. For this reason I studied peripheral cell ruffling and focal adhesion assembly, as these processes occur over a shorter time course. To gain greater insight, I utilised cAMP sensors to simultaneously monitor intracellular cAMP changes and correlate them with ruffling and trafficking of focal adhesion associated proteins.

The third aim of the study was to characterise the specific roles played by PKA and EPAC in the regulation of PDAC migration. To investigate this I utilise selective activators for both of the cAMP effectors. To selectively activate PKA I utilised the cAMP analogue 6Bnz, while selective EPAC activation was achieved using 8pCPT. These sets of experiments were important to discriminate between the possible effectors which could be activated upon global cAMP elevation, and to characterise the individual contribution of PKA and EPAC to changes in the rate of PDAC migration.

CHAPTER 2 – MATERIALS AND METHODS

2.1. Cell culture

PDAC cell lines PANC-1, SUIT-2, BxPC3, CAPAN-2, and MiaPaca-2 were maintained in Dulbecco modified Eagle medium (DMEM) (Invitrogen, Paisley, UK) supplemented with 10% foetal bovine serum (FBS) (Invitrogen, Paisley, UK) and penicillin/streptomycin/L-glutamate (Invitrogen, Paisley, UK) at 100units/mL, 100ug/mL, and 0.29mg/ml respectively. Cell cultures were maintained in standard humidified tissue culture incubators (Wolf Laboratories) at 37 ^{o}C and 5% CO_2. Prior to any imaging experiments, cells were transferred into Na^+-HEPES based extracellular solution (composition of which is 140mM NaCl, 4.7mM KCl, 1.13mM MgCl, 10mM HEPES, 10mM Glucose, 1.8mM CaCl, pH 7.4, and will be referred to as Na^+-HEPES or extracellular solution).

2.2. Exogenous gene expression

Cells were transfected using PromoFectin (PromoKine, UK) reagent according to manufacturer instructions. This reagent was chosen because it is non-liposomal formulation and as a result displays lower cytotoxicity as compared to other liposomal-based transfection reagents. Briefly, a total of 2ug DNA and 4µl PromoFectin was mixed in 100µl of antibiotic-free and serum-free DMEM for 20min at room temperature. Cells were grown in 2ml DMEM + 10%FBS on 35mm glass-bottom culture dishes (MatTek, USA) to approximately 60% confluency and were supplemented with the 100µl volume of the transfection solution, and maintained in the incubator at 37^{o}C and 5% CO_2 for 24 hours. Cells were then washed twice with HEPES based extracellular solution before start of experiments.

2.2.1. Plasmids and constructs

All plasmids were amplified using Qiagen Plasmid Maxi Prep HiSpeed kit. The whole process was performed according to manufacturer instructions. EPAC-based cAMP Förster resonance energy transfer (FRET) sensor CFP(nd)-EPAC (dDEP/CD)-Venus(d) was termed H84 and was a gift from Dr. K. Jalink (The Netherlands Cancer Institute) [see http://research.nki.nl/jalinklab/Constructs.htm and (van der Krogt *et al.*, 2008)]. PKA FRET sensor encoding substrate for PKA (termed AKAR4, containing PKA substrate sequence and Cerulean-Venus FRET pair), allowing visualisation of endogenous PKA activation, was a gift from Dr. J. Zhang (The John Hopkins University School of Medicine) (Depry *et al.*, 2011). PKA-based cAMP FRET sensor (RII-L20-CFP + CAT-YFP) was a gift from Prof. M. Zaccolo (University of Oxford) (Zaccolo *et al.*, 2000). LifeAct-GFP was a gift from Prof. M. Clague and Prof. S. Urbé, (The University of Liverpool) and was originally obtained from Ibidi, UK. LifeAct-RFP was obtained from Ibidi, UK. FAK-YFP was a gift from Dr. G. Bunt (Max-Planck Institute of Experimental Medicine, Germany) (Papusheva *et al.*, 2009). PKI-mCherry was a kind gift from Dr. M. Ginsberg (University of California San Diego) (Tkachenko *et al.*, 2011).

The following constructs were all obtained from plasmid sharing company addgene (www.addgene.org): Paxillin-GFP (Addgene plasmid 15233); principal investigator was Rick Horwitz (Laukaitis *et al.*, 2001). Vinculin-Venus (Addgene plasmid 27300); principal investigator was Martin Schwartz (Grashoff *et al.*, 2010). GIT-GFP (Addgene plasmid 15226); principal investigator was Rick Horwitz (Manabe *et al.*, 2002). Paxillin-PSmOrange (Addgene plasmid 31923); principal investigator was Vladislav Verkhusha (Subach *et al.*, 2011). Note, this plasmid encodes photoswitchable version of mOrange; however in all experiments, low laser light was used to ensure no photoswitching occurred and thus was used as ordinary

mOrange tag with typical excitation and emission spectra. Dominant negative PKA-GFP (Addgene plasmid 16716) was made by Randall Moon (Ungar & Moon, 1996).

All transfections were performed in PANC-1 cells line. Transfection efficiency was typically between 20-30% of the population. Approximately 24 hours after transfection the expression of the constructs was adequate to allow imaging. It is important to mention that after the 24 hour period of transfection, variable levels of expression within the population of cells was seen. Cells that were overexpressing the constructs were not analysed. Only relatively low and medium expressing cells, which displayed regular morphology, were used for analysis.

2.3. Microscopy - Perfusion system

Cells were grown to approximately 80% confluency in 35mm glass-bottom dishes (MatTek, USA), and were placed into a custom made insert designed to accommodate the dish. The insert had attachments to a 5 or 6-way manifold connected to gravity fed perfusion system, which was equilibrated to flow at approximately 0.5ml/min. A controlled vacuum fed suction line was attached to the other side of insert, allowing a constant perfusion through the insert. Depending on the insert used the volume was approximately between 0.3 and 0.8ml, allowing complete solution exchange between approximately 0.75 and 1.5 minutes. The top part of the gravity fed perfusion system had 10ml syringes connected via two-way valve taps, only one syringe was ever open at any one time thus keeping flow rate constant throughout the experiment.

2.3.1. Microscopy - Confocal imaging

Two types of the Leica inverted laser scanning microscopes (LSCM) were used: TCS-SP2-AOBS or TCS-SL. TCS-SP2-AOBS was specifically required for experiments utilising FRET sensors because of the available 405nm laser line. A set of objectives were used to take both low resolution and high resolution images depending on the experiments performed. 10x dry objective (NA=0.3) without any digital zoom was used for imaging stained Boyden chamber inserts. 20x dry objective (NA=0.5) was often used for ruffling and time lapse migration experiments. 40x dry objective (NA=0.85) was sometimes used to image the brighter FRET constructs. 63x oil (NA=1.4) were used to acquire high resolution images. Scan head pinhole diameter, determining the z-thickness of the optical slice, was also varied depending on the requirements of the experiment. The smaller the pinhole was set (measured in Airy units), the thinner the optical slice was obtained. For high resolution images, such as paxillin localisation, pinhole was typically set to 1-2 Airy units. To enable best signal to noise ratio for FRET recordings, larger pinhole diameters were used which ranged between 7 and 31 Airy units.

2.3.2. Microscopy - Fluorochrome excitation and emission

Laser excitation used and emission spectra collected were set to suit the fluorochromes used. In the event of imaging multiple fluorochromes, excitation/emission was in some instances adjusted to minimise spectral bleed through, this usually involved limiting the emission spectra collected to avoid overlapping spectra of both fluorochromes. In general, CFP was excited by 405nm laser and emission was collected between 450-490nm, GFP was excited by 488nm laser and emission collected between 500 and 570nm, YFP was excited by 514nm laser and emission collected between 520 and 590nm, PSmOrange was excited

by 543nm laser and emission collected between 560 and 670nm, RFP and mCherry was excited by 594nm laser and emission collected between 605 and 690nm.

2.3.3. Microscopy - XYT mode of imaging

Leica microscopes were used in the XYT series mode to create two-dimensional images at a fixed Z-plane optical section over time. Single frame acquisition time was dependent on chosen image resolution, number of line average and frequency of scan head. Typically 512x512 pixel resolution along with 400Hz scan head speed and 8 line average was used, resulting 13.44 second duration to fully acquire the image. This cycle was repeated every 15 seconds yielding 4 frames per minute recording for the duration of the experiment. In some experiments 1024x1024 pixel resolution images were chosen, providing higher spatial but lower temporal resolution image series. Additionally scan head could be used in unidirectional mode as described above, or bidirectional mode which halved acquisition time at a cost of producing lower detail images, whilst maintaining same signal to noise ratio. For experiments requiring high level of detail, such as visualisation of small discrete focal adhesion complexes, unidirectional mode was used. In all FRET experiments regions of interest were drawn around whole cells, and bidirectional mode was used. Furthermore, when imaging more than one fluorochrome, either parallel or sequential modes were used in order to minimise spectral bleed through and/or cycle time.

2.4. FRET imaging and analysis

All FRET sensors utilised CFP donor and YFP acceptor FRET pair (or their variants, such as Cerulean and Venus), thus 405nm laser was used for excitation of donor only. Donor emission was collected between 450 and 490nm, while acceptor emission was collected

between 520 and 590nm. Both EPAC-based FRET sensor H84 and PKA sensor AKAR4 are a uni-molecular design, which signifies that the entire sensor is composed of a single protein molecule. Thus, regardless of expression level or intracellular localisation of the construct within individual cells, the ratio of donor to acceptor fluorochromes remains fixed at 1:1. In the case of H84, the binding of cAMP to the sensor's EPAC-based backbone induces a conformational change, which increases the distance between the CFP and YFP fluorochromes, resulting in reduced FRET from the donor to the acceptor. To display increasing cAMP as a function of upward deflection on the y-axis, CFP emission was divided by Venus emission and normalised to initial baseline. In contrast, PKA phosphorylation of the AKAR4 sensor results in conformational change which brings the Cerulean-Venus FRET pair closer together and thus causing an increase FRET. As a result, to display increasing PKA activity as a function of upward deflection on the y-axis, Venus emission was divided by Cerulean emission and normalised to the initial baseline.

PKA-based cAMP FRET sensor RII-L20-CFP + CAT-YFP is of bi-molecular design. Bi-molecular sensors utilise the same principal mechanism of FRET between donor and acceptor fluorochromes, however they comprise of two separate peptides: one peptide has the donor attached, while the other has the acceptor. This arrangement can lead to significant problems if the amount of expression and localisation of both constructs varies significantly between individual cells, and thus there is uneven ratio of donor to acceptor fluorochromes. If the ratio of donor to acceptor was to vary between different compartments of the cell, this could lead to misinterpretation of the results and wrong conclusion that there are differences in FRET in these compartments. This could be detrimental to particular investigations, such as studies which try to measure intracellular gradients of cAMP production within individual cells. To avoid such problems associated

with bi-molecular sensors, additional excitation of the acceptor fluorochrome can be performed. Then, calculations can be used to find the absolute intracellular FRET within the different compartments of the cell, which allows correcting for any differences in FRET induced by an uneven ratio of donor to acceptor fluorochromes. However, in our study, for all the FRET sensors used, the FRET signal was collected from the entire single transfected cells (during analysis the region of interest was drawn around the periphery of the entire cell which was not overlapping with adjacent cells). There were several reasons for this; primarily I were interested in global cAMP signals rather than localised signalling within different compartments of the cell. Secondly, this avoided some of the problems associated with bi-molecular sensors discussed above. The design of the PKA-based cAMP FRET sensor RII-L20-CFP + CAT-YFP is such that elevation of cAMP causes separation of the FRET pair. As a result, to display increasing cAMP as a function of upward deflection on the y-axis, CFP emission was divided by YFP emission and normalised to the initial baseline.

2.4.1. Image processing and data analysis

Adjustments made to images were always performed using linear algorithms in Leica Application Suit AF Lite (Leica Microsystems) or PowerPoint 2007 (Microsoft). Image cropping was performed in PowerPoint 2007. Quantification of time series was performed in Leica Application Suit AF Lite software. Regions of interest were drawn around whole cells and intensity values were exported into Excel 2007 (Microsoft). Following calculations, if any, excel spread sheets were imported into OriginPro 8.5 (OriginLab Corporation, Northampton, MA, USA) in order to plot the graphs required. Results were presented as mean values +/- standard error of the mean.

2.5. Ruffling analysis

A macro developed by (Deming *et al.*, 2008) was used in ImajeJ software (Schneider *et al.*, 2012) to process transmitted light series of images to minimise background intensity fluctuation induced by the perfusion system. Briefly, for each image of a time-lapse stack, the macro produces two Gaussian blurred images at a radius of 1.23 and 0.80. The 1.6:1 ratio of the two values was chosen by the authors to keep the closest approximation of the Difference of Gaussian function to the true Laplacian of Gaussian function. While the absolute values were determined to maximize the discrimination between ruffle and non-ruffle features. Images with the smaller blur radius are subtracted from those with the larger radius. and the resulting difference images are thresholded based on the average image intensity of the whole stack.

Processed image series were used to produce kymographs from selected lines of interest, using a plug-in 'Multiple Kymograph' developed by Jens Rietdorf and Arne Seitz (see: http://fiji.sc/wiki/index.php/Multi_Kymograph).

2.6. Chemicals and other reagents

Forskolin, 8Br-cAMP, H89, and myristoylated PKI (Myr-PKI) were all purchased from (Tocris Biosciences, UK). IBMX was obtained from (Sigma Aldrich, UK). 8-pCPT-2'-O-Me-cAMP and N6-benzoyl-cAMP were acquired from (BioLog, Germany). St-Ht31 active peptide and st-Ht31P control peptide were obtained from (Promega, Madison, WI, USA). All other chemical reagents were purchased from Sigma-Aldrich, UK. All reagents were dissolved in water or dimethyl sulfoxide (DMSO). Experiments which utilised drugs which were dissolved in DMSO, had a corresponding concentration of DMSO placed into the control solution(s). Forskolin stock was made in DMSO to 20mM, while IBMX was made in DMSO to 500mM; thus solution containing 20µM forskolin + 1mM IBMX was 0.3% DMSO.

Accordingly the control solution was supplemented with DMSO to 0.3%. I found that 0.3% DMSO did not influence the cellular ability to migrate relative to the control solution which did not contain any DMSO.

2.7. Migration and Invasion assays

Random cell migration was assessed using 24-well sized Boyden chambers (BD Biosciences, UK) with polyethylene terephthalate (PET) membrane containing 8µm pore size, and were used as specified by the manufacturer. Briefly, 750µl of DMEM culture media + 1%FBS was placed into the bottom well of a 24-well plate and 500µl DMEM + 1% FBS into the top well of Boyden chamber. The 24-well plate was allowed to equilibrate in the incubator set to 37^{o}C and 5% CO_2. Cells were trypsinized for a minimal duration required (typically 2 minutes), then resuspended in DMEM + 1% FBS and seeded in a volume of approximately 500µl into the top well. Migration was allowed to take place in the incubator for the duration of 6 hours. Between 30,000 and 100,000 cells were seeded into the top well of Boyden chambers, depending on cell type and experiment performed. To test random cell invasion, matrigel covered Boyden chambers (BD Biosciences, UK) were used according to manufacturer specification, and the same protocol was used as the above test for random migration. Directional chemotactic cell migration and invasion were assessed by setting up a gradient of FBS across the top and bottom wells. Bottom well was filled with 750µl of DMEM + 10% FBS, while top well with 500µl DMEM + 0% FBS. Trypsinized cells were resuspended in DMEM + 0% FBS in order to preserve the 0-10% FBS gradient during cell seeding into the top well.

Following 6h of incubation in a Boyden chamber, the cells were fixed using 100% methanol for 10 minutes at room temperature (this method of fixation provided sufficient quality for staining and imaging that was required, and is described in the following text). Non-migrated cells were scraped away from top well using forceps with soft tissue paper on the ends. Boyden chambers were then placed into solution containing 10ug/ml RNAaseA for 30 minutes, which was followed by 100ug/ml propidium iodide staining for 10 minutes at room temperature. Any remaining non migrating cells were removed from the top of Boyden chambers for the second time as described above and placed into 24-well plate containing 1ml phosphate buffered saline (PBS) solution per well. In-between each of the steps above two quick PBS washes with PBS was given.

Stained cells were imaged using Leica TCS SP2 inverted LSCM microscope using dry 10x objective. To visualise propidium iodide staining, 514nm laser excitation was used in combination with 570-690nm emission collection. CellProfiler software (Carpenter *et al.*, 2006) was used to automatically identify and quantify individually stained cells, (this eliminated human bias when counting migrated cells in different conditions). Unpaired two-tailed t-test was used to calculate the statistical significance to $p < 0.05$. Statistically significant results were indicated by the * symbol situated above the error bars.

2.8. Scratch assay

Cells were grown in 35mm culture dishes and were allowed to reach 100% confluency. Horizontal and vertical lines were drawn with a marker on the underside of each dish to use as landmark reference points. Using a 200µl pipette tip, which was held by hand, a scratch was made on the cell surface by the application of uniform pressure. Dishes were carefully

washed with PBS to remove any of the non-adherent cells, and 2ml of fresh DMEM + 1% FBS was added. Images were taken at 0 hours soon after the scratch procedure. Further images at the corresponding landmarks were taken 6 and 18 hours following induction of the scratch.

CHAPTER 3 –cAMP ELEVATION INHIBITS PANCREATIC DUCTAL ADENOCARCINOMA MIGRATION

3.1. Elevation of intracellular cAMP inhibits migration of pancreatic cancer cells.

The effect of cAMP signalling on migration was investigated using classical modulators of the pathway such as forskolin and IBMX: both agents cause elevation of intracellular cAMP via activation of adenylyl cyclase and inhibition of phosphodiesterase activity respectively. Migration of PANC-1 cells was measured using Boyden chambers containing DMEM supplemented with 1% FBS in both top and bottom wells. With no gradient of FBS across the chambers, cell migration was non-directional. Cells were treated with control vehicle or cAMP elevating agents for 6 hours, cells which migrated to the bottom of the chambers were quantified. All treatments were normalised relative to the control condition and expressed as a percentage. Treatment of cells with forskolin (20μM) resulted in decreased level of migration to 43%, while IBMX (1mM) inhibited migration to 38%. Combination of forskolin (20μM) + IBMX (1mM) strongly inhibited migration to 4.7% (Figure 3.1); this supported the idea that cAMP that was responsible for the inhibitory effects.

Wound healing assays were used to confirm the Boyden Chamber results. PANC-1 cells were grown to confluency and scratches were induced by a 200μl pipette tip. In these experiments it was necessary to extend migration time to 18 hours to clearly observe migration in the control condition. Relative to the 0 hour time point, some control cells were seen migrating into the scratch as early as 6 hours, and quite clearly by 18 hours. In contrast, majority of forskolin (20μM) + IBMX (1mM) treated cells were not seen to migrate into the scratch at neither 6 nor 18 hours post scratch induction (Figure 3.2).

I wanted to confirm that inhibition of cell migration was not as a result of cell injury induced by cAMP elevation with forskolin (20μM) + IBMX (1mM). Thus I performed cell death assays utilising propidium iodide, which is taken up from the extracellular solution by dead cells as a

result of a loss of plasma membrane integrity. Upon binding to DNA, propidium iodide undergoes an increase in fluorescence. Cells which were labelled with propidium iodide were considered dead. PANC-1 cells were treated with control vehicle or with forskolin (20µM) + IBMX (1mM) for 6 hours and were subsequently exposed to DMEM supplemented with propidium iodide (10µg/ml) for 10 minutes. Stained cell were quantified in each condition, and it was found that there was no significant difference between the numbers of cells stained with propidium (n=3, data not shown). Further experiments were performed for a duration of 24 hours, which also displayed no difference in cell death between the control and forskolin (20µM) + IBMX (1mM) conditions (n=3, data not shown).

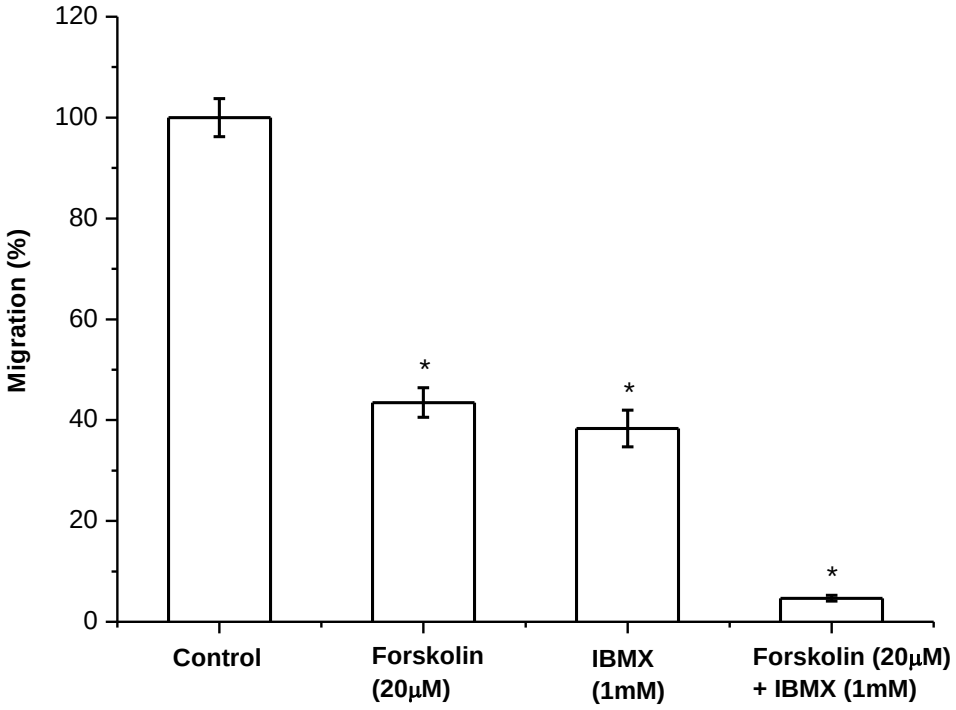

Figure 3.1. cAMP elevating agents reduce migration of PANC-1 cells. Cell migration was investigated using Boyden chambers supplemented with DMEM + 1% FBS in both top and bottom wells. Cells were allowed to migrate from top to bottom wells for 6h post seeding. Results were normalized relative to control and displayed as a percentage. Both adenylyl cyclase activator forskolin (20μM) and non-specific phosphodiesterase inhibitor IBMX (1mM) reduced migration (to 43% and 38% respectively). Combination of forskolin + IBMX resulted in strong inhibition of migration to 4.7% (n=18 Boyden chambers for each condition. At least 3 independent experiments were performed. All results were statistically significant to $p<0.05$ and indicated by * symbol).

Figure 3.2. Scratch assay revealed that cAMP elevation strongly inhibited migration. PANC-1 cell were grown to confluency, after which a scratch was induced with a 200µl pipette tip; cells were imaged at 0, 6, and 18 hours after the scratch. Control cells were clearly able to migrate into the scratch by 18 hour time point. In contrast, forskolin (20µM) + IBMX (1mM) treated cells were not seen to migrate into the induced scratch (n=12 scratches for each condition. Scale bar corresponds to 200µm).

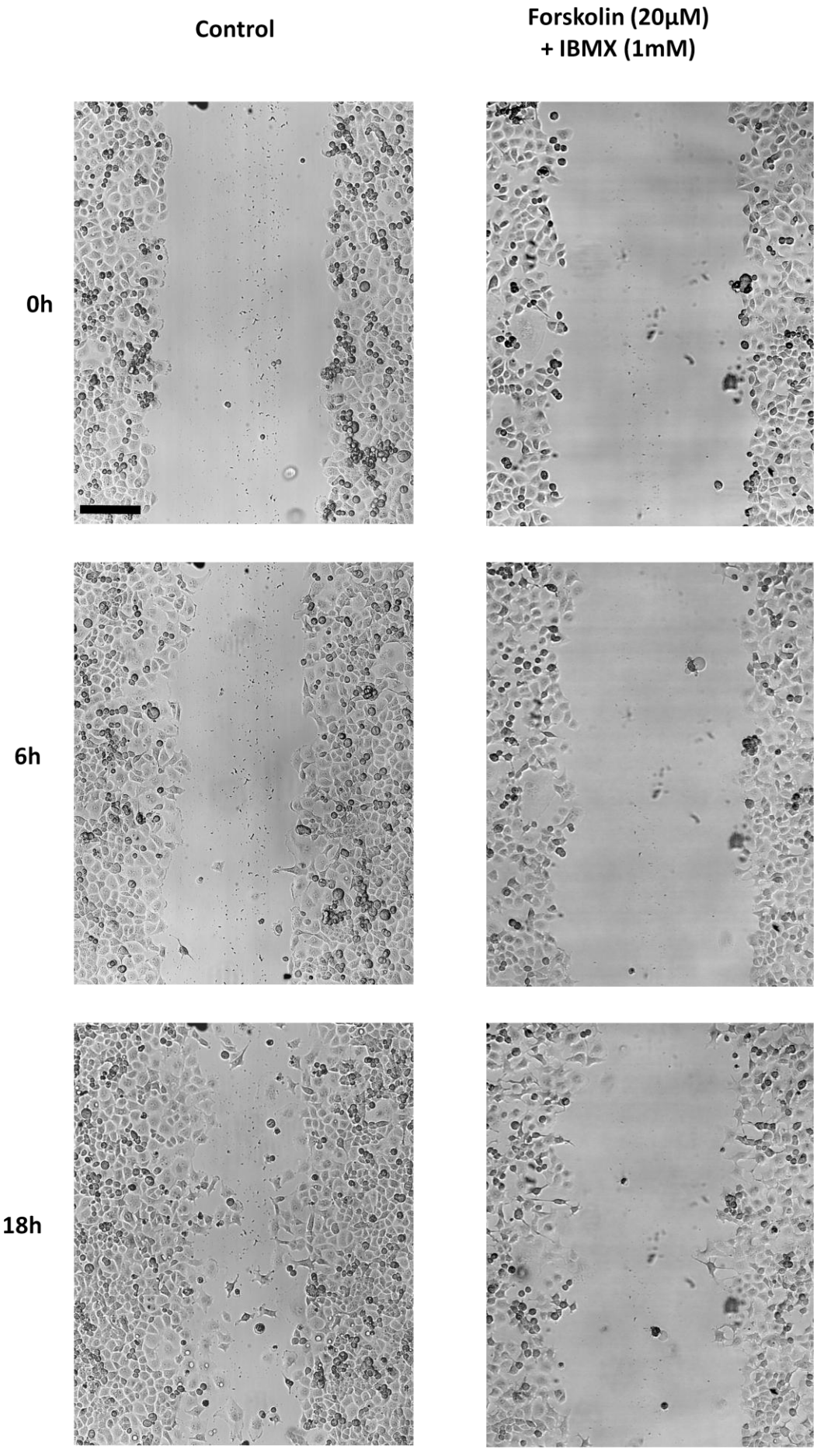
Control
Forskolin (20µM)
+ IBMX (1mM)
0h
6h
18h

To investigate the effects of forskolin and IBMX on intracellular cAMP changes, PANC-1 cells were transfected with EPAC-based cAMP Förster electron resonance energy transfer (FRET) sensor H84; this was developed by Kees, J. and others (van der Krogt *et al.*, 2008) and has proven to be a very robust and reliable tool for measuring intracellular cAMP changes in single cells. The sensor comprised of N-terminal CFP donor fluorochrome, EPAC backbone, and C-terminal Venus acceptor fluorochrome. The positioning of both fluorochromes is very close to each other, and is in such a way that allows FRET to occur.

PANC-1 cells were transfected with EPAC-based cAMP FRET sensor H84 and were imaged 24 hours later. After obtaining a stable baseline of the FRET sensor, forskolin (20µM) was applied and resulted in a modest elevation of cAMP. Addition of forskolin 20µM) + IBMX (1mM) further increased cAMP levels, and resulted in the FRET sensor saturation (Figure 3.3). Relative to the fully saturated FRET signal, application of forskolin (20µM) alone resulted in approximately 32% FRET shift. The order of drug application was reversed to visualise the effects of IBMX (1mM) alone, followed by addition of IBMX (1mM) + forskolin (20µM). It was found that IBMX resulted in similar cAMP increases as with forskolin, resulting in approximately 26% FRET shift (Figure 3.4). These data indicated that application of either drug alone resulted in modest elevation of cAMP, which correlated with their ability to moderately suppress migration. Combination of both drugs resulted in additive large cAMP elevation, which correlated with their ability to strongly suppress migration.

It should be noted that I utilised relatively higher concentration of IBMX then reported in most other studies; typically around 100µM IBMX is used to maximally inhibit phosphodiesterase activity. I have found however, that this is not the case in PANC-1 cells (as shown in Figure 3.5); higher extracellular concentration of the drug was required to

achieve stronger inhibition of phosphodiesterase activity. In these experiments PANC-1 cells expressing H84 sensor were subject to 100µM IBMX, which resulted in very marginal FRET shift. Subsequent application of 1mM IBMX resulted in a substantially larger FRET shift, indicating that further phosphodiesterase inhibition occurred resulting in higher intracellular cAMP rise. Application of 4mM IBMX resulted in only a slightly higher FRET shift (in comparison with 1mM), indicating 1mM IBMX was sufficient to strongly inhibit most of the phosphodiesterase activity (Figure 3.5).

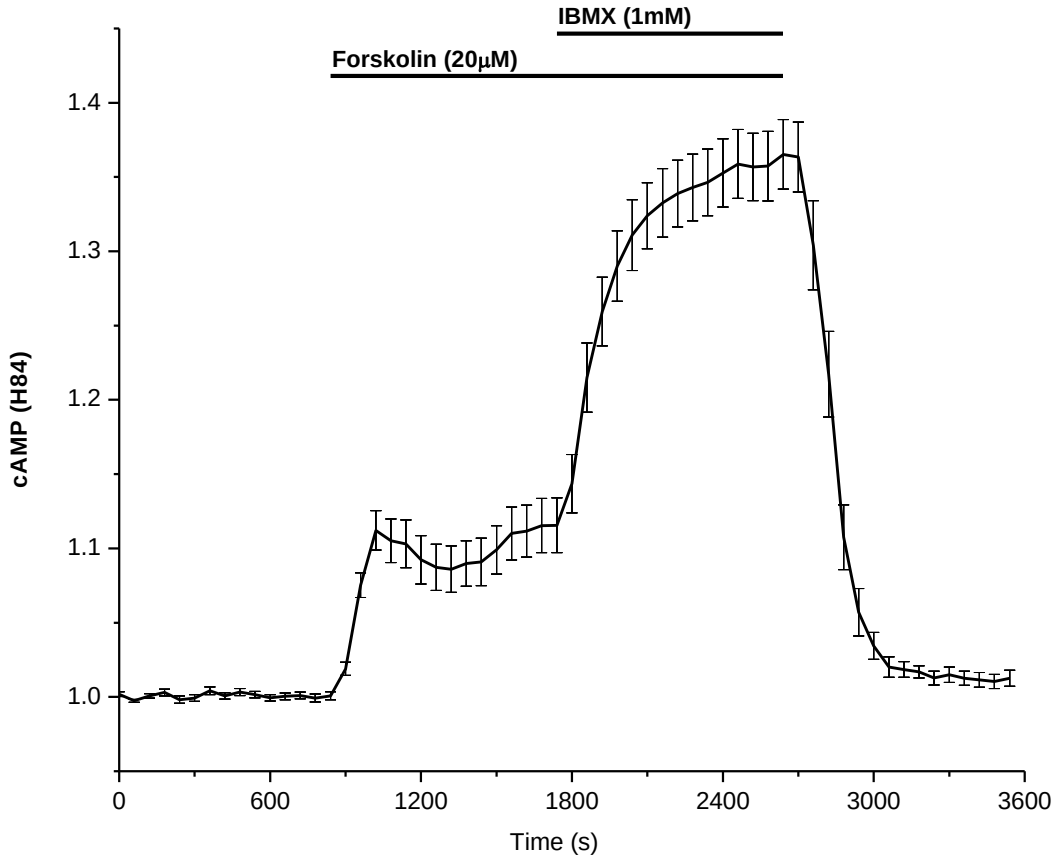

Figure 3.3. The effect of forskolin and combination of forskolin + IBMX on the cAMP level in PANC-1 cells. PANC-1 cells were transfected with EPAC-based FRET sensor H84. Forskolin (20μM) induced a modest rise of cAMP; approximate FRET shift was calculated to be 32% of that achievable for the maximal FRET shift. Combination of forskolin (20μM) + IBMX (1mM) caused a much larger response of H84m and saturated the sensor (n=34 cells. At least 3 independent experiments were performed.)

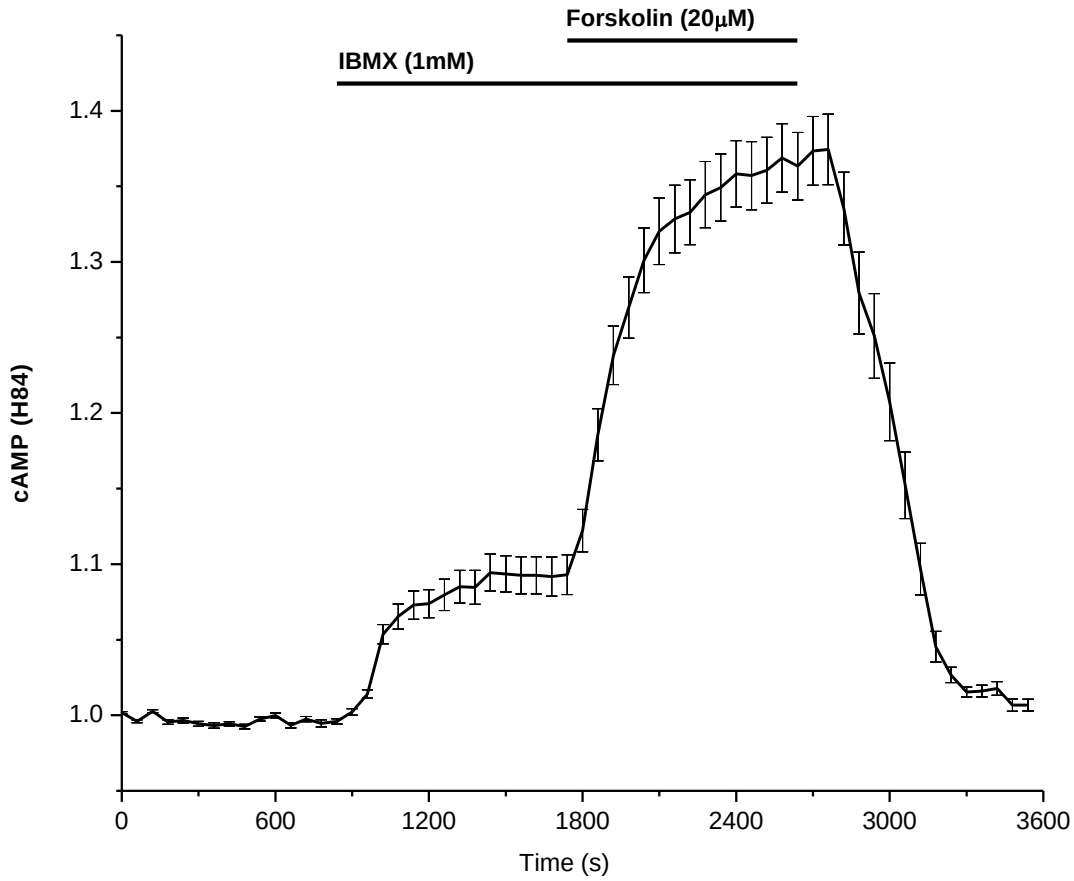

Figure 3.4. The effect of IBMX and combination of forskolin/IBMX on cAMP level in PANC-1 cells. PANC-1 cells were transfected with EPAC-based FRET sensor H84. IBMX (1mM) induced a modest rise of cAMP; approximate FRET shift was calculated to be 26% of that achievable for the maximal FRET shift. Combination of forskolin (20μM) + IBMX (1mM) caused a much larger response of H84, and saturated the sensor (n=54 cells. At least 3 independent experiments were performed.)

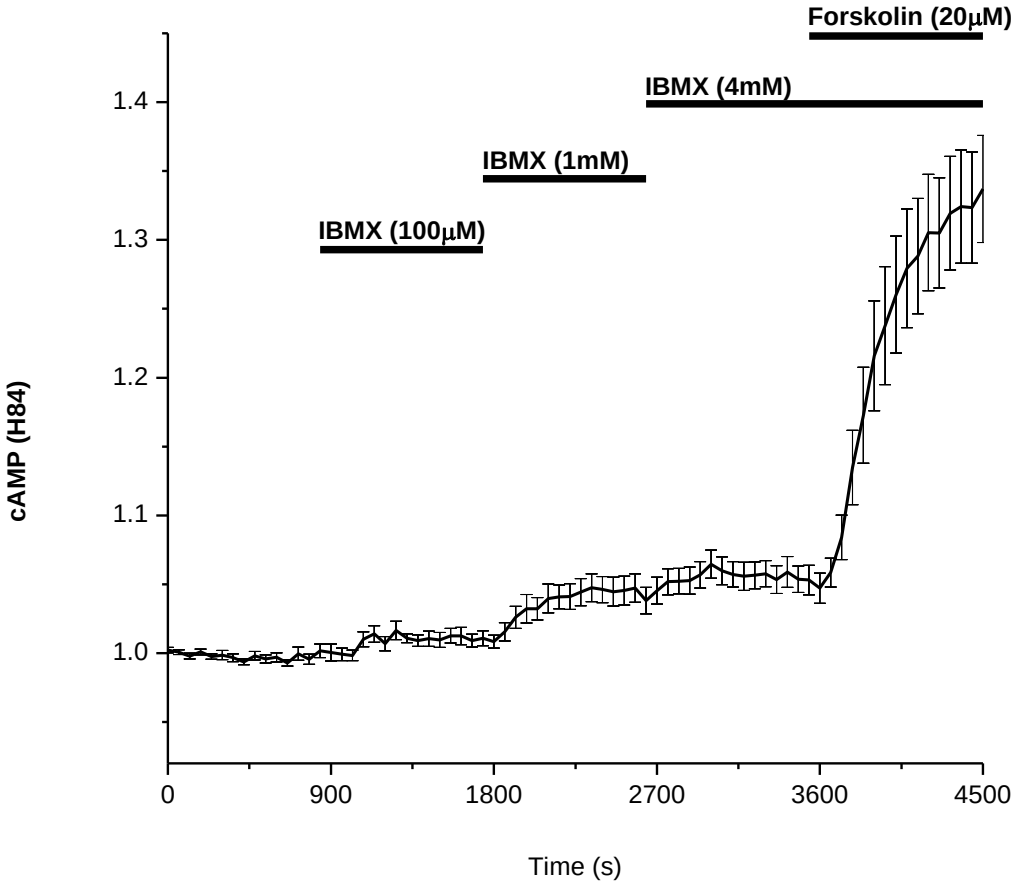

Figure 3.5. Relatively high extracellular concentration of IBMX is required to achieve strong inhibition of PANC-1 phosphodiesterase activity. PANC-1 cells were transfected with EPAC-based FRET sensor H84. IBMX (100μM) induced a very marginal FRET shift. Application of 1mM IBMX caused a larger FRET shift, indicating that substantial rise of intracellular cAMP had occurred as a result of higher phosphodiesterase inhibition. Further application of 4mM IBMX resulted in only a slight further elevation of the FRET signal. Application of forskolin (20μM) + IBMX (4mM) caused a much larger increase of cAMP (n=8 cells. At least 3 independent experiments were performed.)

I wanted to confirm the results obtained with the EPAC-based sensor H84 by using other FRET sensors, which were either based on a PKA backbone or were a direct substrate for endogenous PKA. Firstly, I used PKA-based FRET sensor (RII-L20-CFP + CAT-YFP) developed by Zaccolo, Tsien, Posan and others (Zaccolo *et al.*, 2000). This was a bi-molecular sensor which utilised PKA regulatory subunit fused to CFP, and catalytic subunit fused with YFP. RII-L20-CFP + CAT-YFP FRET sensor was transfected into PANC-1 cells and imaged in a similar manor as with the EPAC-based FRET sensor H84. cAMP elevation results in RII-L20-CFP + CAT-YFP FRET sensor activation, leading to catalytic-YFP subunit dissociation from the regulatory-CFP subunits; resulting in a decline of FRET. Therefore, a ratio of CFP relative to YFP emission was plotted and normalised to the initial baseline. Upward deflection of the graph would indicate increased intracellular cAMP concentrations. Forskolin (20µM) was applied and resulted in approximately 33% FRET shift. Application of IBMX (1mM) together with forskolin resulted in greater activation of PKA, and caused full saturation of the FRET sensor (Figure 3.6).

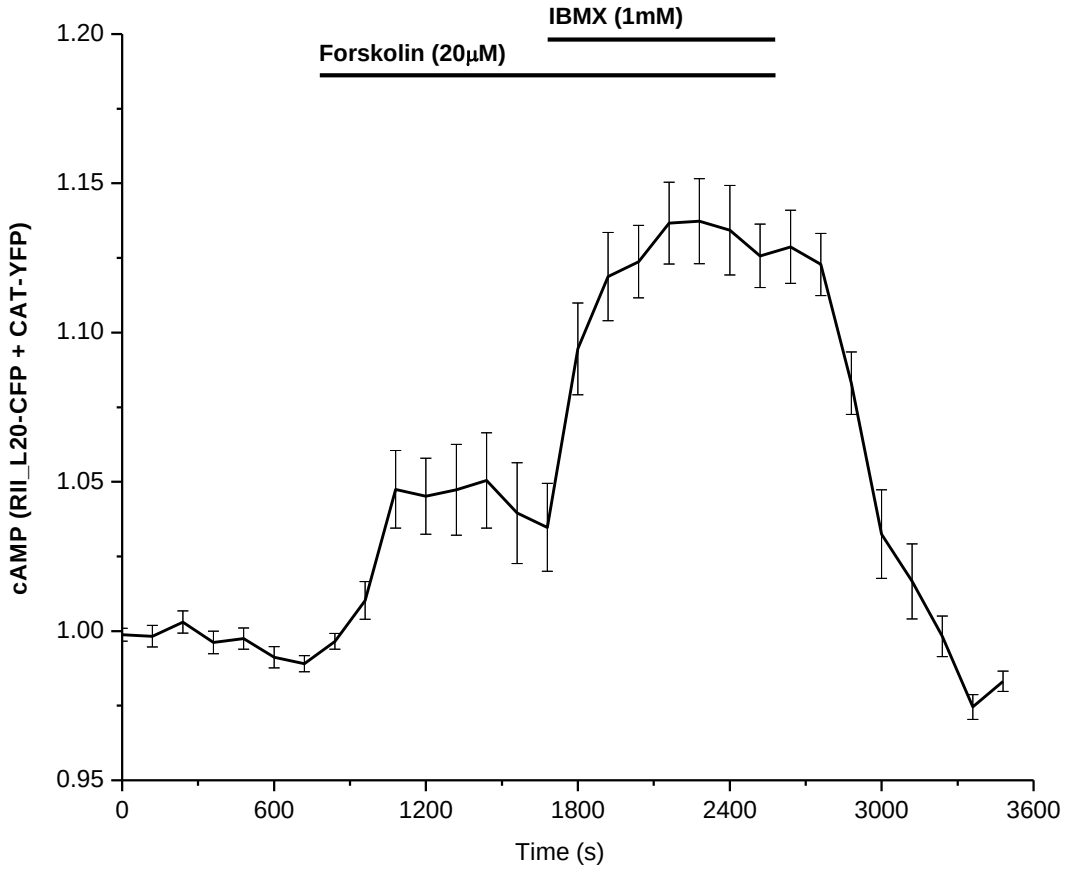

Figure 3.6. PKA-based FRET sensor revealed similar intracellular cAMP changes as seen with EPAC FRET sensor. PANC-1 cells were transfected with PKA-based cAMP FRET sensor RII-L20-CFP + CAT-YFP. Forskolin (20μM) induced a modest rise of cAMP, as seen by the approximate 33% FRET shift. Combination of forskolin (20μM) + IBMX (1mM) resulted a larger increase of cAMP which saturated the sensor (n=19 cells. At least 3 independent experiments were performed.)

I also utilised a FRET sensor which is able to measure endogenous PKA activity (AKAR4), which was developed by Zhang and others (Depry *et al.*, 2011). Unlike the previous sensors mentioned which rely on endogenous cAMP to induce FRET changes, AKAR4 sensor utilises a backbone which is selectively phosphorylated by endogenous PKA; which results in conformational change leading to increased FRET between Cerulean and Venus based fluorochromes. Intracellular phosphatase activity on the other hand dephosphorylates the construct. Thus, the level of AKAR4 FRET is controlled by equilibrium between PKA phosphorylation and phosphatase dephosphorylation events. For this reason it is also worth noting that unlike with the previous two sensors mentioned, AKAR4 full FRET saturation does not correspond to maximum PKA activity. However, the sensor is able to visualise small elevations of PKA activity owing to its great sensitivity profile, and so is extensively used in the field in studies which investigate small gradients and localised intracellular PKA activity. Graphs were plotted with Venus emission relative to Cerulean emission; increase in PKA activity corresponds to elevation of the graph. PANC-1 cell were transfected with AKAR4 construct 24 hours prior to the beginning of the experiments, and where imaged as with the previous FRET sensors used. Application of forskolin (20μM) resulted in a large FRET shift. Application of IBMX (1mM) on top did not induce any further FRET shift, indicating the sensor was fully saturated.

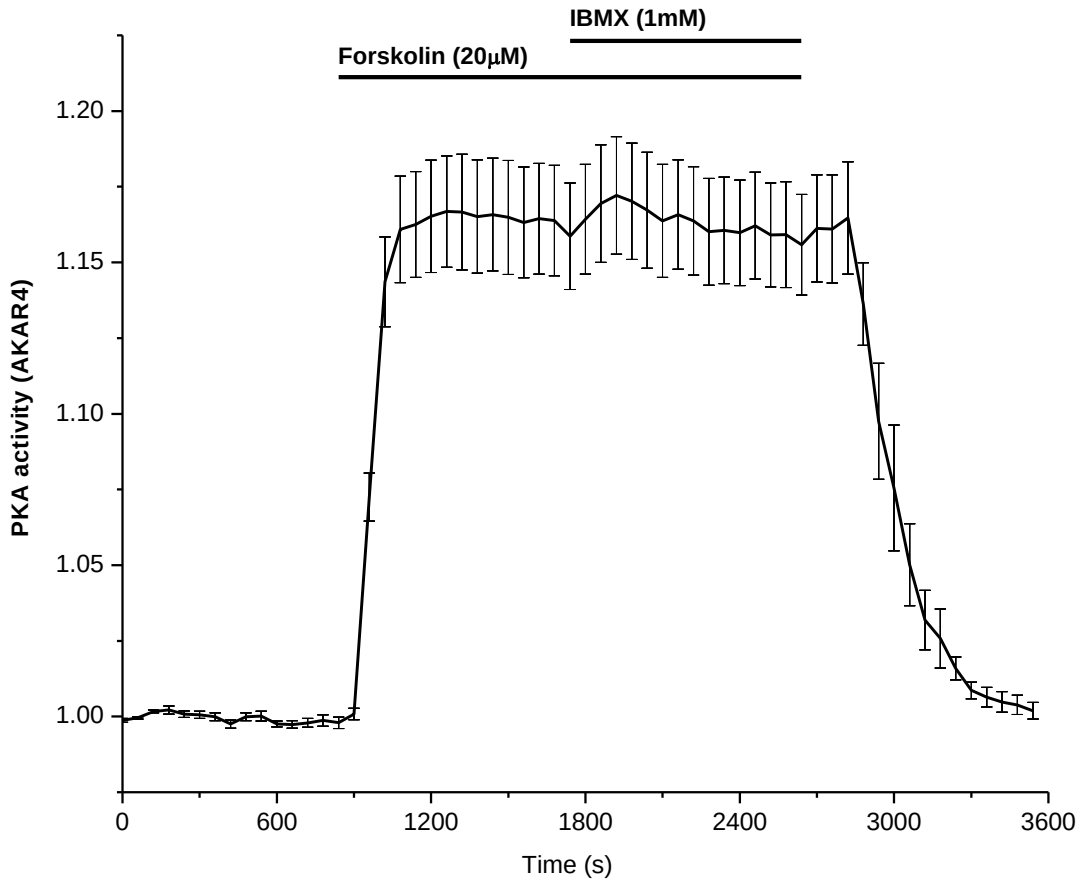

Figure 3.7. PANC-1 cells were transfected with AKAR4 which revealed endogenous activation of PKA following cAMP elevation. PANC-1 cells were transfected with AKAR4 PKA FRET sensor. Forskolin (20μM) was applied and resulted in large FRET shift. Application of forskolin (20μM) + IBMX (1mM) was not able to increase the FRET shift any further, indicating the FRET sensor was already fully saturated (n=10 cells. At least 3 independent experiments were performed.)

3.1.1. Analogue of cAMP inhibits PANC-1 migration.

So far I have seen correlation between endogenous cAMP elevation and inhibition of migration. All of these results were obtained using drugs which manipulate endogenous machinery to raise cAMP levels. However, it is possible that both forskolin and IBMX could have off-target effects, and as a result the inhibition of migration was not specifically due to the cAMP changes. To control for this, I utilised 8Br-cAMP, a non-selective analogue of cAMP. I utilised the same protocols for investigating migration and FRET sensor recording as mentioned previously. I decided to find the concentration of 8Br-cAMP required to induce similar FRET changes as observed with forskolin (20µM) or IBMX (1mM). PANC-1 cells were transfected with EPAC-based FRET sensor H84 to monitor intracellular cAMP concentrations. To our surprise, I found that relatively high extracellular concentration of 8Br-cAMP had to be applied in order to achieve comparable cAMP elevation as induced with either forskolin (20µM) or IBMX (1mM) alone. Application of 2mM 8Br-cAMP resulted in very modest FRET shift which was substantially below that which was caused by either forskolin or IBMX. A higher dose of 8Br-cAMP (6mM) was applied and resulted in further FRET shift which was comparable to the action of either forskolin or IBMX (Figure 3.8). It was found that 2mM 8Br-cAMP induced 12% FRET shift, while 6mM 8Br-cAMP produced 27% shift. As seen from previous results, relative changes induced by forskolin (20µM) were approximately 32%, while for IBMX (1mM) were 26%.

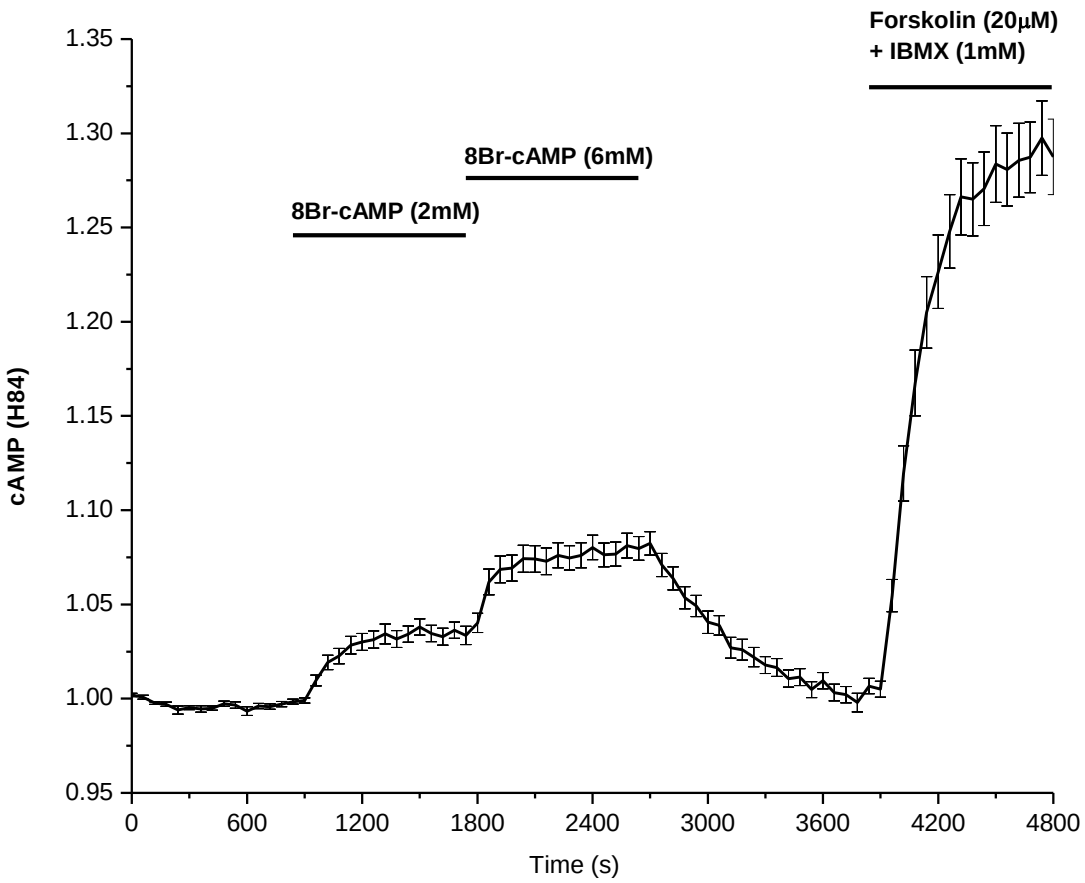

Figure 3.8. Intracellular cAMP levels measured in PANC-1 cells displayed submaximal effect of 2mM and 6mM 8Br-cAMP. PANC-1 cells were transfected with EPAC-based FRET sensor H84. 8Br-cAMP was applied at 2mM followed by a higher concentration of 6mM. After the drugs were washed off, forskolin (20μM) + IBMX (1mM) was applied. Only modest intracellular rise of 8Br-cAMP was achieved with 2mM 8Br-cAMP, which induced only a 12% FRET shift. Higher concentration of 8Br-cAMP (6mM) produced 27% FRET shift (n=37 cells. At least 3 independent experiments were performed.)

I decided to use the two remaining sensors, AKAR4 and PKA-based FRET sensor RII-L20-CFP + CAT-YFP, to confirm 8Br-cAMP was non-selective cAMP analogue, which is able to also activate PKA. Firstly, I utilised AKAR4 to visualise endogenous activation of PKA. Following a stable baseline, sequential doses of 2mM and 6mM 8Br-cAMP were applied. This was followed by a wash period of 20 minutes and a positive control using forskolin (20μM) + IBMX (1mM) to induce maximal FRET shift. 2mM 8Br-cAMP was found to induce approximately 37% FRET shift, while 6mM induced 60% shift (Figure 3.9).

Finally, I used PKA-based FRET sensor RII-L20-CFP + CAT-YFP to confirm the actions of 8Br-cAMP on PKA activity. Sequential doses of 2mM and 6mM 8Br-cAMP were applied, which was followed by a wash period of 20 minutes and a positive control using forskolin (20μM) + IBMX (1mM) to induce maximal FRET shift. 2mM 8Br-cAMP was found to induce approximately 8% FRET shift, while 6mM induced 36% shift (Figure 3.10). Earlier experiments displayed that forskolin (20μM) induced approximately 33% FRET shift with this sensor; indicating 6mM 8Br-cAMP is comparable to 20μM forskolin.

After finding the concentration of the 8Br-cAMP required to induce comparable activation of EPAC and PKA as with either forskolin (20μM) or IBMX (1mM), I were ready to use Boyden chamber assays to investigate the effect of the drug on cell migration. 8Br-cAMP was used at 2mM and 6mM, and was found to inhibit migration to 78% and 24% of the control respectively (Figure 3.11). The higher dose of 8Br-cAMP inhibited migration to a level that was comparable to either forskolin (20μM) or IBMX (1mM) alone. Thus, after considering all the experiments performed so far, it strongly appears that cAMP elevation was responsible for the inhibition of PANC-1 migration.

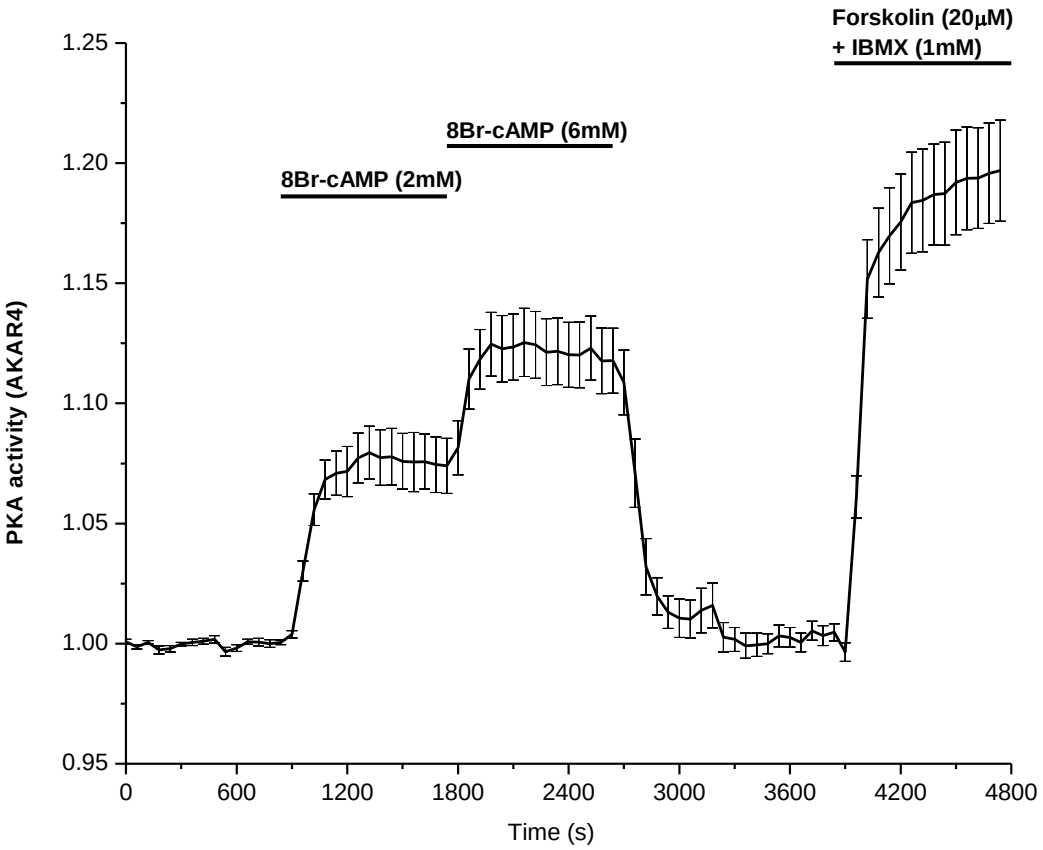

Figure 3.9. Endogenous activation of PKA by 8Br-cAMP was measured in PANC-1 cells using AKAR4 sensor. PANC-1 cells were transfected with AKAR4 PKA FRET sensor. 8Br-cAMP was applied at 2mM followed by 6mM concentration. Control forskolin (20μM) + IBMX (1mM) was applied following a wash period. 2mM 8Br-cAMP was found to induce approximately 37% FRET shift, while 6mM induced 60% shift (n=13 cells. At least 3 independent experiments were performed.)

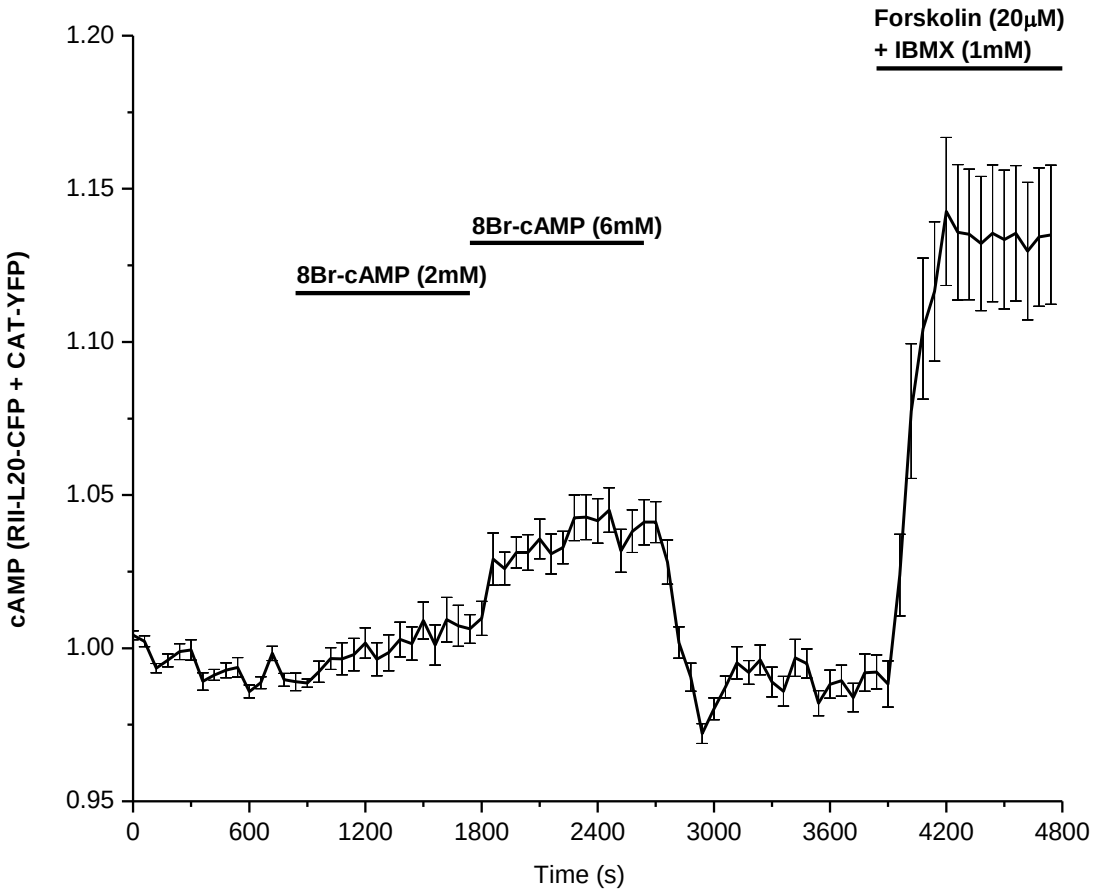

Figure 3.10. Intracellular cAMP levels measured in PANC-1 cells displayed submaximal effect of 2mM and 6mM 8Br-cAMP. PANC-1 cells were transfected with PKA-based FRET sensor RII-L20-CFP + CAT-YFP. 8Br-cAMP was applied at 2mM followed by 6mM. Control forskolin (20μM) + IBMX (1mM) was applied following a wash period. Results indicate only a modest rise of intracellular 8Br-cAMP was achieved following 6mM of extracellular 8Br-cAMP application. 2mM 8Br-cAMP was found to induce approximately 8% FRET shift, while 6mM induced 36% shift (n=8 cells. At least 3 independent experiments were performed.)

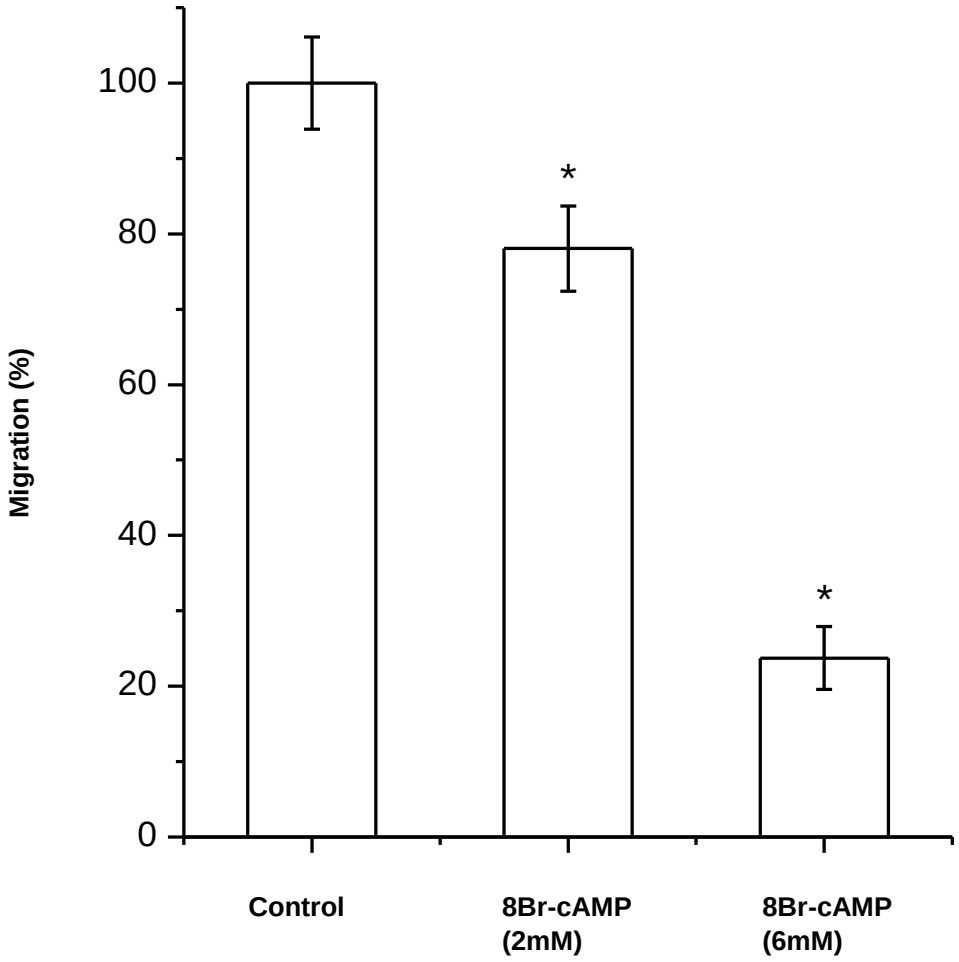

Figure 3.11. cAMP analogue 8Br-cAMP reduced PANC-1 cell migration. Cell migration was investigated using Boyden chambers supplemented with DMEM + 1% FBS in both top and bottom wells. Cells were allowed to migrate from top to bottom chamber for 6h post seeding. 8Br-cAMP, a non-selective cAMP analogue, was used at 2mM and 6mM concentration and resulted in 78% and 24% inhibition of migration respectively (n= 9 Boyden chambers for each condition. At least 3 independent experiments were performed. All results were statistically significant to $p<0.05$ and indicated by * symbol).

3.2. cAMP elevation inhibits migration in a diverse range of PDAC cell lines.

To ensure the effects of cAMP are not specific to the PANC-1 cell line, I tested the effect cAMP on four other diverse pancreatic adenocarcinoma cell lines; Suit-2, BxPC3, Capan-2, and MiaPaca-2. Boyden chamber migration assays were setup as previously described. Cell migration was significantly inhibited in Suit-2 (Figure 3.12), BxPC3 (Figure 3.13), Capan-2 (Figure 3.14), and MiaPaca-2 (Figure 3.15) cells by forskolin (20µM) + IBMX (1mM) to a level of 5.4%, 44%, 47%, and 42% of the control condition respectively. It became quite clear that migration in all cell lines tested was inhibited in response to cAMP, however the responses varied with some cell lines displaying stronger inhibition than others.

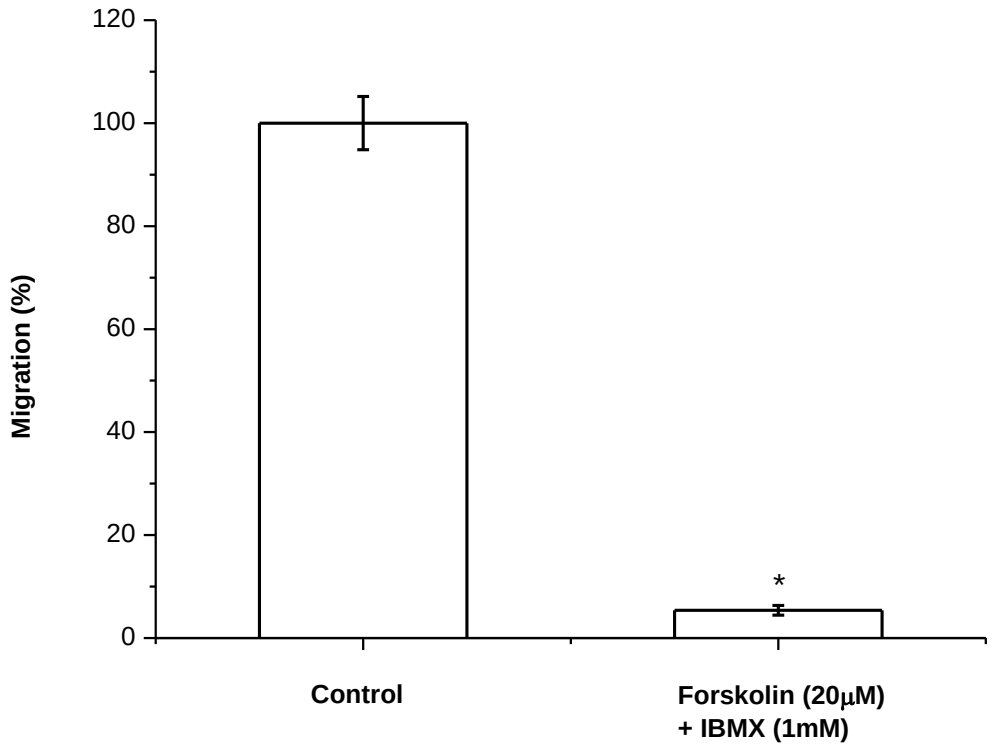

Figure 3.12. cAMP elevating agents reduced migration of SUIT-2 cells. Cell migration was investigated using Boyden chambers supplemented with DMEM + 1% FBS in both top and bottom wells. SUIT-2 cells were allowed to migrate from top to bottom chamber for 6h post seeding. Combination of Forskolin (20μM) + IBMX (1mM) reduced migration to 5.4% of the control (n=6 Boyden chambers for each condition. At least 3 independent experiments were performed. All results were statistically significant to $p<0.05$ and indicated by * symbol)

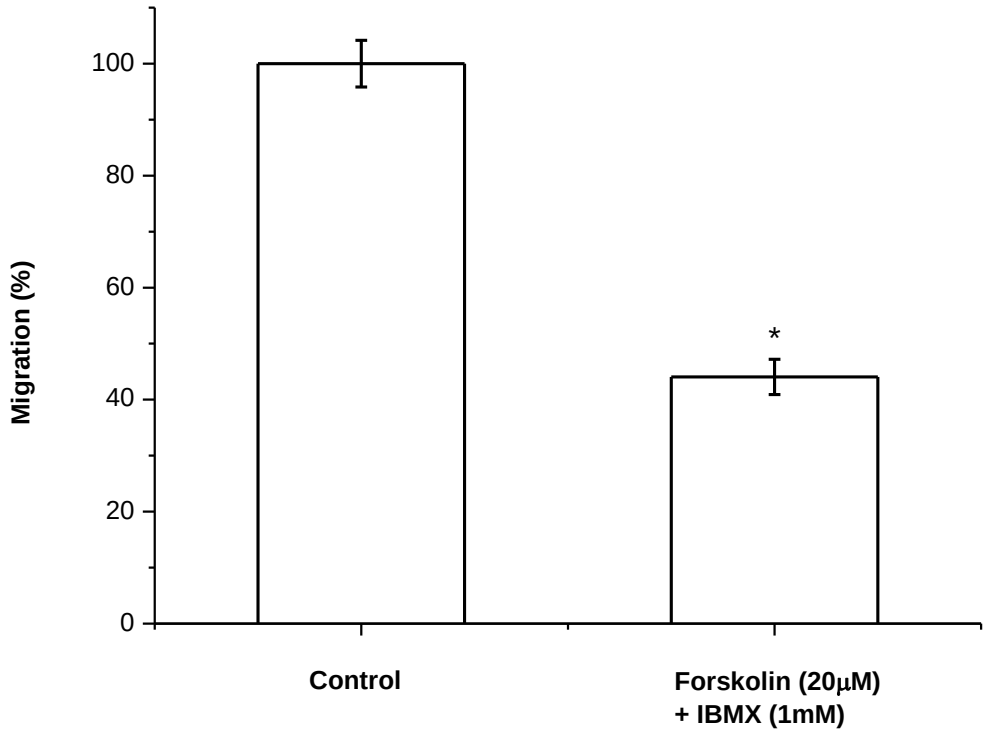

Figure 3.13. cAMP elevating agents reduced migration of BxPC3 cells. Cell migration was investigated using Boyden chambers supplemented with DMEM + 1% FBS in both top and bottom wells. BxPC3 cells were allowed to migrate from top to bottom chamber for 6h post seeding. Combination of Forskolin (20μM) + IBMX (1mM) reduced migration to 44% of the control (n=9 Boyden chambers for each condition. At least 3 independent experiments were performed. All results were statistically significant to $p<0.05$ and indicated by * symbol).

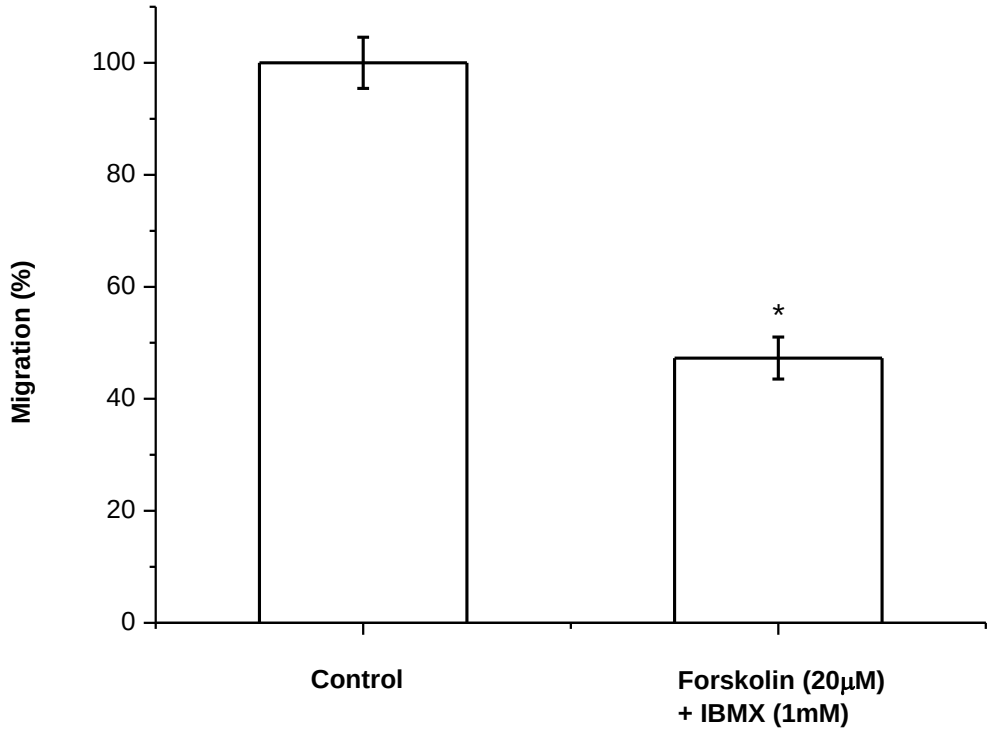

Figure 3.14. cAMP elevating agents reduced migration of CAPAN-2 cells. Cell migration was investigated using Boyden chambers supplemented with DMEM + 1% FBS in both top and bottom wells. CAPAN-2 cells were allowed to migrate from top to bottom chamber for 6h post seeding. Combination of Forskolin (20μM) + IBMX (1mM) reduced migration to 47% of the control, (n=12 Boyden chambers for each condition. At least 3 independent experiments were performed. All results were statistically significant to $p<0.05$ and indicated by * symbol)

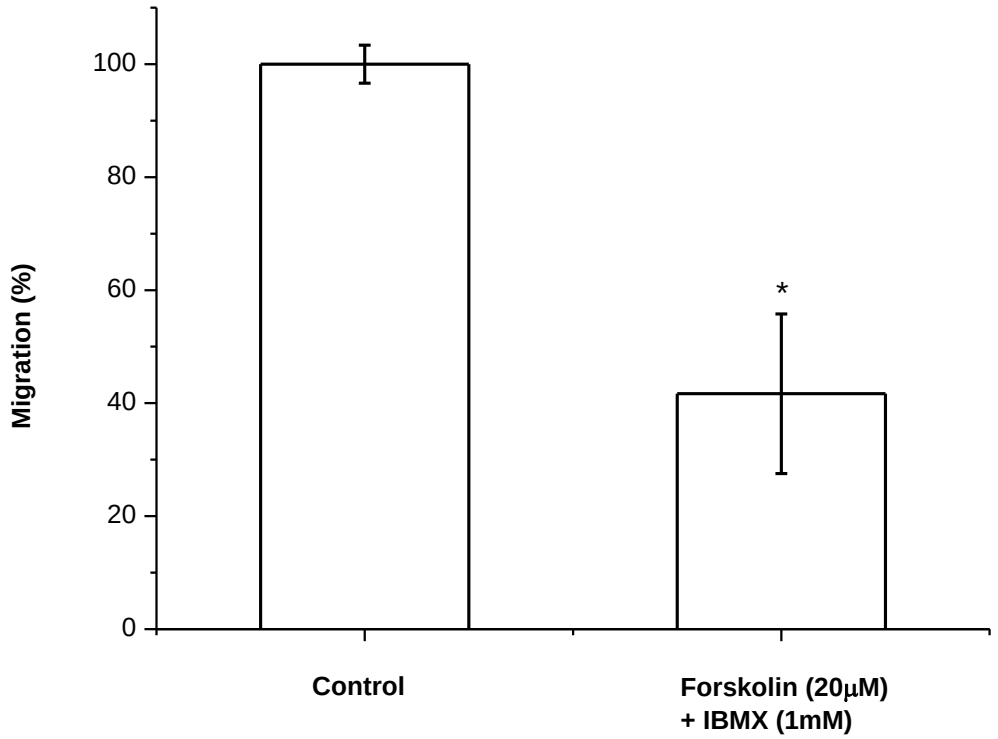

Figure 3.15. cAMP elevating agents reduced migration of MiaPaca-2 cells. Cell migration was investigated using Boyden chambers supplemented with DMEM + 1% FBS in both top and bottom wells. MiaPaca-2 cells were allowed to migrate from top to bottom chamber for 6h post seeding. Combination of Forskolin (20μM) + IBMX (1mM) reduced migration to 42% of the control (n=7 Boyden chambers for each condition. At least 3 independent experiments were performed. All results were statistically significant to $p<0.05$ and indicated by * symbol).

3.3. Cell migration is inhibited when migration is induced by asymmetric FBS gradient.

The effects of cAMP on PANC-1 migration have so far utilised Boyden chambers which tested non-directional migration. Directional migration was investigated using Boyden chambers containing DMEM supplemented with 0% FBS in top and 10% FBS in bottom wells (thus cells seeded into top wells migrated towards higher FBS concentrations in the bottom wells). Combination of forskolin + IBMX inhibited directional migration to 7.3% of the control condition (Figure 3.16).

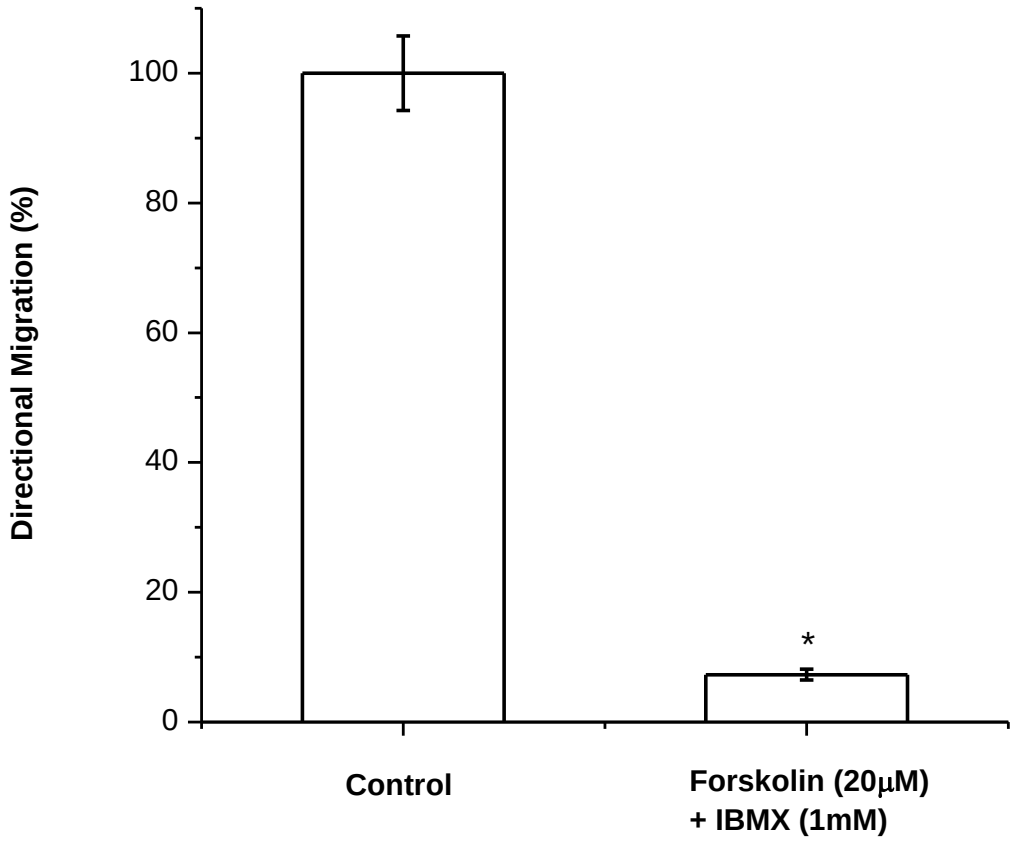

Figure 3.16. cAMP elevation reduces directional migration of PANC-1 cells. In order to investigate directional migration, a gradient of 0-10% FBS was setup within each Boyden chamber. PANC-1 cells were seeded into the top well of Boyden chambers containing DMEM + 0% FBS, whilst the bottom well contained DMEM + 10% FBS. Cells were allowed to migrate from top to bottom chamber for 6h post seeding. Combination of Forskolin (20μM) + IBMX (1mM) inhibited directional migration to 7.3% of the control (n=12 Boyden chambers for each condition. At least 3 independent experiments were performed. All results were statistically significant to $p<0.05$ and indicated by * symbol).

3.4. Cell invasion is inhibited by cAMP elevation in PANC-1 cells.

I felt it was also important to investigate the role of cAMP in the ability of the cells to invade. Boyden chambers were purchased which were covered with a homogenous layer of matrigel; which simulates the extracellular matrix environment. Importantly, the pores were occluded, meaning that PANC-1 cells had to actively degrade the matrix contents in order to successfully invade to the bottom side of the membrane. To induce non-directional invasion, both the top and bottom wells were supplemented with DMEM +1% FBS. Cells were allowed to invade for 6h in either a control vehicle or forskolin (20μM) + IBMX (1mM) condition. Forskolin (20μM) + IBMX (1mM) was found to inhibit cell invasion to 12.1% of the control condition (Figure 3.17). These findings indicated that elevation of cAMP not only inhibited migration, but also strongly suppressed cellular ability to invade.

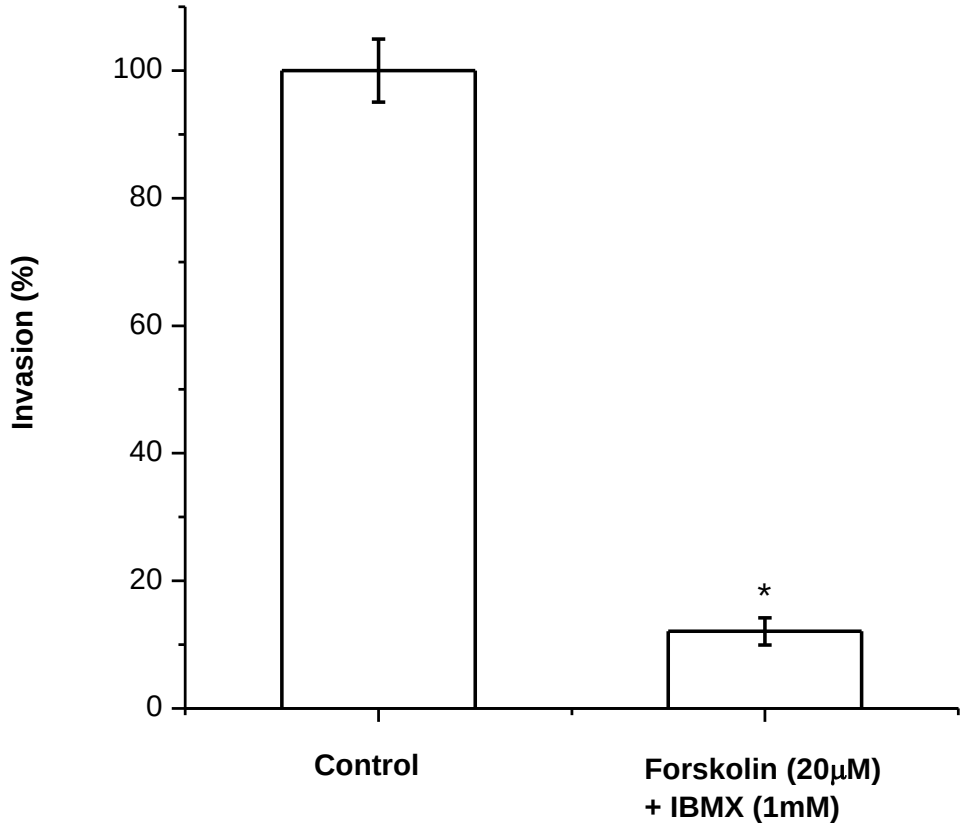

Figure 3.17. The effect of cAMP elevating agents reduces invasion of PANC-1 cells. Cell invasion was examined using matrigel covered Boyden chambers containing DMEM + 1% FBS in the top and bottom wells. Cells were allowed to migrate from top to bottom chamber for 6h post seeding. Combination of Forskolin (20μM) + IBMX (1mM) inhibited invasion to 12.1% of the control (n=6 Boyden chambers for each condition. At least 3 independent experiments were performed. All results were statistically significant to $p<0.05$ and indicated by * symbol).

3.5. Directional invasion induced by asymmetric FBS gradient is suppressed by cAMP.

I investigated directional invasion, which was induced by the use asymmetrical FBS gradient; DMEM + 0% FBS in the top and DMEM + 10% FBS in the bottom wells of matrigel covered Boyden chambers was used. Forskolin (20µM) + IBMX (1mM) inhibited directional invasion to 11.8% of the control condition (Figure 3.18). Thus, the strong inhibition of migration and invasion in both non-directional and directional modes of migration, suggests that cAMP elevation is able to inhibit effective cell movement in a variety of cell migration and invasion modes.

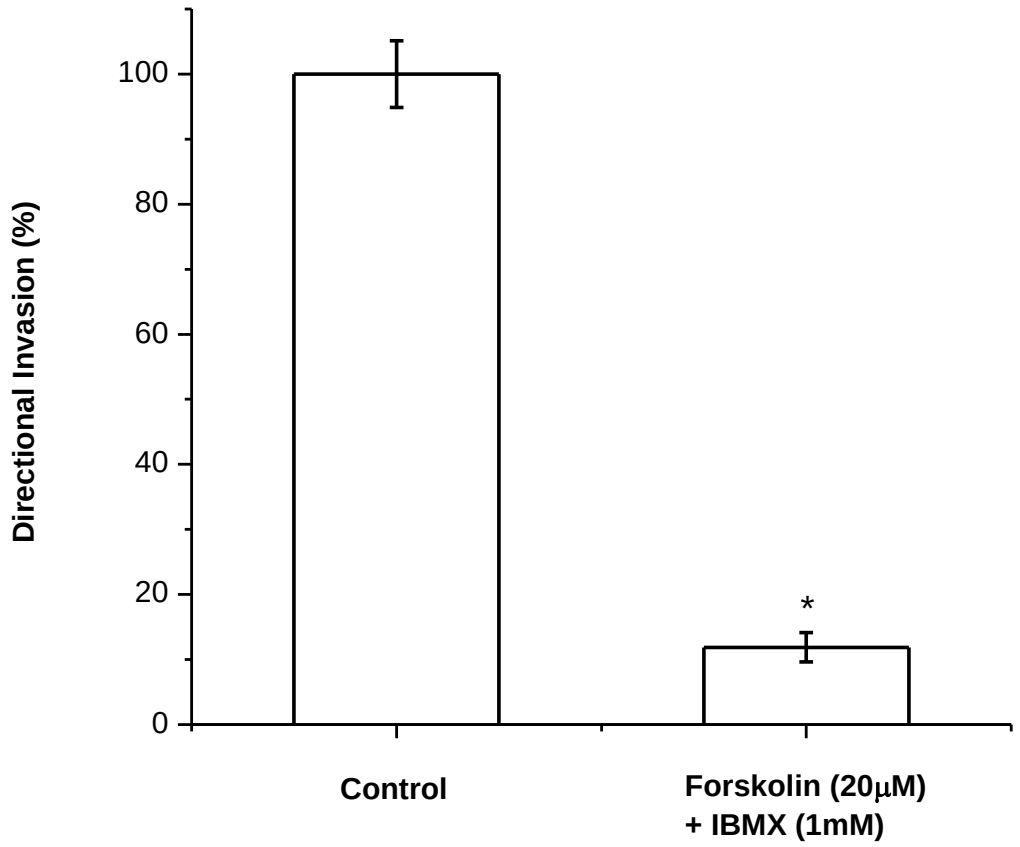

Figure 3.18. Effect of cAMP elevating agents reduces directional invasion of PANC-1 cells. To test directional cell invasion, a gradient of 0-10% FBS was setup within each matrigel covered Boyden chamber. PANC-1 cells were seeded into the top well of Boyden chambers containing DMEM + 0% FBS, whilst the bottom well contained DMEM + 10% FBS. Cells were allowed to migrate from top to bottom chamber for 6h post seeding. Combination of Forskolin (20μM) + IBMX (1mM) inhibited directional invasion to 11.8% of the control condition (n=6 Boyden chambers for each condition. At least 3 independent experiments were performed. All results were statistically significant to $p<0.05$ and indicated by * symbol).

Summary of the key results in Chapter 3.

I have successfully utilised EPAC based cAMP sensor and AKAR4 to monitor correspondingly cAMP and PKA activity in PANC-1 cells. I observed cAMP increases induced by forskolin, IBMX and 8Br-cAMP. Increase of cAMP, induced by all of these substances, resulted in the inhibition of migration of PANC-1 cells, as revealed in experiments utilising Boyden Chamber assay. The strength of the inhibition of migration directly correlated with the amplitude of cAMP increase. Not only random migration but also directional migration and invasion of PANC-1 cells were inhibited by cAMP elevation. Importantly, migration of four other pancreatic cancer cell lines was also inhibited by cAMP increase, suggesting that this phenomenon is common for all cell lines derived from this type of cancer.

CHAPTER 4 – RAPID AFFECT OF cAMP INCREASE ON RUFFLING, STRESS FIBRES, ACTIN DYNAMICS, AND FOCAL ADHESIONS.

4.1. cAMP elevation inhibits cell ruffling.

Having determined that cAMP plays a role in modulating migration, I next set out to test the effects of cAMP increase on cellular processes integral for migration. I decided to investigate the effect of cAMP on events which can contribute towards efficient migration such as cell ruffling, focal adhesion assembly, and cytoskeletal arrangement. Firstly, I decided to focus on cell ruffling events in PANC-1 cells. Lamellipodial extensions, which can lead to the formation of ruffles, are frequently observed as important structures which are associated with cell migration and invasion (Cramer *et al.*, 1997; Svitkina & Borisy, 1999). Ruffle composition is actin rich, which is tightly controlled through the actions Rho GTPases such as Rac1, RhoA, and Cdc42 (Schweiger, 1991; Suetsugu *et al.*, 2003; Svitkina, 2007; Machacek *et al.*, 2009; Pollitt & Insall, 2009; Campellone & Welch, 2010). Careful cooperation between these GTPases and their downstream effectors results in membrane protrusion and retraction cycles. Following acquisition of time-lapse videos of migrating PANC-1 cells, I frequently observed prominent peripheral ruffling at the front leading edge of polarised migrating cells (n>50, data not shown). With this in mind, I set out to investigate whether a correlation between cAMP effect on migration and ruffling existed. PANC-1 cells were seeded onto glass bottom dishes and imaged 24 hours later. In these experiments ruffling cells were recorded for a control period of time in order to ensure stable ruffling kinetics were maintained. Application of forskolin (20μM) + IBMX (1mM) quickly inhibited cell ruffling (Figure 4.1). Ruffle inhibition remained for the duration of the drug application. After a wash period, ruffle formation was quickly restored. To visualise ruffling kinetics over time, the time-lapse images were used to create a kymograph from a specified line of interest. One can clearly see stable ruffling kinetics during the control period (Figure 4.1). Addition of forskolin (20μM) + IBMX (1mM) resulted in compete ruffle inhibition within approximately 300-400s (Figure 4.1). Washing the drugs off resulted in quick (200-300s) restoration of ruffle formation (Figure 4.1).

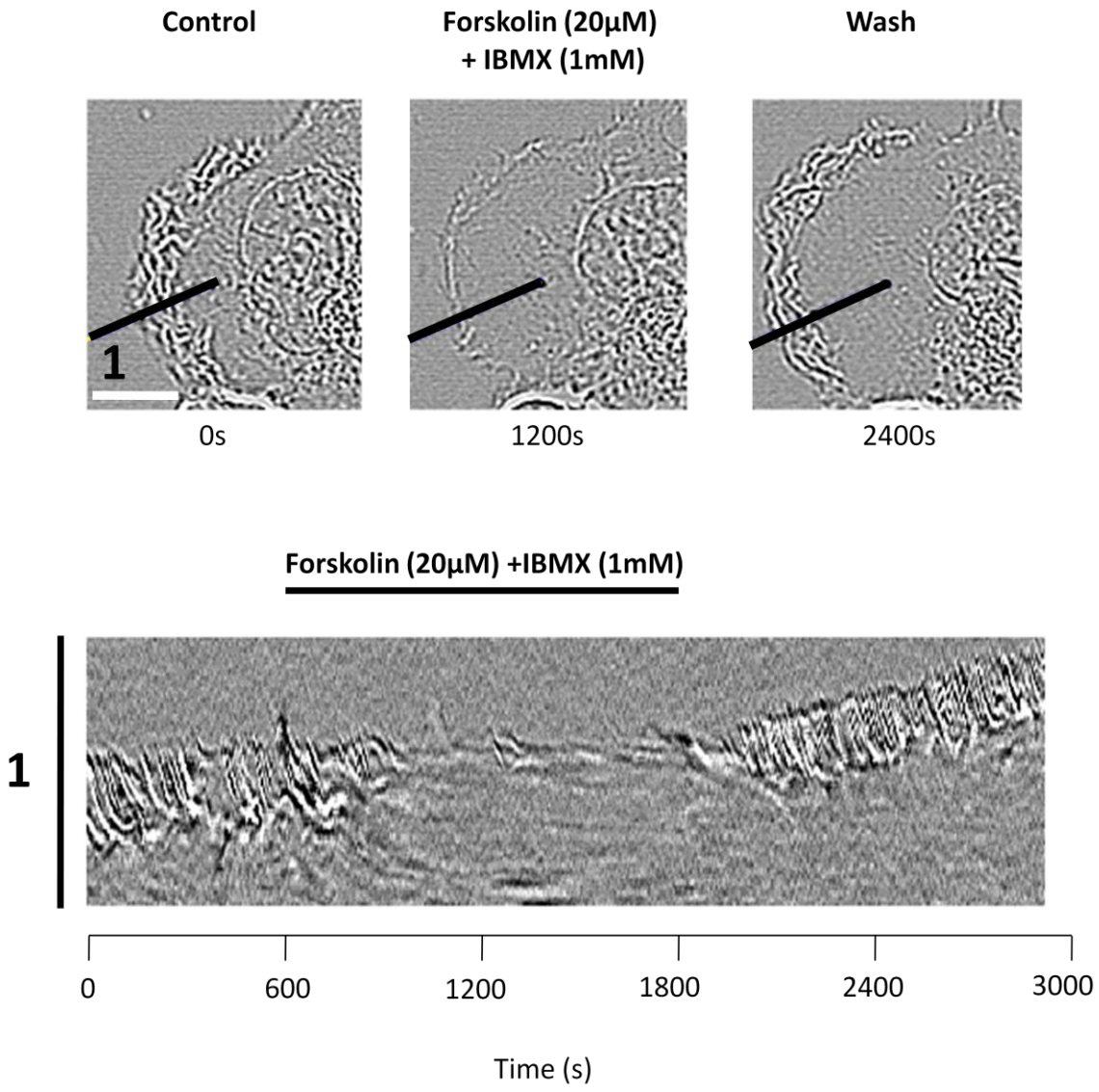

Figure 4.1. PANC-1 peripheral ruffling was reversibly inhibited with forskolin (20µM) + IBMX (1mM). Peripheral cell ruffling can be seen in images of PANC-1 cells, and was further visualised over time with the use of a kymograph constructed using the line of interest indicated (1). After 600s of ruffling, cells were subject to forskolin (20µM) + IBMX (1mM) application. Within approximately 300s, ruffle formation inhibited. After a wash of the drugs, ruffles began to form within approximately 200s (n > 50 cells. At least 3 independent experiments were performed. Scale bar corresponds to 10µm).

Ruffles are rich in actin, I therefore hypothesised that inhibition of ruffling could be accompanied with the inhibition of cortical actin dynamics. To test this hypothesis PANC-1 cells were transfected with LifeAct-GFP, which is an F-actin marker. In these experiments cells with stable ruffling kinetics were imaged for the duration of the control period (Figure 4.2). Simultaneous recording of LifeAct-GFP revealed its localisation within the ruffling structures. Inhibition of ruffling induced by forskolin (20μM) + IBMX (1mM) resulted in simultaneous loss of LifeAct-GFP staining within the corresponding ruffling structures (Figure 4.2). Upon complete ruffle inhibition, LifeAct-GFP was seen to be diffusely distributed within the cytosol, with minimal peripheral staining (Figure 4.2). Upon the wash of the drug, LifeAct-GFP was seen to redistribute back towards the cell periphery, and its intensity increased proportionally with the size of ruffling structures. Within a few minutes, full recovery of ruffling was seen, with corresponding LifeAct-GFP distribution within the ruffle structures. These data strongly indicated that elevation of cAMP did not simply inhibit ruffle kinetics, but rather inhibited the formation of ruffles. It is also interesting to note that advancement of the leading edge of the migrating cell was immediately stopped by the action of cAMP. This can be seen from the kymographs; during the control period the ruffles advance forward, which is indicated by their movement further upward in the kymograph. Upon cAMP elevation, ruffles are inhibited and the leading edge no longer advances forward. Following wash of the cAMP elevating drugs, ruffle structures appear again at the same level on the kymograph as seen just before they were inhibited. Once the ruffles establish, the leading edge of the cell advances forward again. These results suggest that the effect of cAMP on the rate of migration is immediate.

Figure 4.2. Actin distribution within ruffling structures of PANC-1 cells was reversibly inhibited with forskolin (20µM) + IBMX (1mM). PANC-1 cells were transfected with LifeAct-GFP in order to visualise actin distribution. Both transmitted light and LifeAct-GFP images are displayed at the top of the figure. Corresponding kymographs for both transmitted light and LifeAct-GFP are created from line of interest (1) and (2) respectively (same position of the lines of interest was used in transmitted light and fluorescent images), and are displayed below the images. High density of actin can be seen within corresponding cell edge lamellipodial extensions. Combination of cAMP elevating agents resulted in reversible ruffle inhibition and a large reversible decrease in corresponding LifeAct-GFP staining (n=6 cells. At least 3 independent experiments were performed. Scale bar corresponds to 10µm).

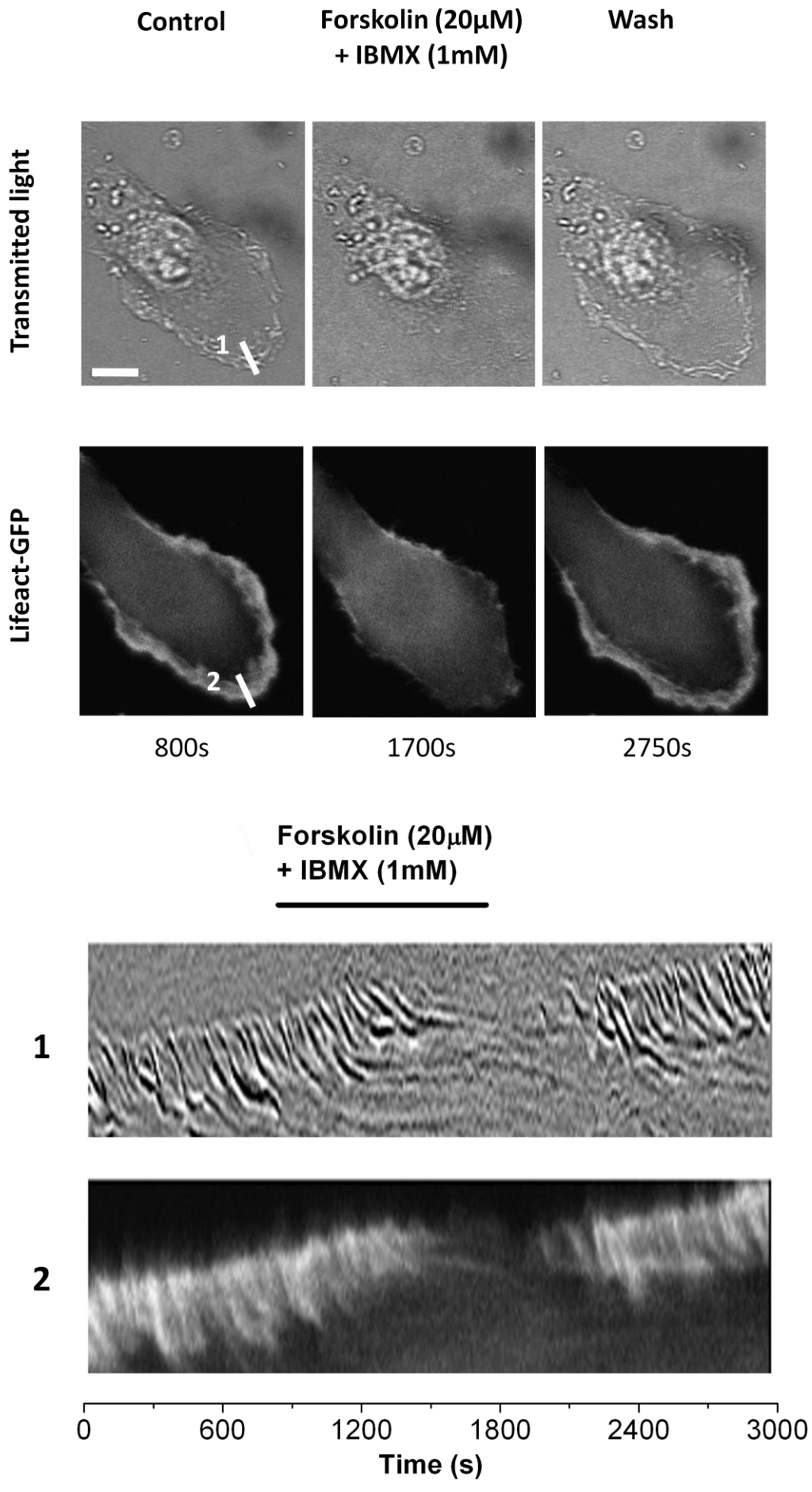
Control
Forskolin (20μM)
+ IBMX (1mM)
Wash
Transmitted light
Lifeact-GFP
1
2
800s
1700s
2750s
Forskolin (20μM)
+ IBMX (1mM)
1
2
0
600
1200
1800
2400
3000
Time (s)

To investigate whether there is a direct relationship between cAMP and ruffling, I decided to monitor endogenous cAMP levels using the EPAC-based cAMP FRET sensor H84, while simultaneously monitoring ruffling. For these experiments I selected cells which were adequately transfected with EPAC-based FRET sensor H84 and displayed stable ruffling kinetics for the duration of the control period (Figure 4.3). Application of forskolin (20µM) + IBMX (1mM) resulted in elevation of endogenous cAMP levels. Simultaneous observation of ruffle kinetics revealed a relationship between ruffling and cAMP levels (Figure 4.3). Ruffling inhibition was typically quite abrupt and occurred when the FRET shift of the sensor was approximately 50%. Ruffle structures were usually fully inhibited by the time maximal FRET shift was achieved. Ruffling remained inhibited for the duration of cAMP elevation. Upon removal of the drugs, cAMP would typically return to baseline levels within 300-600s (Figure 4.3). Immediately upon the return of cAMP to baseline, ruffles structures started to appear. All of the effects developed rapidly, with very little delay between the rise of intracellular cAMP and the inhibition of ruffling. Thus the action of cAMP on the ruffle kinetics is very likely to be as a result of direct signalling events such as phosphorylation (rather than due to cAMP-dependent changes in gene expression).

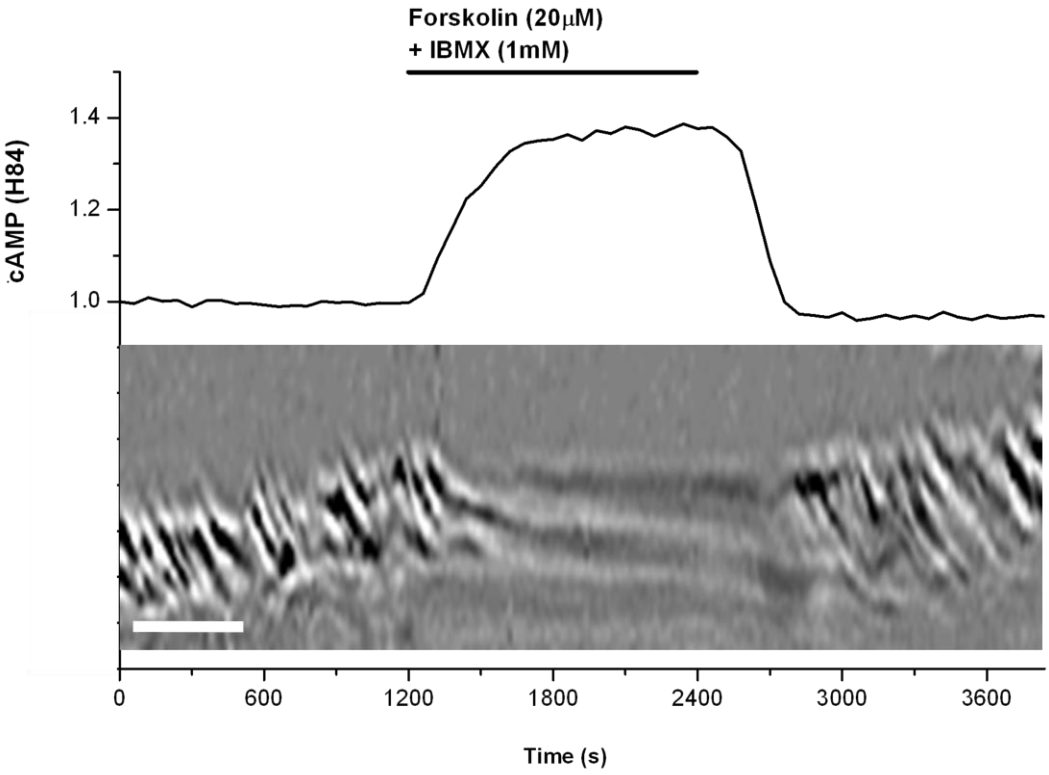

Figure 4.3. Simultaneous recording of cAMP and cell ruffling. PANC-1 cells were transfected with EPAC-based FRET sensor H84. It was found that upon cAMP elevation with forskolin (20μM) + IBMX (1mM), cell ruffling was inhibited. Upon cAMP returning to basal levels, ruffling was re-established (n=3 cells. 3 independent experiments were performed. Scale bar corresponds to 5μm).

4.2. Key focal adhesion protein paxillin dissociates from focal adhesions in response to cAMP elevation.

I next focused on focal adhesion assembly and the effect, if any, that cAMP elevation has on key focal adhesion associated proteins. As mentioned within the introduction, there are many proteins that can localise into focal adhesions structures. However, there are a few key proteins which have been well studied and shown to be important for cell motility. I decided to investigate the focal adhesion associated protein paxillin, based on the fact that it is one of the key focal adhesion proteins responsible for modulation of various downstream effectors such as RhoA, Rac1 and CDC42 Rho GTPases (Brown & Turner, 2004). I utilised constructs encoding for paxillin-GFP, which enabled us to monitor its intracellular distribution in individual cells. PANC-1 were transfected with this construct and the effect of cAMP elevation on paxillin presence in focal adhesions was investigated. In these experiments, I have found that application of forskolin (20µM) + IBMX (1mM) resulted in rapid loss of paxillin in response to cAMP elevation (Figure 4.4). The effect was also found to be quickly reversible upon wash of the drugs.

Figure 4.4. Elevation of intracellular cAMP induces paxillin trafficking out of focal adhesions. Paxillin-GFP construct was transfected into PANC-1 cells. Cells were imaged for a control period of 300s. Application of forskolin (20μM) + IBMX (1mM) (from 300 to 900s), caused paxillin to traffic out of focal adhesions. After a washing off the drugs (900 to 3000s), paxillin trafficked back into focal adhesions (n >30. At least 3 independent experiments were performed. Scale bar corresponds to 10μm).

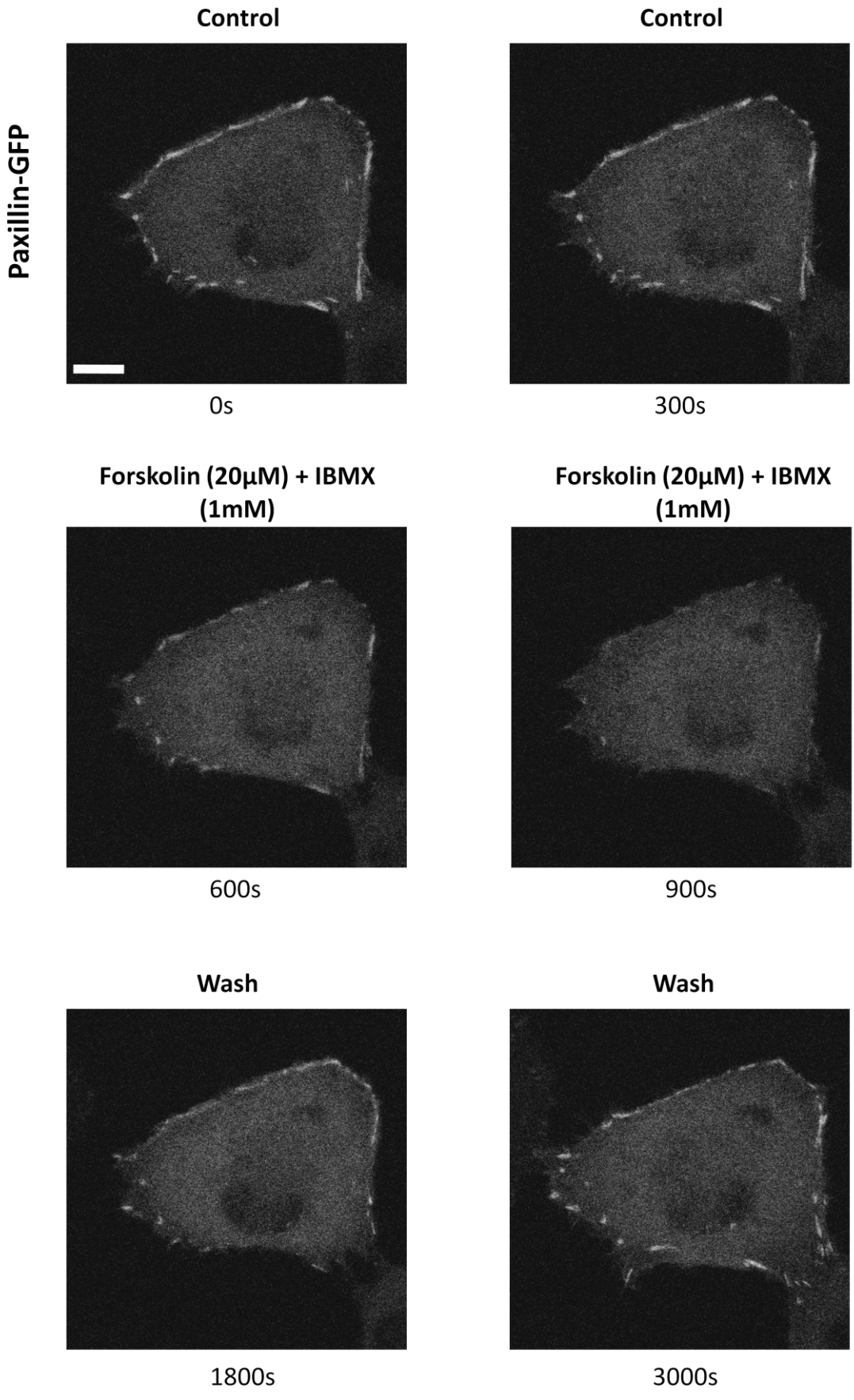
Paxillin-GFP
Control
Control
0s
300s
Forskolin (20µM) + IBMX (1mM)
Forskolin (20µM) + IBMX (1mM)
600s
900s
Wash
Wash
1800s
3000s

To further investigate the effect of cAMP on paxillin localisation, PANC-1 cells were co-transfected with EPAC-based FRET sensor H84 and paxillin-PSmOrange. To quantify the relative amount of paxillin within focal adhesions, regions of interest were drawn around each of the clearly visible focal adhesions (F_{Fa}). Next to each focal adhesion devoid of focal adhesions, a corresponding region of interest was drawn in the vicinity of the focal adhesion (F_C). Thus a ratio of paxillin intensity within a focal adhesion relative to adjacent cytosolic staining revealed the relative level of paxillin incorporation within the focal adhesion. Combining the paxillin ratio with the simultaneous cAMP FRET sensor recording, enabled us to simultaneously visualise dynamics of intracellular cAMP levels and paxillin focal adhesion incorporation within single live cells. An example of such experiment is shown in Figure 4.5. Forskolin (20µM) + IBMX (1mM) was applied, which resulted in elevation of cAMP. Simultaneous recording of paxillin revealed that elevation of cAMP caused paxillin to traffic out of focal adhesions (Figure 4.5). Upon removal of the drugs, cAMP levels returned back to baseline, which was accompanied by paxillin trafficking back into focal adhesion. Interestingly, paxillin was seen to start moving back into focal adhesions before basal level of cAMP was achieved; unlike ruffling which started to recover after basal levels of cAMP were achieved. This could be perhaps expected, as paxillin acts as a scaffold to bind proteins which control ruffling. Furthermore, the rapid action of cAMP on paxillin in focal adhesions, suggests that the effect of cAMP is direct (i.e. not modulated by cAMP-dependent changes in gene expression).

Figure 4.5. Correlation of cAMP concentration and paxillin presence in focal adhesions. PANC-1 cells were transfected with EPAC-based FRET sensor H84. Cells were co-transfected with paxillin-PSmOrange, enabling simultaneous observation of its focal adhesion distribution. The ratios (F_{Fa}/F_C, see page 84) obtained from focal adhesions (outlined in the image situated in the middle of the figure, and indicated by white circles) were averaged to give a single trace. It was found that upon cAMP elevation with forskolin (20μM) + IBMX (1mM), content of paxillin in focal adhesions was greatly reduced. Upon cAMP returning to basal levels, paxillin was seen to traffic back into focal adhesions (n=4 cells. At least 3 independent experiments were performed. Scale bar corresponds to 10μm).

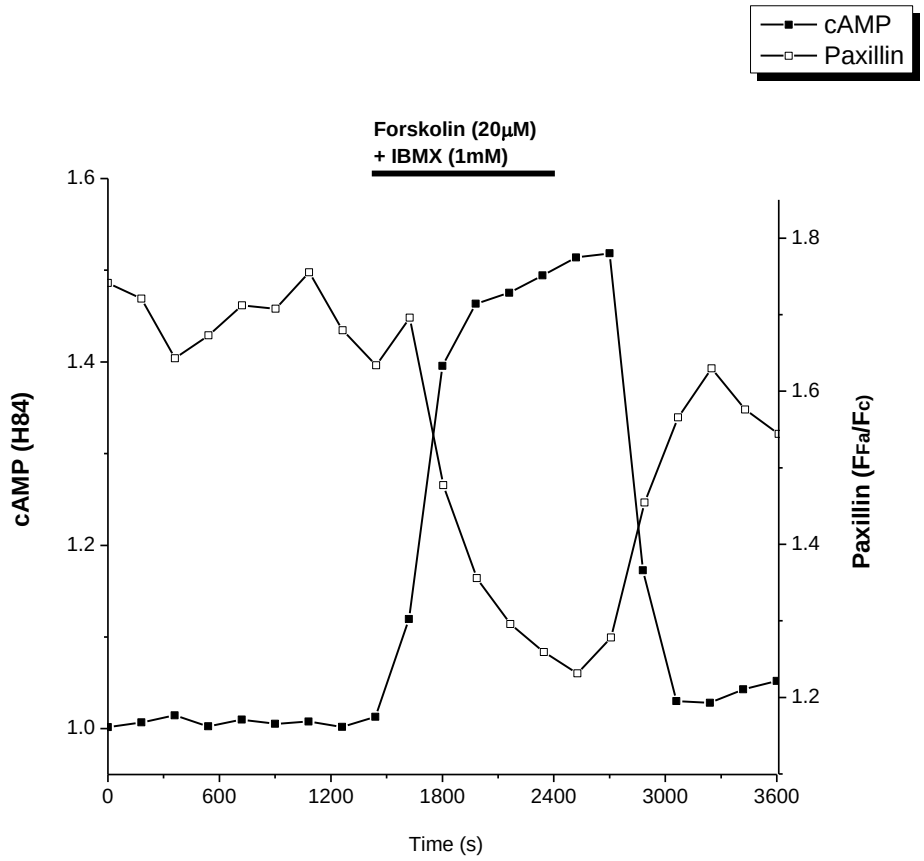
cAMP
Paxillin
Forskolin (20μM)
+ IBMX (1mM)
cAMP (H84)
Paxillin (FFa/Fc)
Time (s)
1.6
1.4
1.2
1.0
1.8
1.6
1.4
1.2
0
600
1200
1800
2400
3000
3600

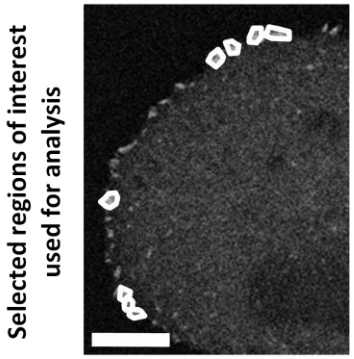
Selected regions of interest
used for analysis

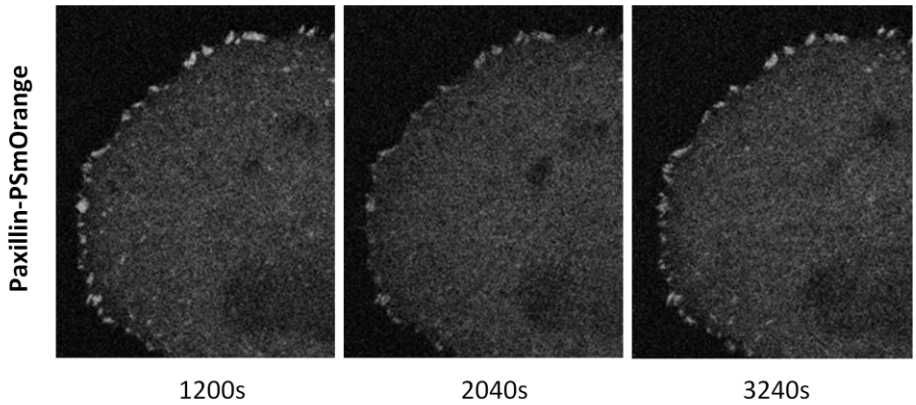
Paxillin-PSmOrange
1200s
2040s
3240s

4.3. cAMP elevation reversibly inhibits actin stress fibre formation.

To further investigate the role of cAMP in the inhibition of migration, I focused on the cytoskeletal arrangement of actin; more specifically stress fibre formation. Actin stress fibres are important structures which are connected to the focal adhesion complexes and are used by the cell to produce tractional forces (Cox & Huttenlocher, 1998). Stress fibres usually terminate at focal adhesions, where they are attached via linker proteins such as vinculin and talin (Critchley, 2009). PANC-1 cells were transfected with LifeAct-GFP in order to visualise actin stress fibres. In our experiments, forskolin (20μM) + IBMX (1mM) was applied for a period of 30 minutes; this resulted in the breakdown of stress fibres (Figure 4.6). Removal of the cAMP elevating agents resulted in quick reversal of stress fibre formation.

Figure 4.6. Actin stress fibre were disassembled by forskolin (20µM) + IBMX (1mM) in PANC-1 cells. In order to visualise actin stress fibres, PANC-1 cells were transfected with LifeAct -GFP. Cells were imaged for a control period of 600s. The application of forskolin (20µM) + IBMX (1mM) from 600s to 2400s, resulted in stress fibre disassembly. Removal of forskolin + IBMX at 2400s resulted in the restoration of stress fibres (n=6. At least 3 independent experiments were performed. Scale bar corresponds to 10µm).

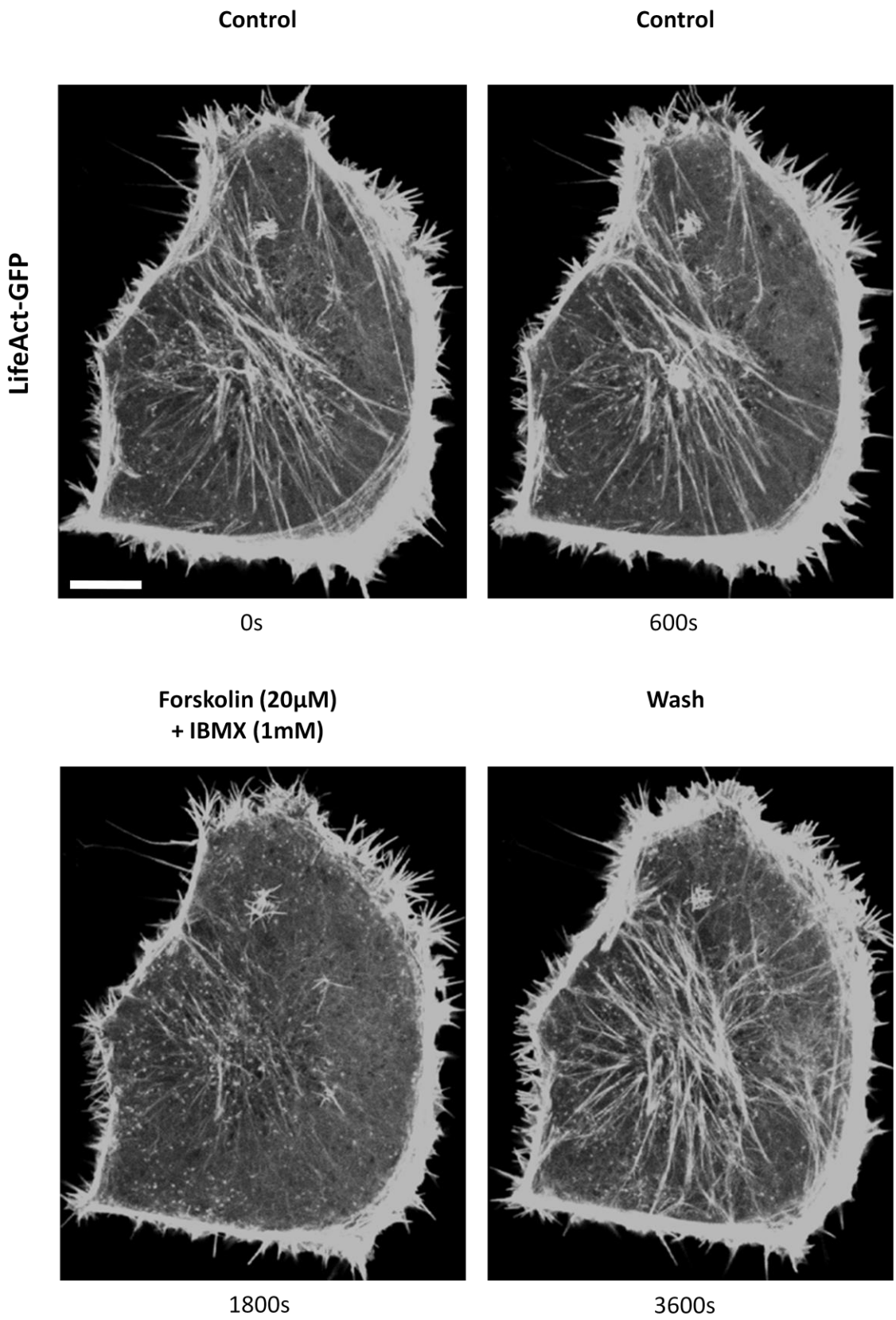
Control
Control
LifeAct-GFP
0s
600s
Forskolin (20µM)
+ IBMX (1mM)
Wash
1800s
3600s

I next decided to establish the relationship between cAMP and stress fibres. PANC-1 cells were transfected with EPAC-based FRET sensor H84 and LifeAct-RFP; results of the experiment are shown in Figure 4.7. To visualise stress fibre formation over time, a kymograph was generated from a line of interest running through the middle of the cell. Three sample images were chosen from the time series of the recording to show stress fibres before, during and after application of forskolin (20µM) + IBMX (1mM) (see lower part of Figure 4.7). The line of interest drawn to generate the kymograph is displayed in the left image. Cells were chosen which displayed good expression of both constructs. Forskolin (20µM) + IBMX (1mM) was applied, resulting in elevation of cAMP. Simultaneous recording of LifeAct-RFP revealed inverse correlation of the density of stress fibres and cAMP levels. Most stress fibres started to dissipate around the time when the cAMP sensor was displaying approximately 50% FRET shift (Figure 4.7). Some stress fibres were noted to take longer than others to dissipate, however all showed decreased fluorescence intensity following cAMP elevation. Removal of forskolin + IBMX resulted in lowering of cAMP back towards baseline levels. Stress fibres stared to form immediately after basal levels of cAMP were achieved.

Figure 4.7. Simultaneous recording of cAMP and actin stress fibres revealed cAMP-dependent disassembly of stress fibres. PANC-1 cells were transfected with EPAC-based FRET sensor H84. Cells were co-transfected with LifeAct-RFP in order to visualise actin stress fibres. Three sample images were chosen from the time series, before, during and after application of forskolin (20µM) + IBMX (1mM) (see lower part of the figure). A line of interest was drawn in the centre of the cell to generate a kymograph of the stress fibre status over time (shown in lower left image). Elevation of cAMP resulted in stress fibre disassembly. Recovery of cAMP back to basal level resulted in restoration of stress fibres (n=3 cells. At least 3 independent experiments were performed. Scale bar corresponds to 10µm).

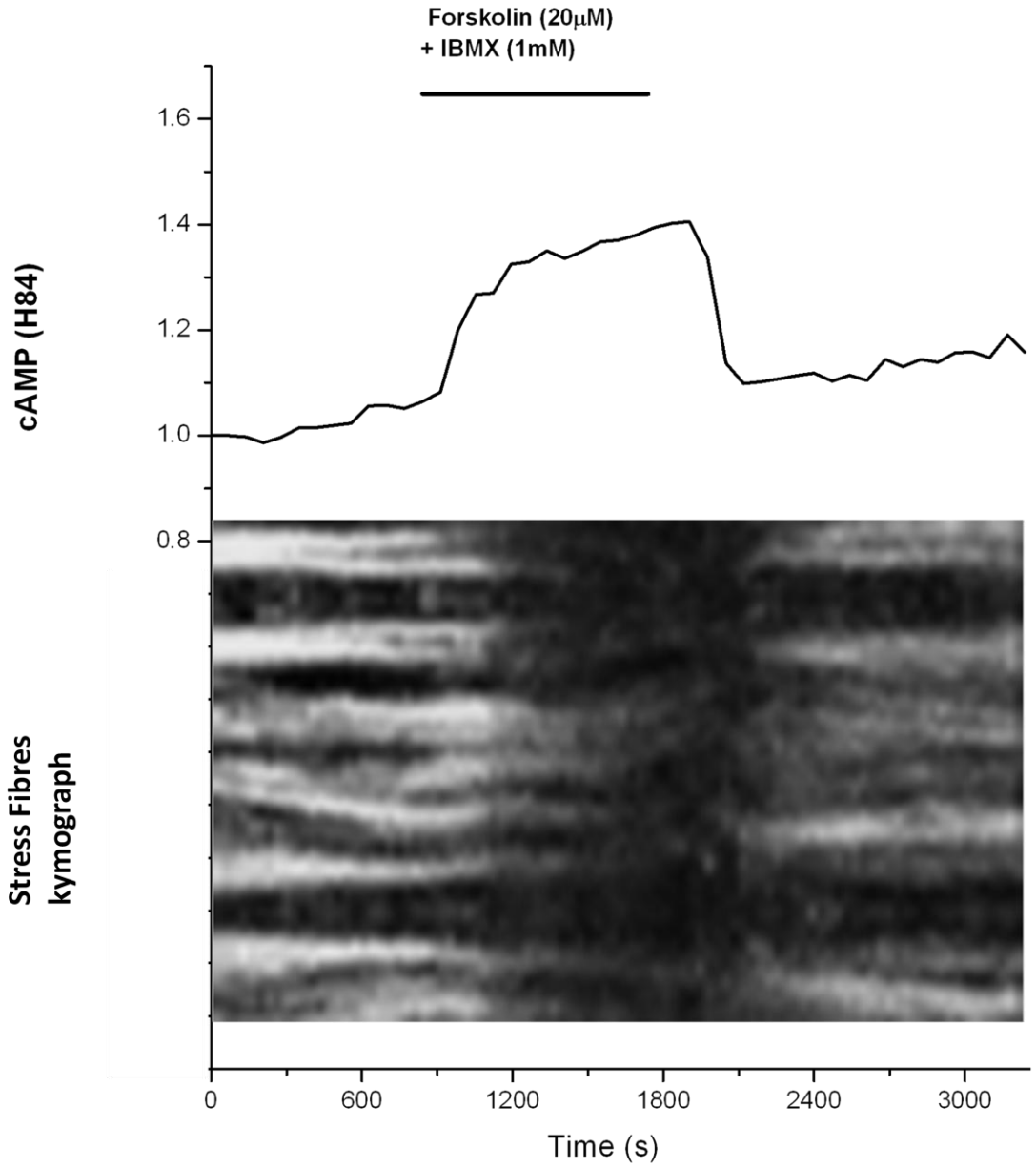
Forskolin (20μM)
+ IBMX (1mM)
cAMP (H84)
1.6
1.4
1.2
1.0
0.8
Stress Fibres
kymograph
0
600
1200
1800
2400
3000
Time (s)

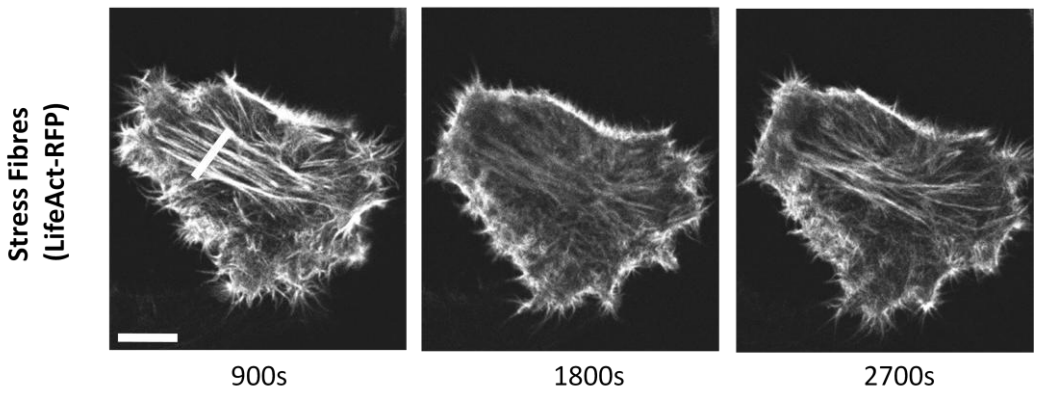
Stress Fibres
(LifeAct-RFP)
900s
1800s
2700s

Summary of the key results in Chapter 4.

I have successfully developed protocols for monitoring ruffling, formation and dynamics of focal adhesion and localisation of stress fibres. Results of experiments reported in this chapter indicate that cAMP increase inhibits a number of cellular processes closely associated with migration. Treatment with forskolin and IBMX resulted in the inhibition of ruffling, and in loss of actin at the leading edge of migrating cells. cAMP increase triggered the loss of paxillin from focal adhesions and stopped dynamic remodelling of focal adhesions. Finally cAMP elevation resulted in disassembly of stress fibres in PANC-1 cells. Importantly, the simultaneous monitoring of cAMP levels and ruffling, focal adhesion dynamics and stress fibre localisation revealed that the inhibition of the processes associated with migration develops well before the saturation of the cAMP probe (in other words, within the physiological range of cAMP effectors).

CHAPTER 5 – DOWNSTREAM EFFECTORS OF cAMP SIGNALLING HAVE OPPOSING ROLES IN MODULATING MIGRATION

5.1. Selective EPAC activation potentiates migration.

So far I have discovered that cAMP elevation inhibits migration in various PDAC cell lines. Further investigation utilising PANC-1 cells revealed effects of cAMP are immediate with respect to its inhibitory action on ruffles, stress fibre, and focal adhesion assembly. However, what is not yet clear is through which effector(s) cAMP is mediating its actions. To investigate this question, I utilised selective cAMP analogues. EPAC selective analogue, 8pCPT, was chosen to see if EPAC is at all involved in modulating PANC-1 migration. However, I first utilised both EPAC and PKA FRET sensors in order to find a dose at which 8pCPT will strongly activate EPAC, but would not significantly activate PKA; as high doses of 8pCPT could potentially activate PKA. PANC-1 cells were transfected with EPAC-based cAMP FRET sensor and various doses of 8pCPT were tested (data not shown). It was found that 300µM 8pCPT caused near maximal FRET shift, thus indicating strong activation of EPAC (Figure 5.1). Importantly however, there was no saturation of the FRET sensor in most of the cells imaged. Thus, I chose to work with 300µM 8pCPT for all the subsequent experiments. I next decided to confirm this concentration of drug was selective for activation of EPAC. PANC-1 cells were transfected with AKAR4 and imaged 24 hours post transfection. 8pCPT (300µM) did not induce any noticeable FRET shift of the PKA sensor (Figure 5.2). Following a wash off period, positive control was applied, consisting of forskolin (20µM) + IBMX (1mM), which displayed a FRET shift as expected. This was a good indication that selective EPAC activation was achieved with 300µM 8pCPT, with no significant cross activation of endogenous PKA.

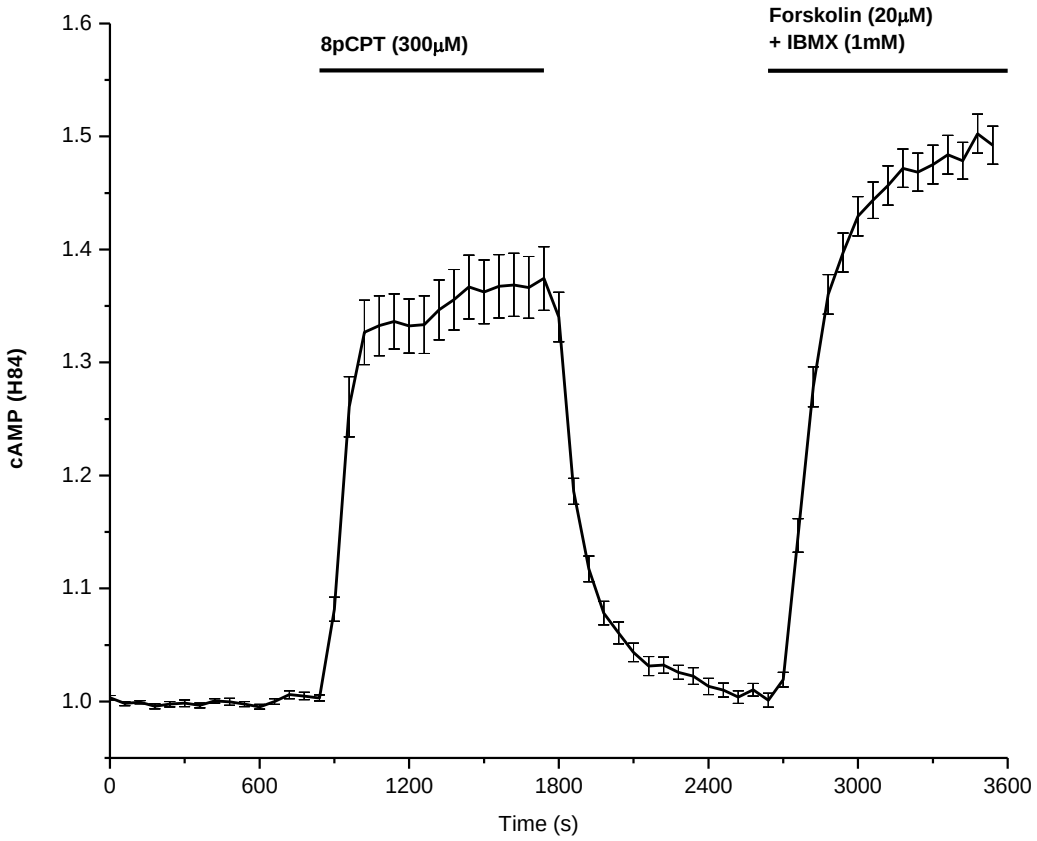

Figure 5.1. EPAC activation was verified using EPAC-based FRET sensor, revealing near maximal EPAC activation with 300µM 8pCPT. PANC-1 cells were transfected with EPAC-based FRET sensor H84. 8pCPT (300µM) was applied and resulted in strong activation of the EPAC FRET sensor. Following wash off period, forskolin (20µM) + IBMX (1mM) was applied to induce maximal FRET shift (n=30 cells. At least 3 independent experiments were performed).

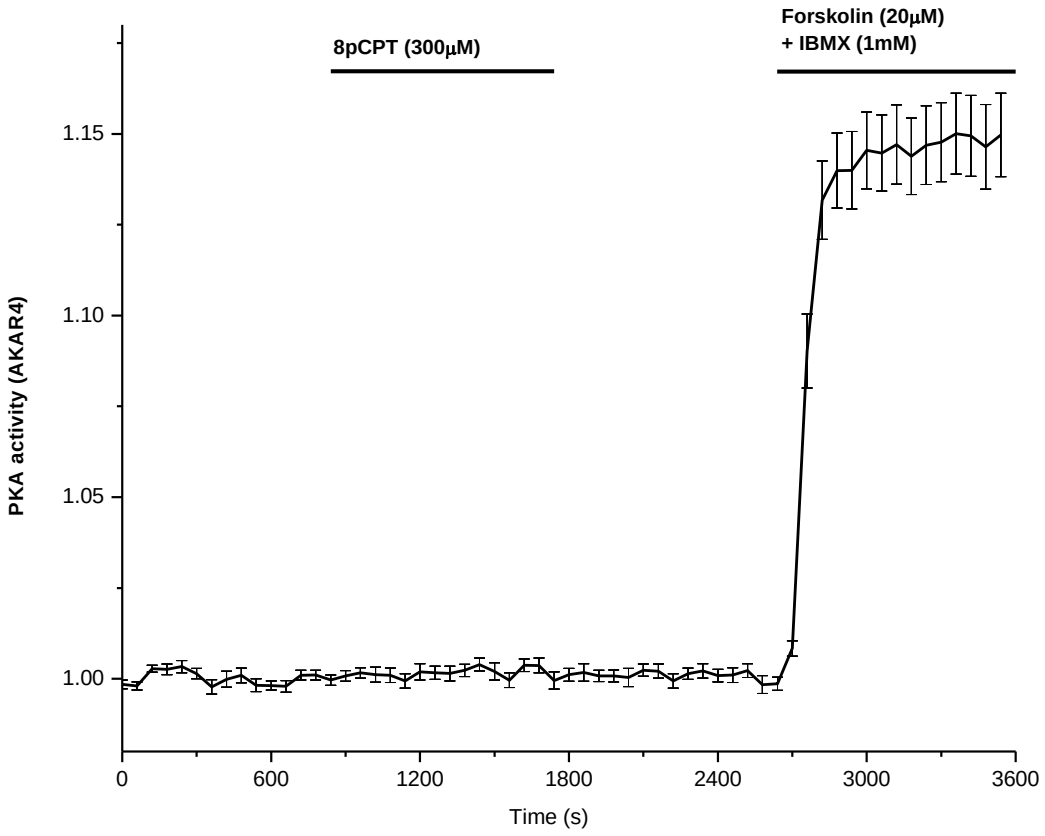

Figure 5.2. AKAR4 revealed no significant endogenous PKA activation with 300μM 8pCPT. PANC-1 cells were transfected with AKAR4. 8pCPT (300μM) did not induce in any significant PKA activation. Following a wash off period, forskolin (20μM) + IBMX (1mM) was applied and resulted in a typical FRET shift (n=21 cells. At least 3 independent experiments were performed).

Having established the correct dose to achieve strong but selective activation of EPAC, PANC-1 cells were subjected to Boyden Chamber experiments to test if EPAC activation is responsible for the inhibition of migration. Cells were treated with control vehicle or 8pCPT (300μM) for 6 hours, and migration was assed as previously described. Surprisingly, I found that EPAC activation resulted in potentiation of migration to 154% of the control condition (Figure 5.3). This was very interesting finding for two main reasons. Firstly, the effects of selective EPAC activation in PANC-1 cells has never been characterised before. Secondly, this data indicated that another effector is likely responsible for the inhibition of migration that is induced through cAMP elevation.

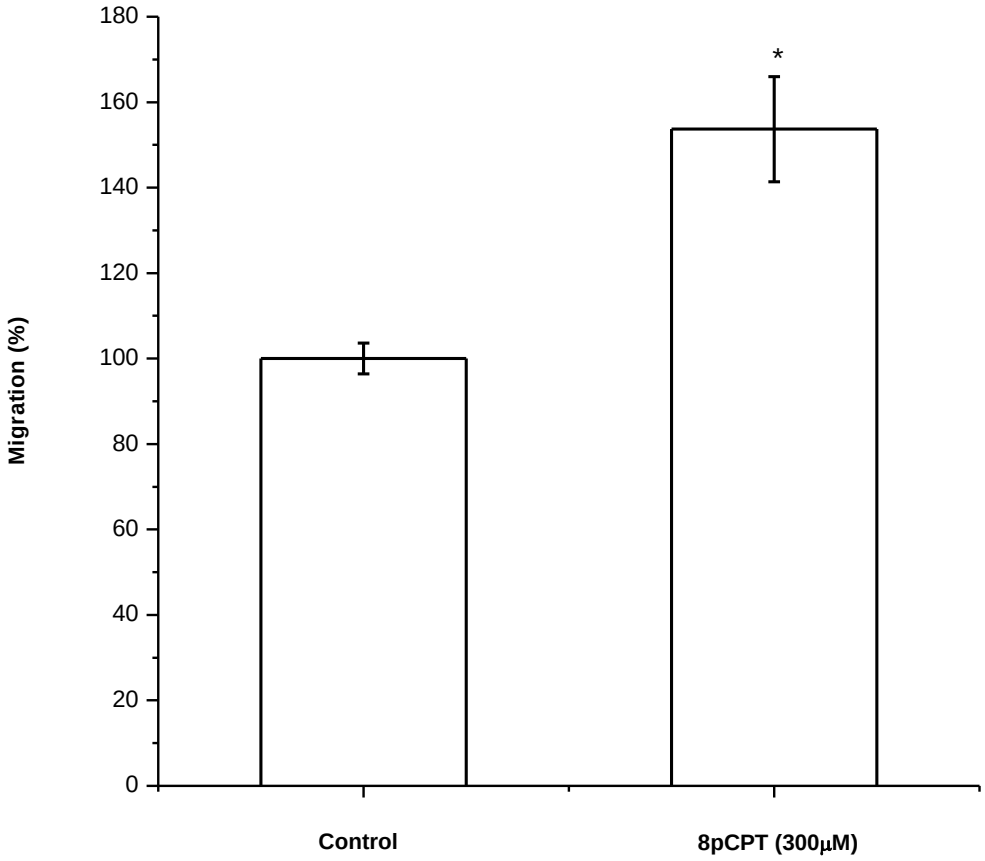

Figure 5.3. Selective EPAC activation using cAMP analogue 8pCPT resulted in potentiation of migration. Cell migration was investigated using Boyden chambers supplemented with DMEM + 1% FBS in both top and bottom wells. PANC-1 cells were allowed to migrate from top to bottom chamber for 6h post seeding. Results were normalised and displayed as a percentage. EPAC activation with 8pCPT (300μM) led to increased migration rate of 154% relative to the control condition (n=16 Boyden chambers for each condition. At least 3 independent experiments were performed. All results were statistically significant to $p<0.05$ and indicated by * symbol).

5.2. Selective PKA activation inhibits cell migration.

Surprised by the previous findings, I were now interested to find out the role of PKA in modulating migration. I used a similar approach as described for 8pCPT, to find an appropriate selective dose of a PKA activator. I utilised another cAMP analogue, 6Bnz, which is known to be a selective PKA activator. I utilised both PKA and EPAC FRET sensors in order to find a concentration at which 6Bnz will strongly activate PKA, but would not significantly activate EPAC. PANC-1 cells were transfected with AKAR4 and various doses of 6Bnz were tested (data not shown). It was found that, like with the non-selective analogue 8Br-cAMP, a similar and high concentration of 6Bnz was required to achieve moderate PKA activation. For this reason, I decided to use 6mM 6Bnz in all the following experiments. PANC-1 cells were transfected with AKAR4 and the cells were subjected to application of 6mM 6Bnz which was seen to induce FRET of the probe (Figure 5.4). These results indicate that PKA activation was achieved with 6Bnz. I next decided to determine whether the concentration of 6Bnz used was selective for activation of PKA. PANC-1 cells were transfected with EPAC-based cAMP FRET sensor and imaged 24 hours post transfection. Following a stable baseline, 6Bnz was applied at 6mM and did not induce any noticeable FRET shift in any of the cells imaged (Figure 5.5). Following a wash off period, positive control was applied, consisting of forskolin (20μM) + IBMX (1mM), which displayed a normal FRET shift as expected. This was a good indication that selective PKA activation was achieved, with no cross activation of EPAC. PANC-1 cells were subjected to Boyden chamber experiments to see if selective PKA activation by cAMP is responsible for the inhibition of migration. Cells were treated with control vehicle or 6Bnz (6mM) for 6 hours, and migration was assed as described previously. Selective PKA activation resulted in the inhibition of migration to 54% of the control (Figure 5.6).

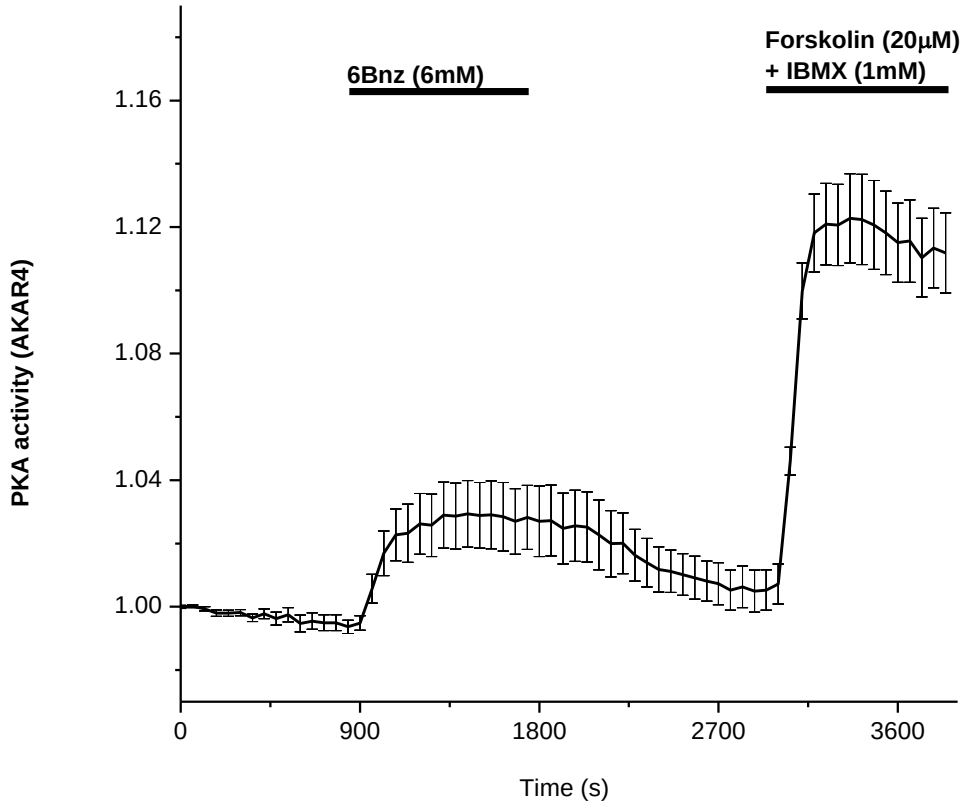

Figure 5.4. Endogenous PKA activation by 6Bnz was verified using FRET sensor containing a substrate for PKA. PANC-1 cells were transfected with AKAR4. 6Bnz was applied at 6mM and caused a moderate FRET shift, indicating endogenous PKA was activated. After a wash off period, forskolin (20μM) + IBMX (1mM) was applied to induce maximal FRET shift (n=28 cells. At least 3 independent experiments were performed).

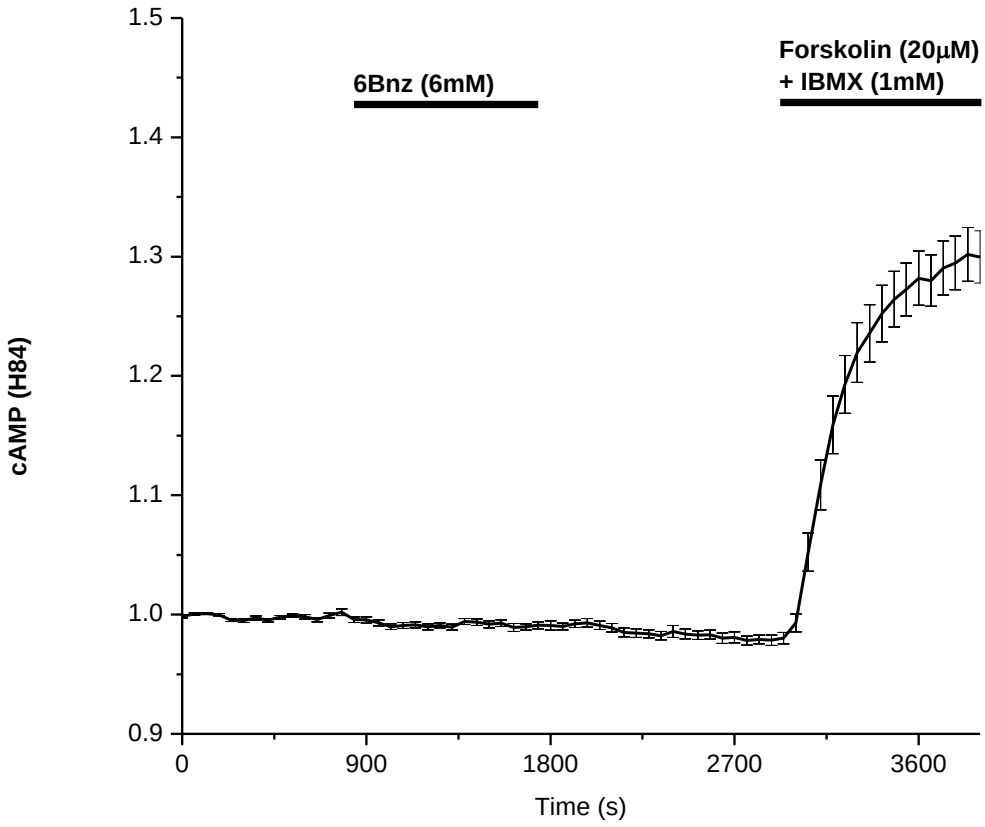

Figure 5.5. 6Bnz did not induce resolvable FRET response of the EPAC-based FRET sensor. PANC-1 cells were transfected with EPAC-based FRET sensor H84. 6Bnz was applied at 6mM concentration. After a wash off, forskolin (20μM) + IBMX (1mM) was applied to induce maximal FRET shift. No EPAC activation was achieved in any of the cells imaged (n=29 cells. At least 3 independent experiments were performed).

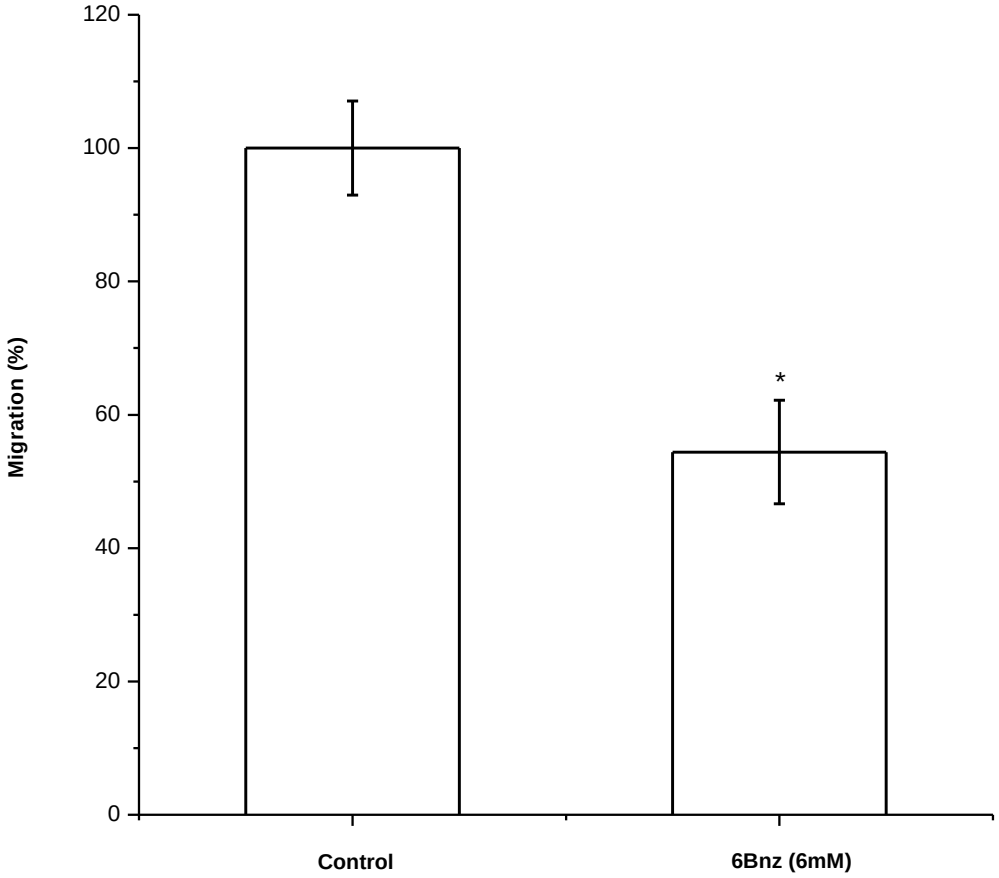

Figure 5.6. Selective PKA activation using 6Bnz shows inhibition of PANC-1 migration. Cell migration was investigated using Boyden chambers supplemented with DMEM + 1% FBS in both top and bottom wells. Cells were allowed to migrate from top to bottom chamber for 6h post seeding. Results were normalised relative to control and displayed as a percentage. Selective PKA activation was achieved using cAMP analogue 6Bnz at 6mM, which led to decreased migration rate to 54% relative to the control condition (n=7 Boyden chambers for each condition. At least 3 independent experiments were performed. All results were statistically significant to $p<0.05$ and indicated by * symbol).

5.3. PKA activity correlates with ruffling.

Having obtained data which displayed selective PKA activation can result in inhibition of migration, I set out to further confirm these results by using selective inhibitors of PKA to reverse the effects induced by cAMP elevation. I decided to test a hypothesis that PKA activation is responsible for ruffle inhibition, paxillin dissociation from focal adhesions, as well as inhibition of migration. I first decided to establish the relationship between endogenous PKA activity and ruffle formation. PANC-1 cells were transfected with AKAR4 and imaged 24 hours later. Transfected cells were chosen which were displaying stable ruffle kinetics for the duration of the control period. Upon application of forskolin (20µM) + IBMX (1mM), endogenous PKA activity increased as expected and fully saturated the FRET sensor. Typically between 300-600s post elevation of cAMP, ruffling would be inhibited. Upon removal of cAMP elevating drugs, ruffles were seen to start forming immediately after basal PKA levels were restored (figure 5.7). These observations would suggest intracellular PKA activity is linked with ruffling formation.

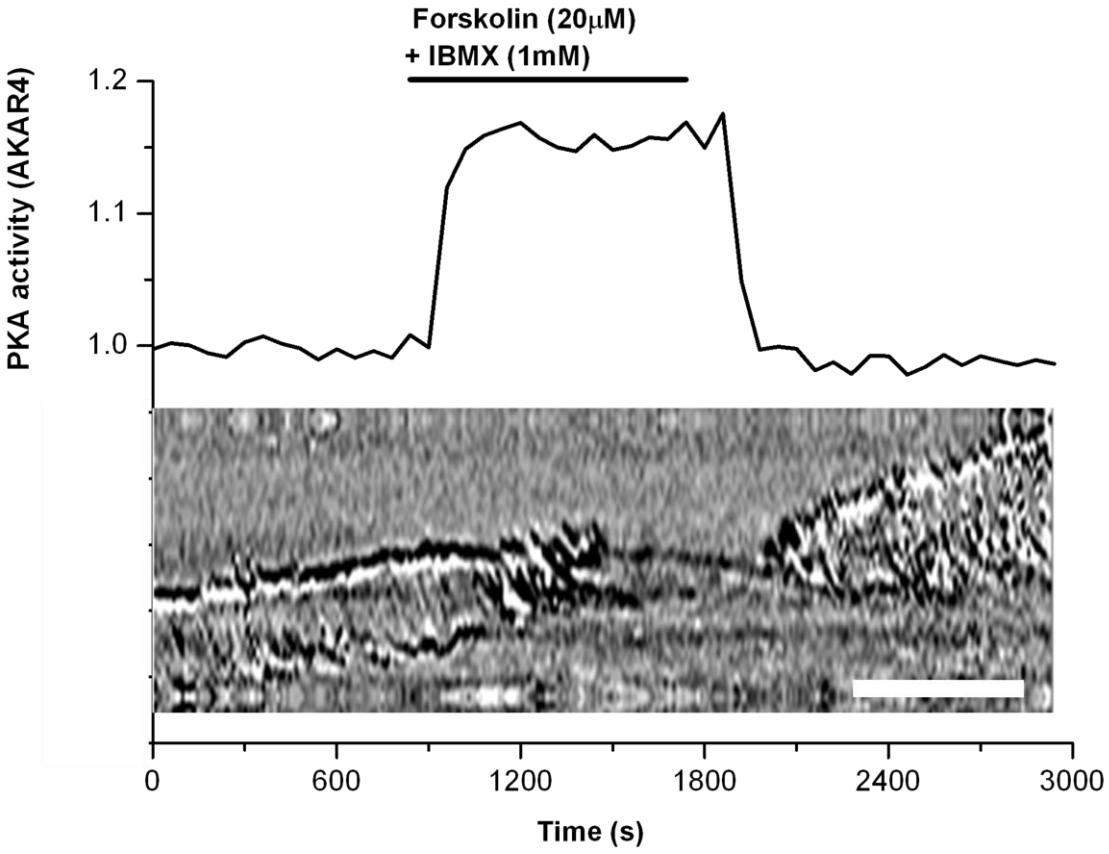

Figure 5.7. Simultaneous recording of endogenous PKA activity and cell ruffling revealed a relationship between the two variables. PANC-1 cells were transfected with the AKAR4. It was found that upon cAMP elevation with forskolin (20μM) + IBMX (1mM), resulted in activation of endogenous PKA and inhibition of cell ruffling. Upon return to basal level of PKA activity, ruffles were seen to start forming again (n= 9 cells. At least 3 independent experiments were performed. Scale bar corresponds to 10μm).

5.3.1. Selective PKA activation using 6Bnz induces paxillin translocation out of focal adhesions.

I next decied to investigate the effect of selective PKA activation on paxillin localisation within focal adhesions. PANC-1 cells were transfected with paxillin-GFP and imaged 24 hours later. I have found that unlike with forskolin (20µM) + IBMX (1mM), which caused strong paxillin loss from focal adhesions; 6mM 6Bnz caused a milder effect which was only seen in half of the cells imaged (23 out of 46). The cells that did respond displayed a clear loss of paxillin from the focal adhesion structures (Figure 5.8). Upon removal of 6Bnz, paxillin was seen to start trafficking back into the focal adhesions. The observations were quite clear, and suggested that selective PKA activation can cause paxillin loss from focal adhesion structures. I wanted to test the effect of selective EPAC activation on paxillin localisation. PANC-1 cells were again transfected with paxillin-GFP and imaged 24 hours later. Following a control period, 8pCPT (300µM) was applied for an extensive period of time. However, no loss of paxillin from focal adhesion structures was seen (Figure 5.9). I therefore concluded that the loss of paxillin from focal adhesion structures induced by global elevation of cAMP with forskolin (20µM) + IBMX (1mM) was as a result of PKA activation.

Figure 5.8. Selective PKA activation using 6Bnz induces paxillin translocation out of focal adhesions. PANC-1 cells were transfected with paxillin-GFP. After 900 second control period, cells were treated with 6Bnz (6mM) for 1800 seconds which induced paxillin translocation out of focal adhesion into the cytosol. Paxillin was seen to traffic back into focal adhesion upon wash of the drugs. This was observed in 23 out of 46 cells imaged (n=46 cells. At least 3 independent experiments were performed. Scale bar corresponds to 10μm).

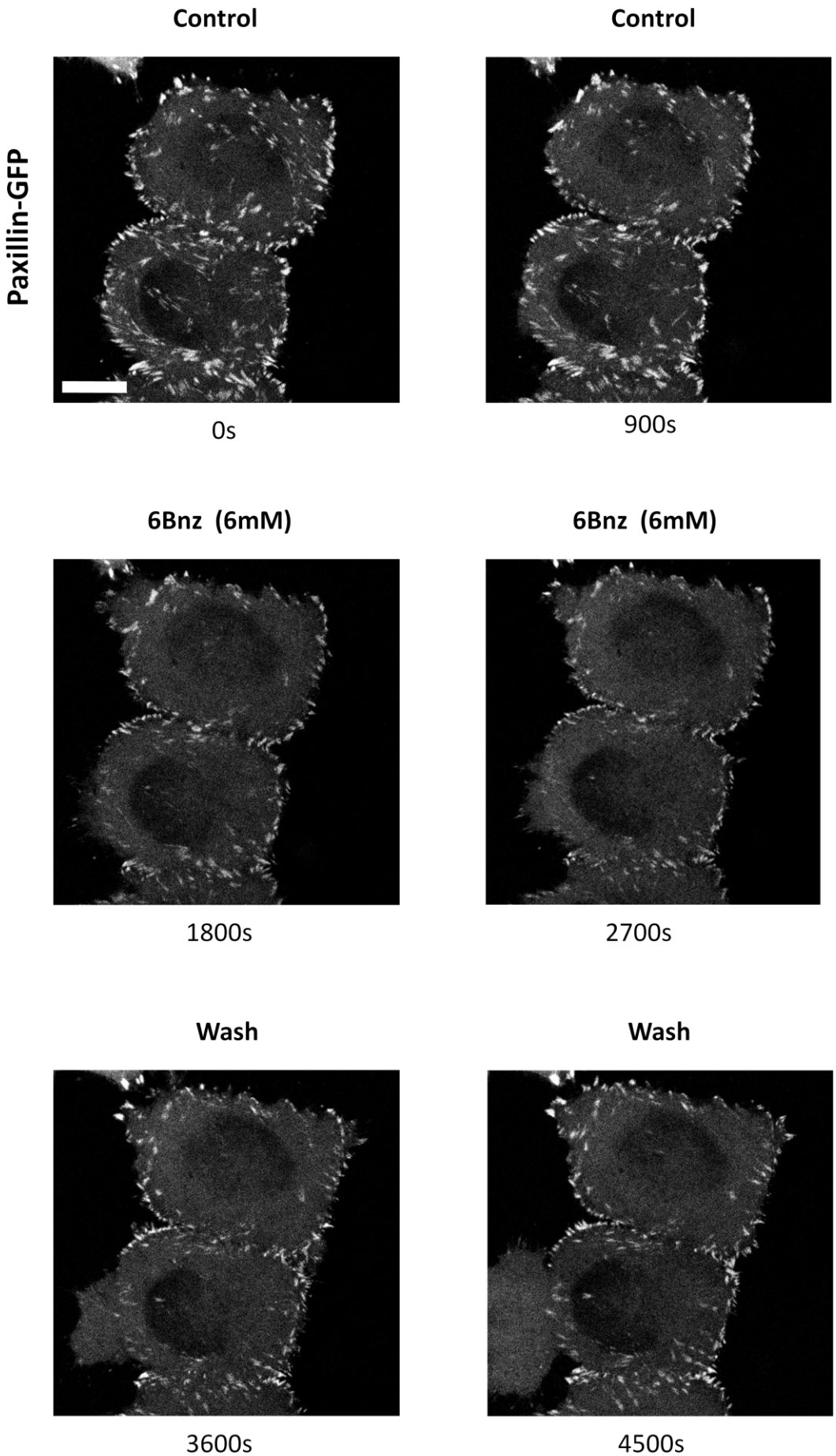
Control
Control
Paxillin-GFP
0s
900s
6Bnz (6mM)
6Bnz (6mM)
1800s
2700s
Wash
Wash
3600s
4500s

Figure 5.9. Selective EPAC activation using 8pCPT did not affect paxillin localisation. PANC-1 cells were transfected with paxillin-GFP. After 600 second control period, PANC-1 cells were treated with 8pCPT (300μM) for an extended period of 3000 seconds, which did not result in any paxillin localisation changes (n=5 cells. At least 3 independent experiments were performed. Scale bar corresponds to 10μm).

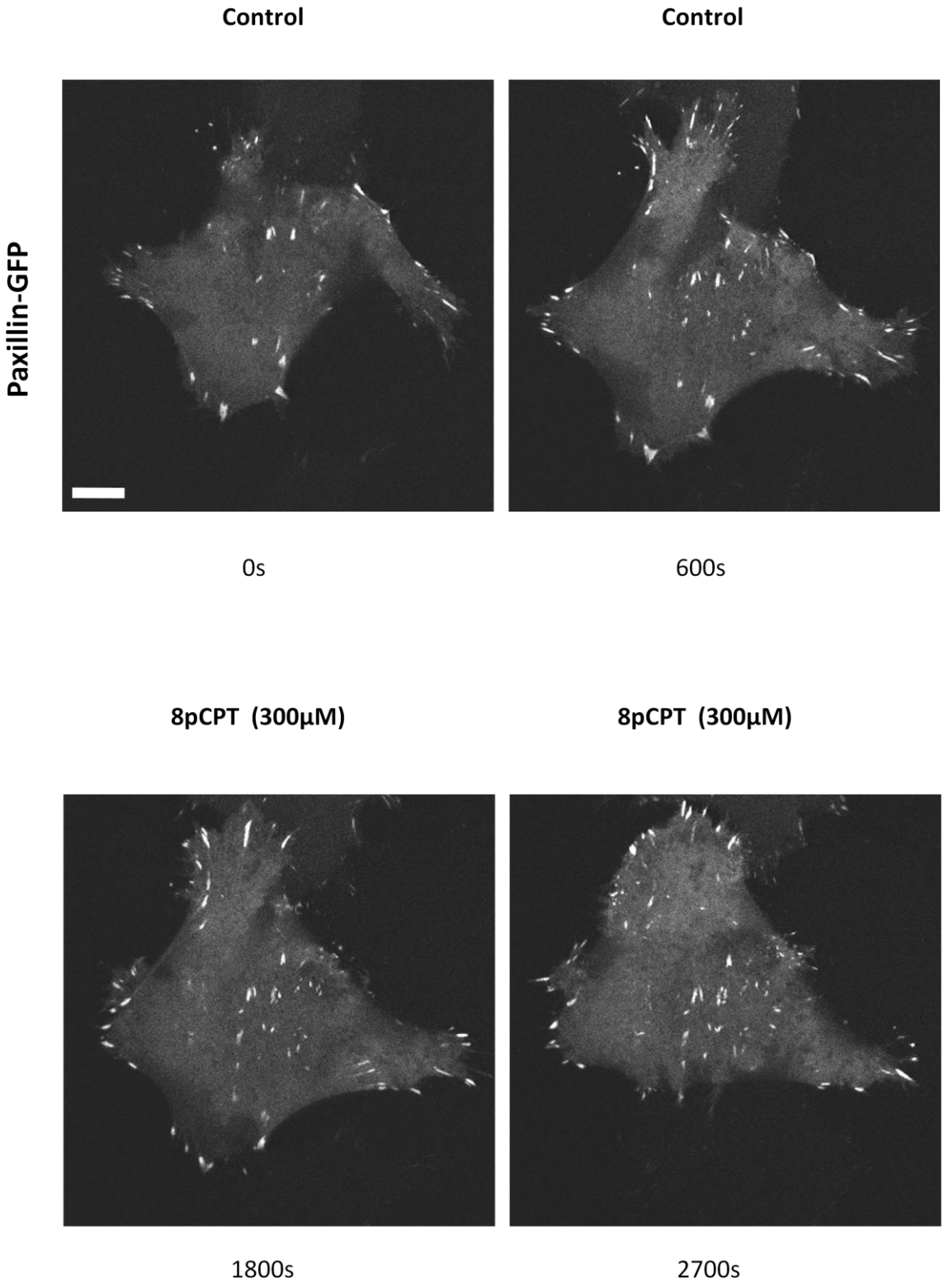
Control
Control
Paxillin-GFP
0s
600s
8pCPT (300µM)
8pCPT (300µM)
1800s
2700s

5.4. Testing PKA inhibitors.

Following observations suggesting that ruffle formation correlated with endogenous PKA activity, and selective activation of PKA inhibited migration and reduced paxillin within focal adhesions; I decided to further test the actions of PKA by using selective inhibitors of PKA. I decided to use a highly potent and selective PKA inhibitor peptide (PKI). I acquired a cell-permeable myristoylated form of PKI which was termed (Myr-PKI). PANC-1 cells were transfected with AKAR4 and imaged 24 hours later. Forskolin (20µM) + IBMX (1mM) was applied, resulting in elevation of PKA activity. Application of Myr-PKI (2µM) in combination with cAMP elevating drugs did not however reduce FRET of the sensor (Figure 5.10). This was quite surprising, considering Myr-PKI should be a highly potent drug. At the end of the experiment, another PKA inhibitor (H89) was used as a control to see if PKA inhibition could bring the AKAR4 sensor back to baseline. Although H89 is a potent inhibitor of PKA, the drug also has been shown to inhibit many other kinases at similar concentrations as required to inhibit PKA (Lochner & Moolman, 2006). For this reason, I chose to not to use H89 for our main experiments and opted to use highly selective and potent inhibitors of PKA, such as PKI (Glass *et al.*, 1986; Kumar & Walsh, 2002). Nonetheless, for the purpose as a control, H89 (10µM) was applied along with forskolin (20µM) + IBMX (1mM) + Myr-PKI (2µM), and resulted in complete reversal of the FRET sensor signal back to baseline. These data displayed that despite elevation of PKA activity with forskolin (20µM) + IBMX (1mM), inhibition of PKA should bring the AKAR4 signal back to baseline. These results therefore suggested that Myr-PKI (2µM) was not inhibiting PKA as expected. As I know, AKAR4 is quickly saturated before PKA activity is maximal, therefore it is possible that Myr-PKI (2µM) did partially inhibit PKA, but this was not visualised because of the FRET sensor limitation. However, it is still important to note that Myr-PKI was unable to strongly block PKA activity, as compared to the H89.

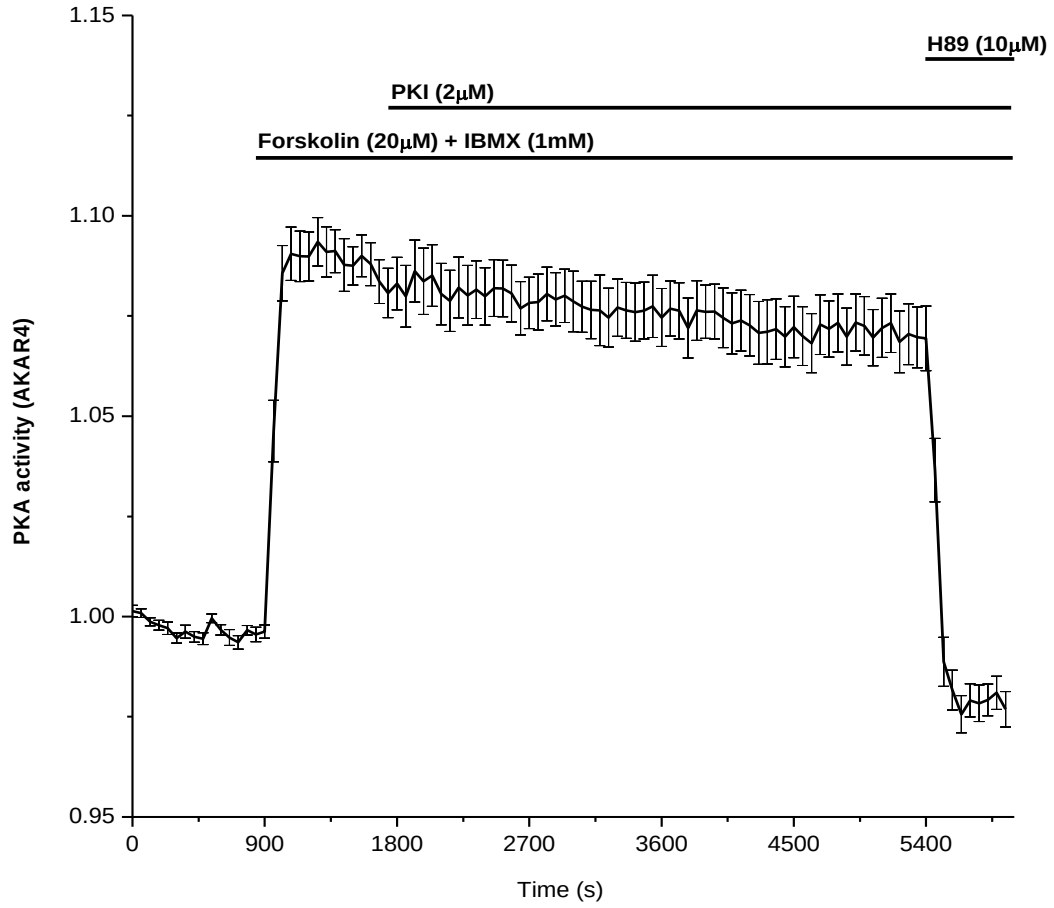

Figure 5.10. Myristoylated-PKI application did not result in the inhibition of endogenous PKA. PANC-1 cells were transfected with AKAR4. Forskolin (20μM) + IBMX (1mM) was applied and resulted in maximal FRET shift. Subsequent prolonged application of Myr-PKI (2μM), in continuing presence of forskolin + IBMX, and did not result in any obvious PKA inhibition. Application of H89 (10μM) to Myr-PKI + forskolin + IBMX resulted in a potent and quick inhibition of PKA activity (n=13 cells. At least 3 independent experiments were performed).

I went on to use a different protocol that would enable us to probe more subtle effects, if any, that Myr-PKI had on PKA activity. PANC-1 cell were transfected with AKAR4, and low dose forskolin (10μM) was applied to trigger moderate (non-saturating) FRET sensor response. This resulted in approximately 56% FRET shift, indicating PKA activity was elevated within the cells (Figure 5.11a). This was followed by application of forskolin (20μM) + IBMX (1mM) to ensure a much larger activation of endogenous PKA had occurred, which caused full saturation of the FRET sensor. In parallel, another dish of PANC-1 cells was pre-treated with Myr-PKI (2μM) for 24 hours prior to imaging (Figure 5.11b). Using the same protocol of drug application had revealed the low dose forskolin (10μM) response was not significantly affected and was displaying approximately 43% FRET shift. Subsequent application of forskolin (20μM) + IBMX (1mM) resulted in full saturation of the FRET sensor, indicating PKA activity was not inhibited by Myr-PKI.

Figure 5.11. 24 hour pre-treatment with myristoylated-PKI did not result in the inhibition of endogenous PKA. PANC-1 cells were transfected with AKAR4. In control cells, application of low dose of forskolin (10μM) resulted in approximately 56% FRET shift, and full sensor activation was achieved with forskolin (20μM) + IBMX (1mM) (**a**, n=46 cells. At least 3 independent experiments were performed). In cells pre-treated with Myr-PKI (2μM) for 24 hours prior to the experiment, and was maintained throughout the duration of the experiment. Low dose forskolin (10μM) was applied and resulted in approximately 43% FRET shift. Following this, forskolin (20μM) + IBMX (1mM) was applied and resulted in full FRET sensor saturation (**b**, n=12 cells. At least 3 independent experiments were performed).

a

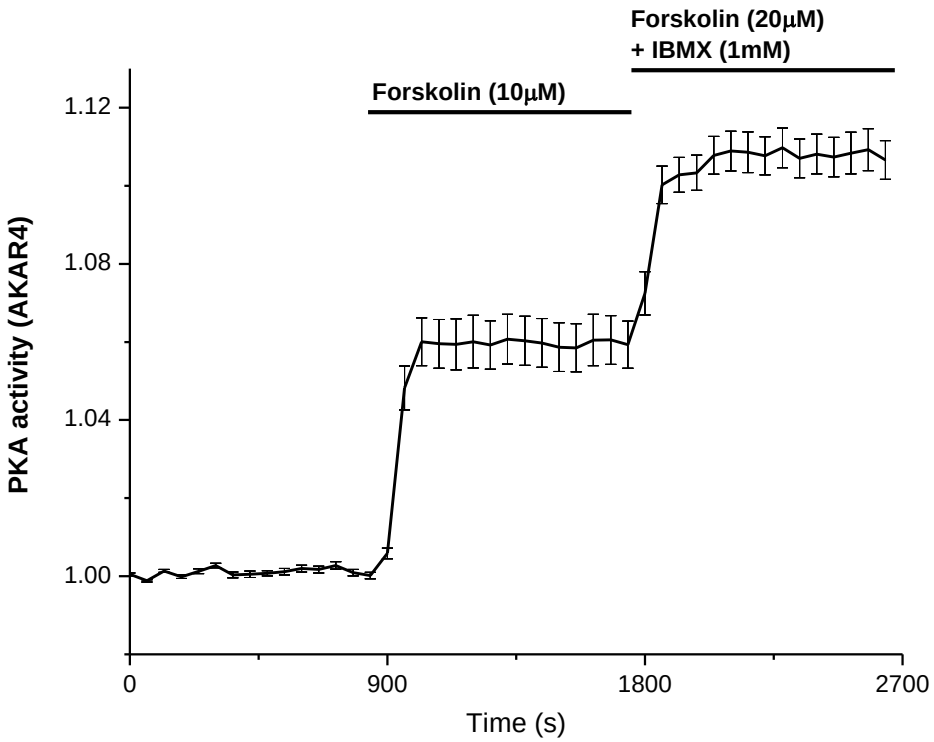
Forskolin (20μM)
+ IBMX (1mM)
Forskolin (10μM)
PKA activity (AKAR4)
1.12
1.08
1.04
1.00
0
900
1800
2700
Time (s)

b

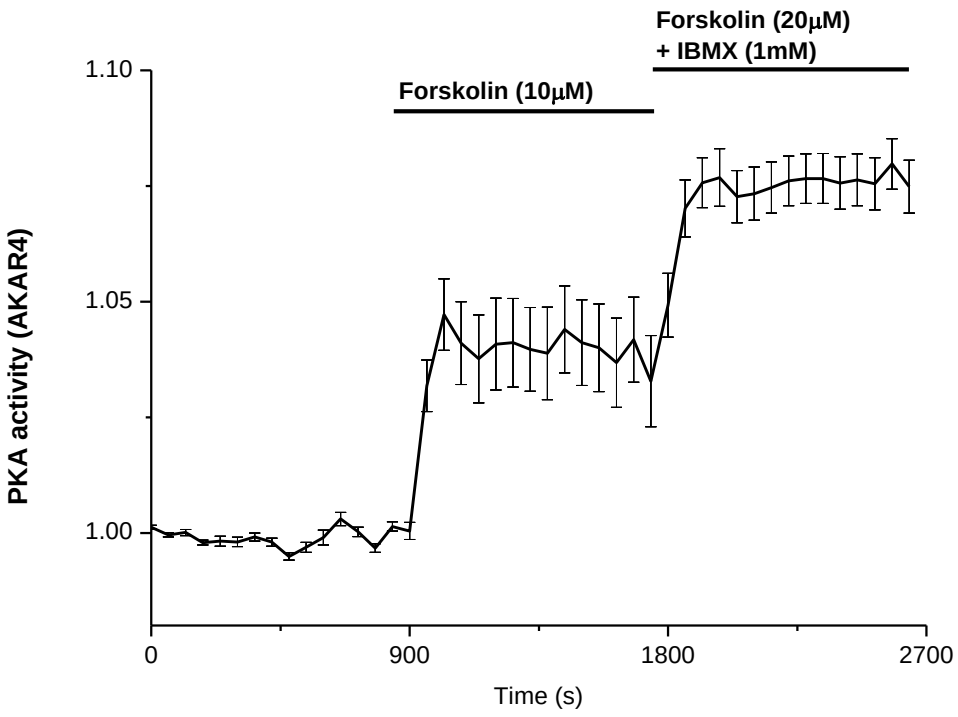
Forskolin (20μM)
+ IBMX (1mM)
Forskolin (10μM)
PKA activity (AKAR4)
1.10
1.05
1.00
0
900
1800
2700
Time (s)

Following experiments were performed by pre-treating PANC-1 cell with Myr-PKI (2μM) for 48 hours (Figure 5.12) and 96 hours (Figure 5.13). Remarkably, even with 48 hour pre-treatment period, low dose forskolin (10μM) response was unaffected as compared to control cells. With 96 hours of pre-treatment, the low dose forskolin (10μM) response was dampened to approximately 24% FRET shift, which was lower than the 56% FRET shift in control cells. However, application of forskolin (20μM) + IBMX (1mM) in all experiments resulted in quick saturation of the FRET sensor. This was an intriguing finding, suggesting that moderate level of PKA suppression can be attained after prolonged incubation with Myr-PKI. The very slow effect could be potentially explained by low permeability or slow accumulation of the compound.

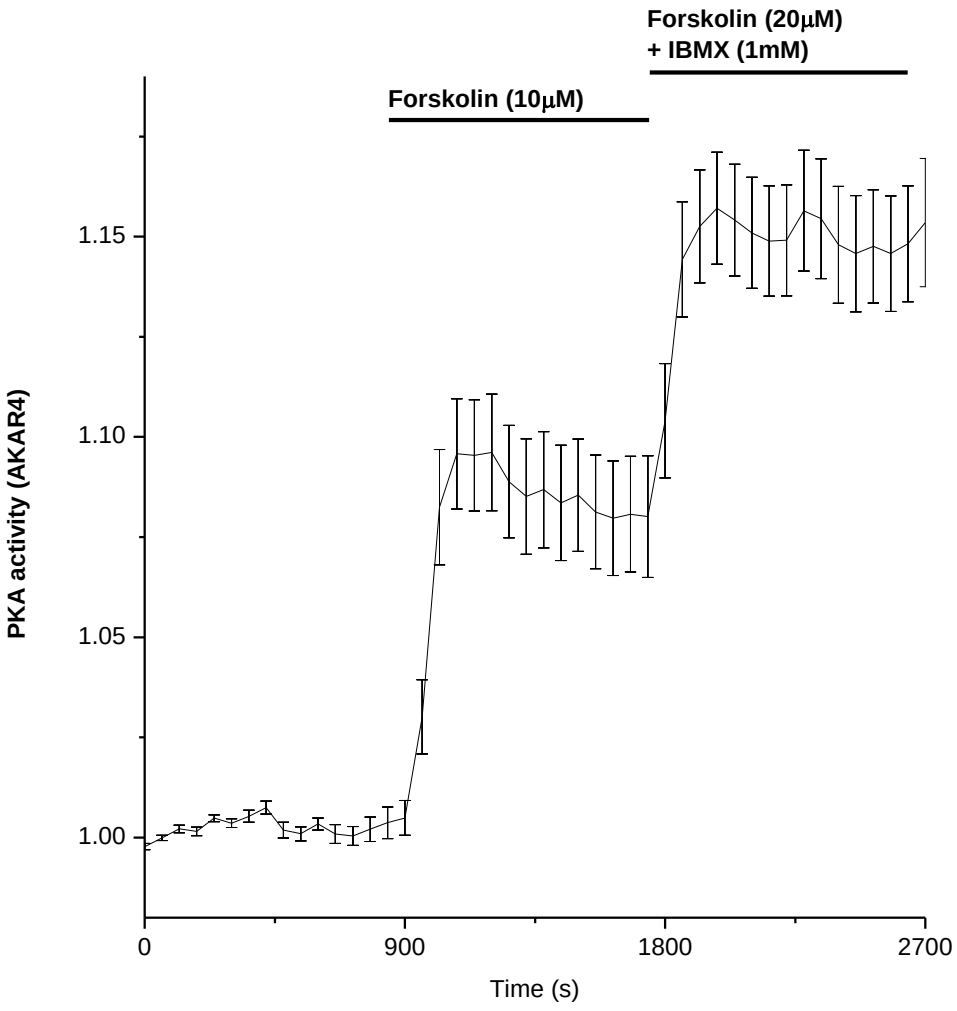

Figure 5.12. 48 hour pre-treatment with myristoylated-PKI did not result in the inhibition of endogenous PKA. PANC-1 cells were transfected with AKAR4 PKA FRET sensor. Cells were pre-treated with Myr-PKI (2μM) for 48 hours prior to the experiment, which was also maintained throughout the duration of the experiment. Low dose of forskolin (10μM) was applied and resulted in approximately 51% FRET shift. Following this, forskolin (20μM) + IBMX (1mM) was applied and resulted in full FRET sensor saturation (n=18 cells. At least 3 independent experiments were performed).

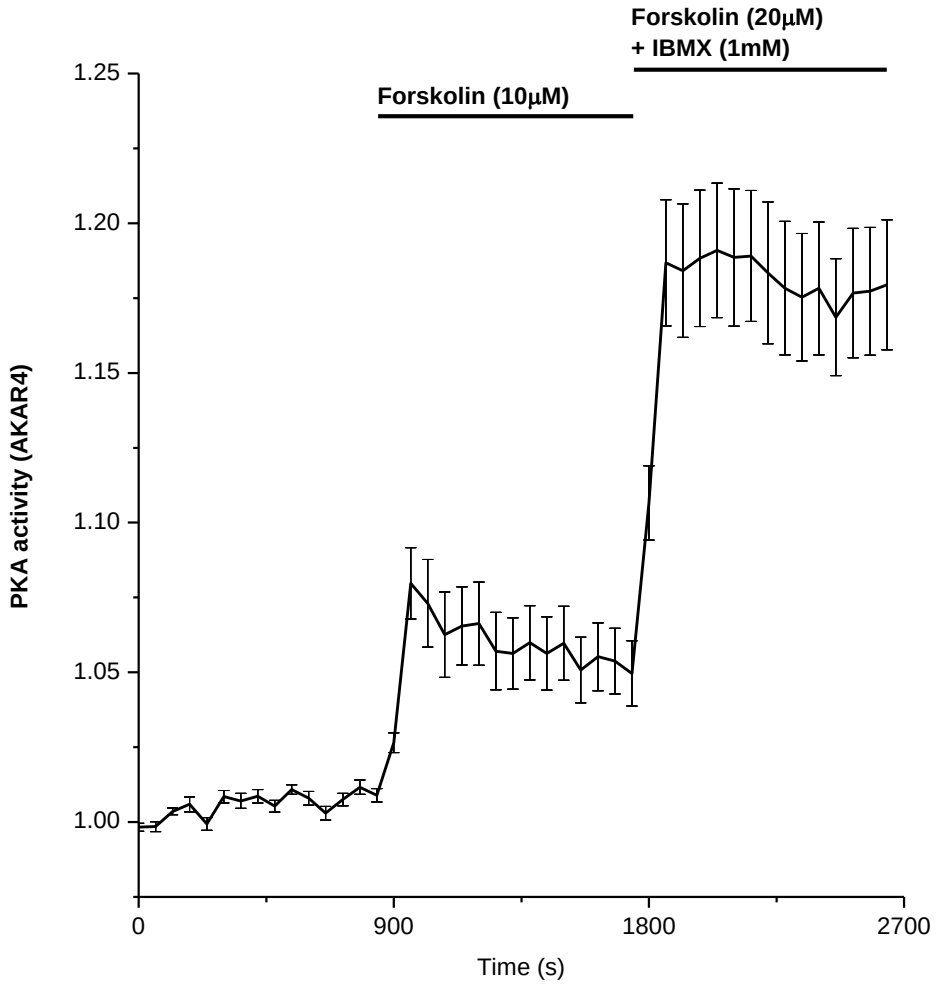

Figure 5.13. 96 hour pre-treatment with myristoylated-PKI partially suppressed the inhibition of endogenous PKA. PANC-1 cells were transfected with AKAR4. Cells were pre-treated with Myr-PKI (2μM) for 96 hours prior to the experiment, which was also maintained throughout the duration of the experiment. Low dose of forskolin (10μM) was applied and resulted in approximately 24% FRET shift. Following this, forskolin (20μM) + IBMX (1mM) was applied and resulted in full FRET sensor saturation (n=13 cells. At least 3 independent experiments were performed).

In pursuit of achieving selective and potent inhibition of PKA, I next decided to focus our attention on using a plasmid which encoded full length PKI protein. PKI was tagged with mCherry which allowed the visualisation of individual cells expressing the protein as well as quantification of the relative amount of intercellular expression amongst the cell population. I decided to use the same protocol as previously used with Myr-PKI in order to enable direct comparison of the data. PANC-1 cells were transfected with AKAR4 and PKI-mCherry constructs, and did not show any significant FRET shift in response to low dose forskolin (10µM). Further application of forskolin (20µM) + IBMX (1mM), which was expected to further increase endogenous PKA activation, also did not result in any significant FRET shift (Figure 5.14). Furthermore, it was also noted that even weakly expressing cells displayed full PKA inhibition, as evident from the lack of any significant FRET shift. Inhibition of endogenous PKA activity by PKI-mCherry thus appeared to be very potent and gave us confidence that strong endogenous PKA inhibition was attained.

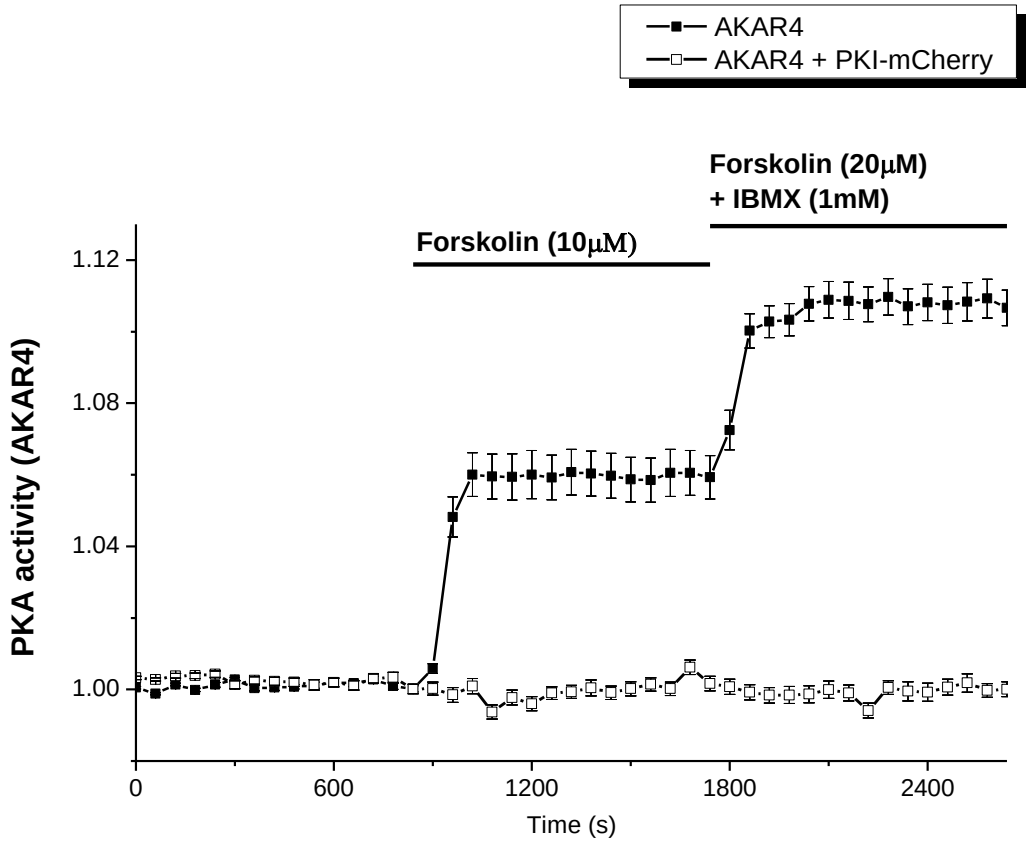

Figure 5.14. PKI-mCherry expression potently inhibits endogenous PKA activity. The experiment from Figure 5.11a (cell transfected with AKAR4) was compared with PANC-1 cells that were transfected with AKAR4 and PKI-mCherry (n=51 cells. At least 3 independent experiments were performed). Results of both set of experiments were combined on a single graph to allow direct comparison of the data. In AKAR4 expressing cells, application of low dose of forskolin (10μM) resulted in approximately 56% FRET shift, and full sensor activation was achieved with forskolin (20μM) + IBMX (1mM). Cells expressing AKAR4 + PKI-mCherry displayed no FRET shift to either low dose forskolin (10μM) or the combination of forskolin (20μM) + IBMX (1mM).

5.5. PKI-mCherry prevents the effect of cAMP induced inhibition of ruffling.

Having established PKI-mCherry was able to potently inhibit endogenous PKA activity, despite the activation induced by forskolin (20μM) + IBMX (1mM), I next proceeded to investigate the role PKA in the inhibition of ruffling, paxillin trafficking out of focal adhesions, and inhibition of migration. First, I decided to investigate the effect of PKA inhibition on cell ruffling. PANC-1 cell were transfected with PKI-mCherry and imaged 24 hours later. It is worth noting that typical transfection efficiency which was achieved for most of the constructs used was around 30%. Thus, following transfection with PKI-mCherry, I found both transfected and non-transfected population of cells within the same dish. This was partially a favourable situation, as I were able to image both cell populations within the same experiment. As mentioned previously though, PKI-mCherry appeared to be very potent, so that even low expressing cells displayed inhibition of PKA. Thus, it was important to clearly separate transfected cells from non-transfected cell population. To achieve this, high laser power corresponding to mCherry excitation was used at the beginning and end of the experiments, which clearly separated low expressing cells from the non-expressing cells. Following the start of experiment, cells were chosen from both populations which displayed stable ruffle kinetic for the duration of the control period. Cells were then subjected to application of forskolin (20μM) + IBMX (1mM). Non-expressing cells displayed typical inhibition of ruffle formation. In contrast, majority of PKI-mCherry expressing cells continued to ruffle (Figure 5.15). These results indicate that PKA activation appeared to be the key process responsible for the inhibition of ruffling.

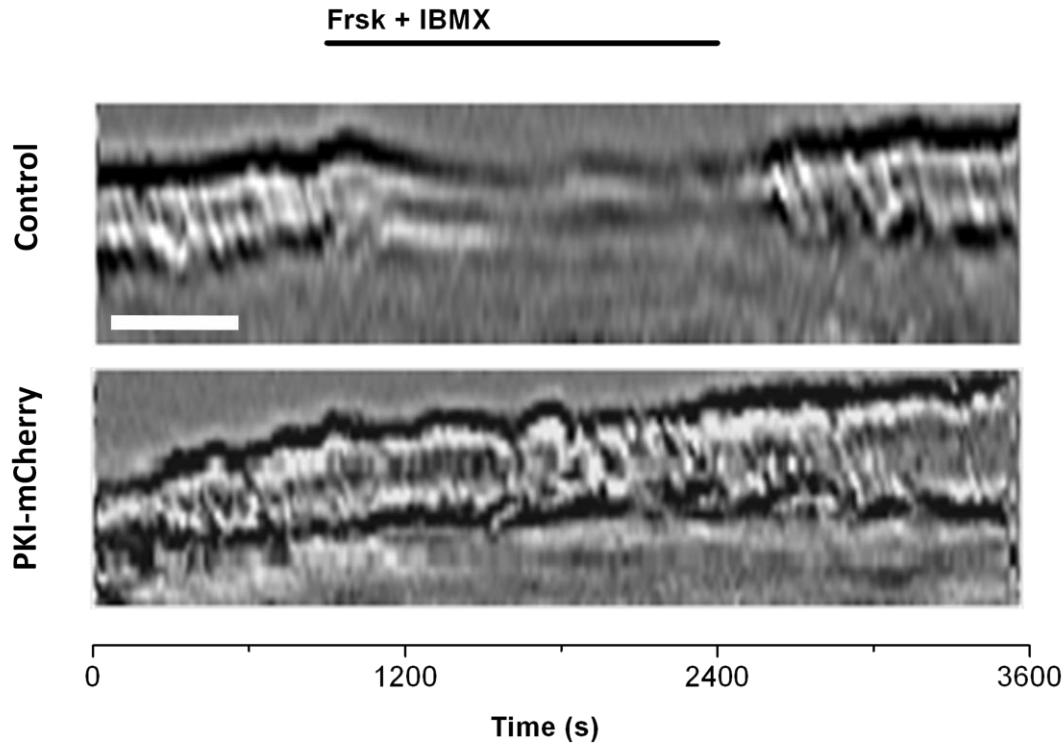

Figure 5.15. Expression of PKI-mCherry prevented ruffle inhibition induced by elevation of cAMP. PANC-1 cells were transfected with PKI-mCherry (n=36 cells. At least 3 independent experiments were performed). Of the transfected cells, 30 out of 36 cells continued to ruffle in the presence of forskolin (20μM) + IBMX (1mM). In contrast, adjacent non transfected cells showed typical reversible inhibition of ruffling. Scale bar corresponds to 5μm.

To confirm the results obtained with PKI-mCherry, which displayed that PKA inhibition prevented ruffle inhibition induced by cAMP, I utilised another genetically encoded inhibitor of PKA: dominant negative PKA tagged with GFP (dnPKA-GFP). The mechanism by which inhibition of endogenous PKA is achieved, is through expression of a regulatory subunit of PKA which contains mutated residues at the docking site responsible for interaction with the catalytic subunits. This causes altered binding of the endogenous catalytic subunits in such a way, that they can't dissociate, and thus they remain in an inactive state. Provided the construct is sufficiently expressed, it will outcompete endogenous regulatory subunits, and thus would have a net effect of inhibiting global endogenous PKA signalling.

In order to determine the ability of dnPKA to suppress PKA activation induced with forskolin (20µM) + IBMX (1mM), PANC-1 cells were dual transfected with AKAR4 and dnPKA-GFP. Cells were imaged approximately 24 hours after transfection. Dual transfected cells displayed greatly suppressed PKA activation in response to forskolin (20µM) + IBMX (1mM). Approximately 90% of cells displayed strong inhibition of PKA, so much so that no significant shift in the FRET ratio could be seen (Figure 5.16a). In the remaining 10% of the cells, responses varied, with some cells showing no apparent dampening of PKA activity, while others displayed a slower rate of change of the FRET ratio shift, indicating that some level of PKA suppression was achieved (Figure 5.16b). Unlike PKI-mCherry, dnPKA-GFP did not induce strong inhibition in all the cells, but rather in the majority of cells. Thus in any subsequent experiments utilising this construct, especially involving single cell observations, cells were co-transfected with AKAR4 to monitor PKA activity and ensure that it was indeed inhibited.

Figure 5.16. Transfection of dnPKA resulted in strong suppression of endogenous PKA activity in the majority of PANC-1 cells. PANC-1 cells were transfected with AKAR4. Cells were co-transfected with dnPKA-GFP. Forskolin (20μM) + IBMX (1mM) were applied, however no FRET shift was seen, indicating that PKA activity was strongly suppressed. This was observed in 20 out of the 24 cells, and a representative trace of a single cell is show in upper part of the figure (**a**). However, 4 out of the 24 cells displayed AKAR4 responses; representative trace is displayed in lower part of figure (**b**) (n=24 cells. At least 3 independent experiments were performed).

a

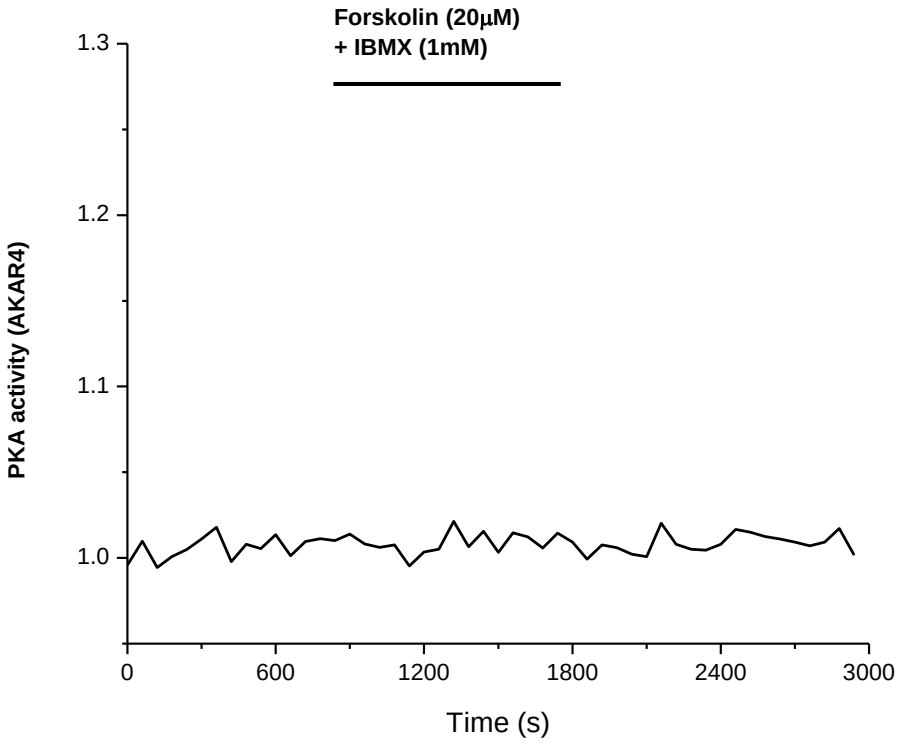
Forskolin (20μM)
+ IBMX (1mM)
PKA activity (AKAR4)
1.3
1.2
1.1
1.0
0
600
1200
1800
2400
3000
Time (s)

b

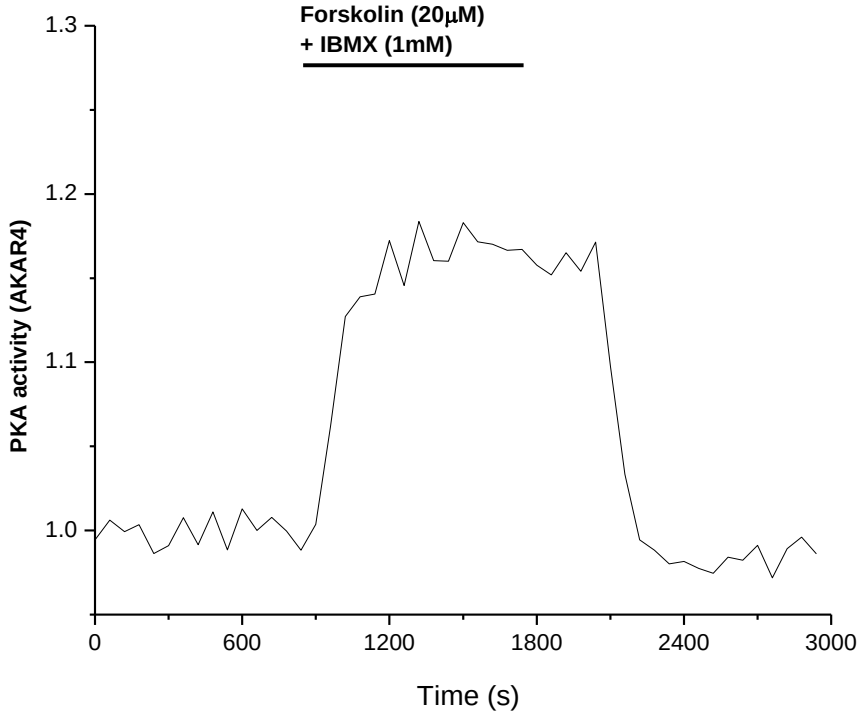
Forskolin (20μM)
+ IBMX (1mM)
PKA activity (AKAR4)
1.3
1.2
1.1
1.0
0
600
1200
1800
2400
3000
Time (s)

Having established dnPKA-GFP was able to strongly inhibit PKA in the majority of transfected cells, I wanted to confirm the results obtained with PKI-mCherry and ruffling experiments. As mentioned previously, not all cells displayed strong inhibition of PKA, thus I decided to co-transfect cells with both dnPKA-GFP and the AKAR4. This enabled us to monitor both the intracellular PKA activation along with ruffle formation. PANC-1 cells were transfected with AKAR4 and dnPKA-GFP, and were imaged 24 hours later. Forskolin (20µM) + IBMX (1mM) induced the characteristic inhibition of ruffles in non-expressing cells (data not shown). Duel transfected cells however, displayed no significant shift in AKAR4 FRET ratio, and did not display inhibition of ruffling (Figure 5.17). These results confirmed previous observations made with PKI-mCherry, supporting the finding that inhibition of ruffling by elevation of cAMP is due to activation of endogenous PKA.

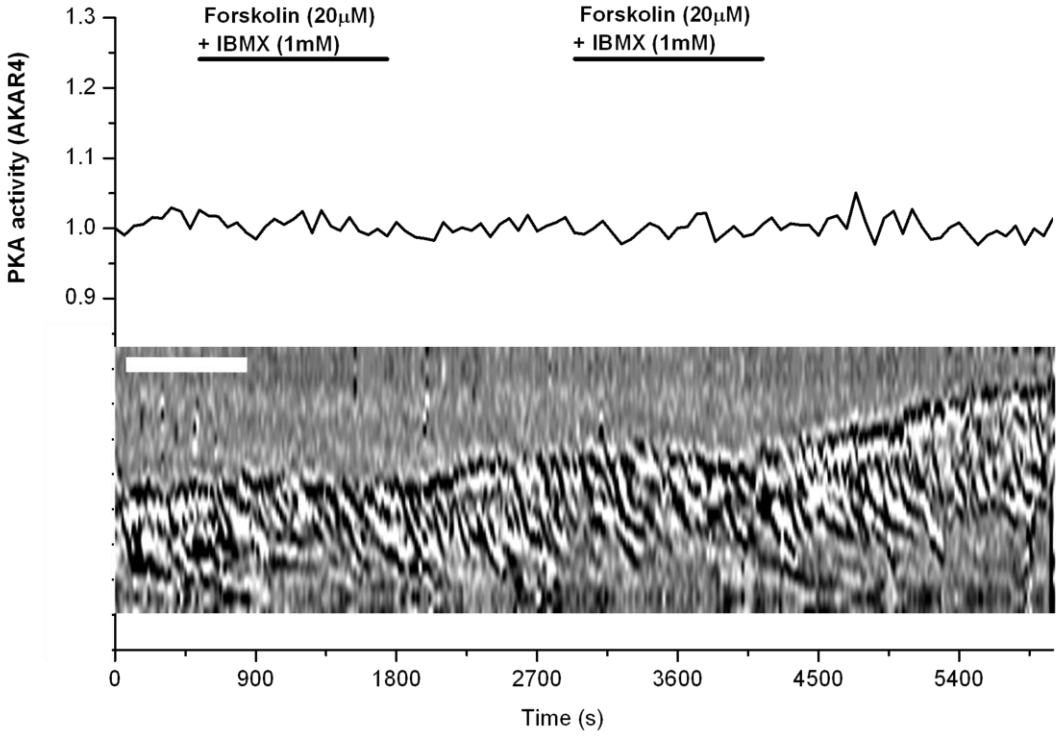

Figure 5.17. Genetic inhibition of endogenous PKA prevented ruffle inhibition induced by elevation of cAMP. PANC-1 cells were transfected with AKAR4. Cells were co-transfected with dnPKA-GFP. Forskolin (20μM) + IBMX (1mM) was applied, however the PKA FRET sensor confirmed that endogenous PKA was strongly suppressed in this cell. Simultaneous recording of ruffling, revealed that PKA suppression prevented ruffle inhibition by forskolin/IBMX (n= 3 cells. 3 independent experiments were performed. Scale bar corresponds to 5μm).

5.6. Selective PKA inhibition prevents the loss of paxillin from focal adhesions in response to cAMP elevation.

I next concentrated on establishing whether PKA inhibition would prevent cAMP induced loss of paxillin from focal adhesions. PANC-1 cells were transfected with paxillin-GFP alone or in combination with PKI-mCherry. Cells were imaged for 15 minutes as a control period; this was followed by 30 minutes of forskolin (20μM) + IBMX (1mM) treatment. Cells that did not express PKI-mCherry displayed typical loss of paxillin out of focal adhesions in response to forskolin + IBMX application (Figure 5.18). In cells expressing PKI-mCherry however, paxillin loss from focal adhesions was greatly reduced.

In order to quantify the effect of forskolin + IBMX on paxillin trafficking, its fluorescence within focal adhesions was compared to cytosolic levels as previously described. Very briefly, regions of interest were drawn around each of the clearly visible focal adhesions. Corresponding regions of interest was drawn in the vicinity of the focal adhesion. A ratio of paxillin intensity within a focal adhesion relative to adjacent cytosolic fluorescence was calculated to reveal the level of paxillin incorporation within the focal adhesion. After the data was combined for paxillin (Figure 5.18) and paxillin + PKI-mCherry (Figure 5.19) cells, it was found that PKA inhibition significantly prevented paxillin loss from focal adhesions (Figure 5.20). Immediately prior to addition of forskolin (20μM) + IBMX (1mM), the ratio of focal adhesion to cytosolic paxillin was calculated for paxillin-GFP only expressing cells as 2.24. Cells expressing both paxillin-GFP and PKI-mCherry displayed a ratio of 2.13. Following elevation of cAMP by forskolin (20μM) + IBMX (1mM) for 30 minutes in paxillin transfected cells, the ratio was reduced to 1.32; while paxillin + PKI-mCherry expressing cells displayed a drop to only 1.82, which was significantly higher than that for the control condition.

Figure 5.18. Cell transfected with paxillin-GFP displayed typical loss of paxillin from focal adhesions in response cAMP elevation. PANC-1 cells were transfected with paxillin-GFP. After a 900 second control period, forskolin (20μM) + IBMX (1mM) was applied for a duration of 1800 seconds. Paxillin-GFP transfected cells displayed typical loss of paxillin out of focal adhesions in response to cAMP elevation (n=23 cells. At least 3 independent experiments were performed. Scale bar corresponds to 10μm).

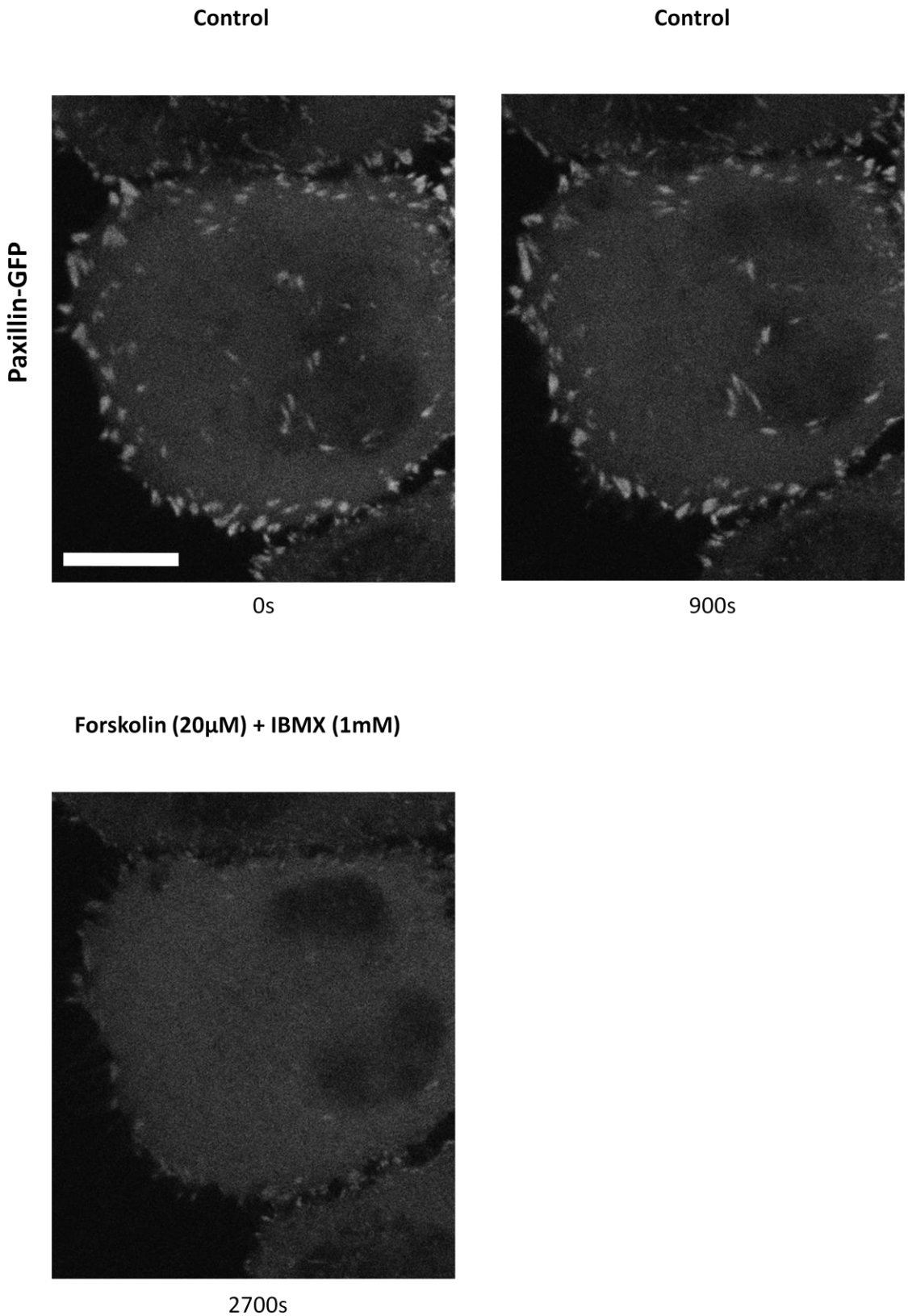
Control
Control
Paxillin-GFP
0s
900s
Forskolin (20µM) + IBMX (1mM)
2700s

Figure 5.19. In cells expressing paxillin-GFP and PKI-mCherry, paxillin loss from focal adhesions in response to forskolin + IBMX was suppressed. PANC-1 cells were duel transfected with paxillin-GFP and PKI-mCherry. After a 900 second control period, forskolin (20μM) + IBMX (1mM) was applied for a duration of 1800 seconds. Duel transfected cells displayed much reduced loss of paxillin out of focal adhesions in response to cAMP elevation (n=29 cells. At least 3 independent experiments were performed. Scale bar corresponds to 10μm).

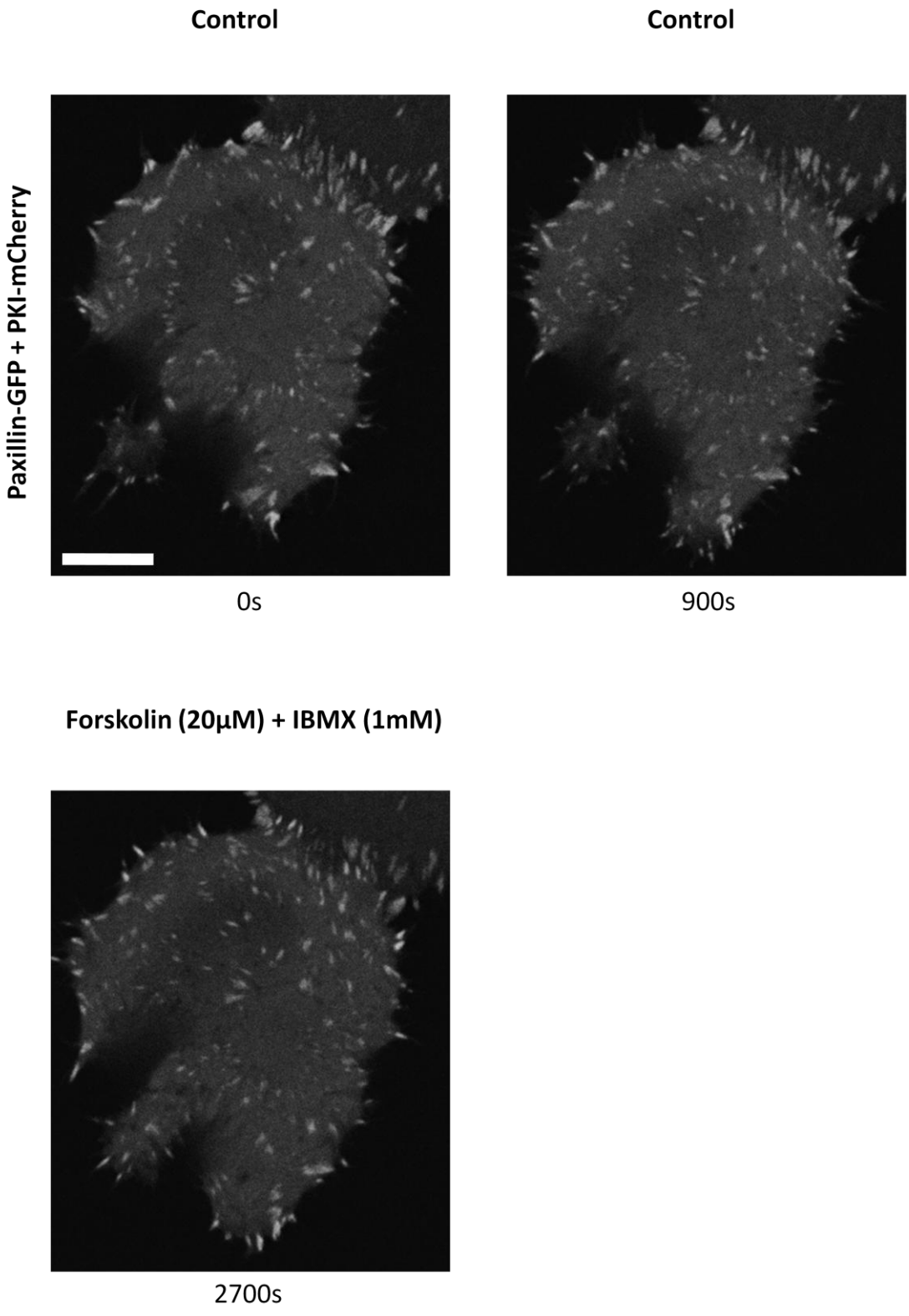
Control
Control
Paxillin-GFP + PKI-mCherry
0s
900s
Forskolin (20µM) + IBMX (1mM)
2700s

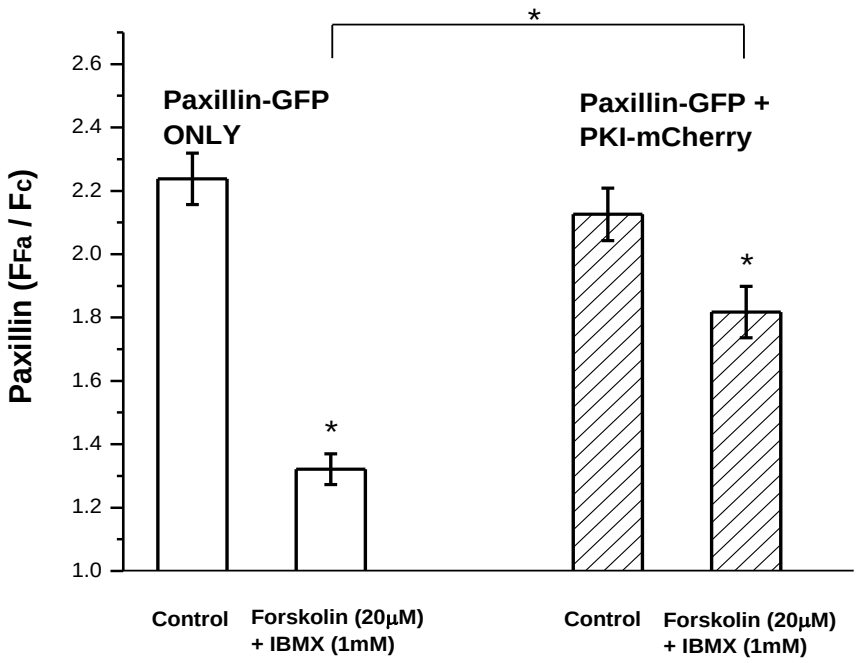

Figure 5.20. Inhibition of PKA prevents paxillin loss from focal adhesions in response to cAMP elevation. PANC-1 cells were transfected with paxillin-GFP only (n=23 cells) or in combination with PKI-mCherry (n=29 cells). Cells were imaged for a 900 second control period, after which forskolin (20μM) + IBMX (1mM) was applied for 1800 seconds. For both single and dual transfected cells, the focal adhesion incorporated paxillin relative to cytosolic paxillin was calculated immediately before application of drugs, and 1800 seconds after. Immediately prior to drug application, cells expressing paxillin-GFP displayed 2.24 fold higher fluorescence in focal adhesions relative to the cytosol. After 1800 seconds of forskolin (20μM) + IBMX (1mM) treatment, paxillin ratio was reduced to 1.32. Immediately prior to drug application, cells expressing paxillin-GFP and PKI-mCherry displayed 2.13 fold higher fluorescence in focal adhesions relative to the cytosol. After 1800 seconds of forskolin (20μM) + IBMX (1mM) treatment, paxillin ratio was reduced to only 1.82; displaying a significant rescue relative to paxillin-GFP expressing cells. (At least 3 independent experiments were performed. Results that were statistically significant to $p<0.05$ are indicated by * symbol).

5.7. Selective PKA inhibition prevents the induced inhibition of migration.

Having confirmed the involvement of PKA signalling in controlling ruffling and paxillin focal adhesion trafficking, I now turned our attention to migration of PANC-1 cells. I used Boyden chambers to measure migration as previously described. However, one key difference which was employed specifically for these set of experiments was the use of Boyden chambers with a membrane which that prevented the bleed-through of fluorescence from top of the membrane to the bottom side (BD Fluoroblok coating). Thus, there was no need to remove non-migrated cells from the top well, and the chambers could be imaged live without fixation. This was advantageous in this particular situation, as I were interested in only imaging transfected cells. Two experiments were performed in parallel; cells were either transfected with PKI-mCherry or a plasmid encoding mCherry only. Each set of cells was treated with a control vehicle or forskolin (20µM) + IBMX (1mM). Following 6 hours of migration, transfected cells which migrated to the bottom of the membrane were imaged. The number of drug treated cells were normalised to the corresponding control condition, and displayed as a percentage. Application of forskolin (20µM) + IBMX (1mM) was found to inhibit migration of mCherry only transfected cells to 13% of the control. However, PKI-mCherry expressing cells displayed a significant rescue of migration to 48% of their corresponding control (Figure 5.21). As with paxillin, I do not see a complete rescue of migration when I inhibit PKA. This would suggest that other effectors besides PKA could be involved in further suppressing PANC-1 migration. However it is important to note that the results indicate that PKA plays a major role in inhibiting cell migration.

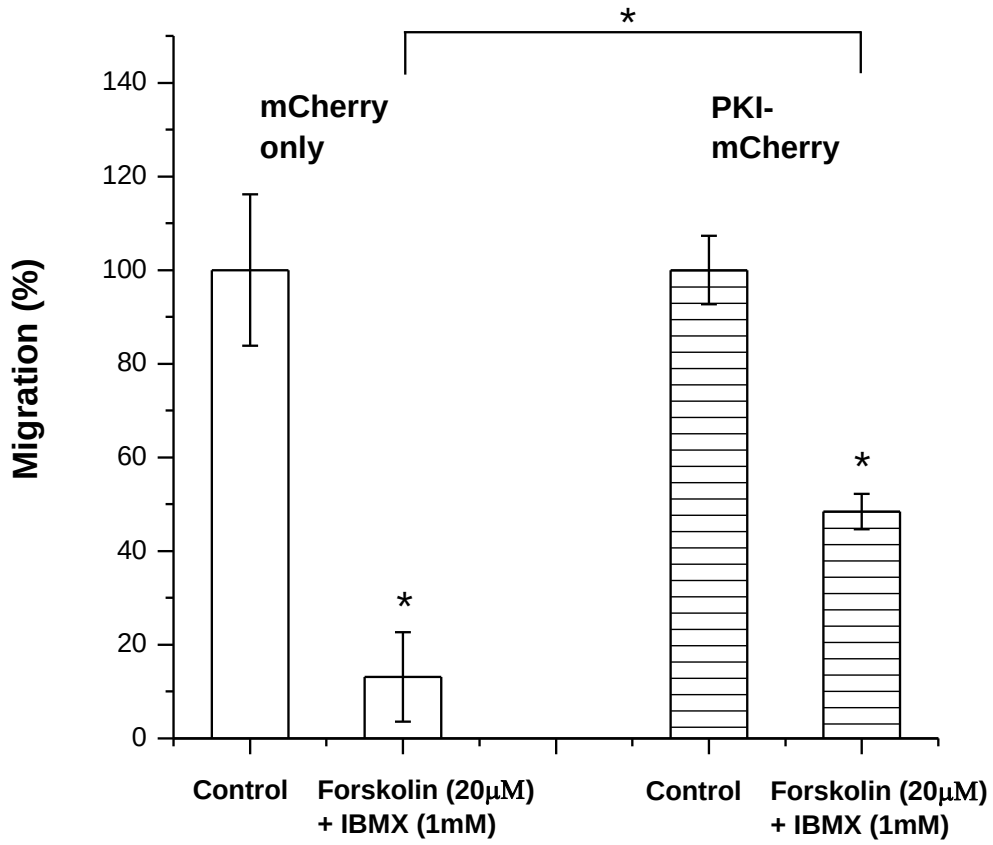

Figure 5.21. PKI-mCherry significantly suppresses forskolin + IBMX induced inhibition of migration. Cell migration was investigated using Boyden chambers supplemented with DMEM + 1% FBS in both top and bottom wells. Cells were allowed to migrate from top to bottom wells for 6h post seeding. Results were normalized relative to the corresponding control and displayed as a percentage. PANC-1 cell were either transfected with PKI-mCherry or a vector encoding mCherry only. Each group was treated with control vehicle or forskolin (20μM) + IBMX (1mM); mCherry only expressing cells were inhibited to 13% relative to their control, while PKI-mCherry expressing cells were inhibited to only 48% relative to their control (n=6 Boyden chambers for each condition. At least 3 independent experiments were performed. Results that were statistically significant to $p<0.05$ are indicated by * symbol).

5.7.1. PKA inhibition induces cell migration.

Having established that PKA activation inhibits PANC-1 migration, I wanted to find out whether inhibiting basal PKA activity would affect migration. PANC-1 cells were transfected with either PKI-mCherry or a plasmid encoding mCherry only. It was found that inhibition of PKA accelerated migration rate to 139% relative to cells expressing mCherry (Figure 5.22). This result was not however statistically significant (P=0.0998). This result suggested that PKA signalling in plays a net negative role in controlling migration; thus when PKA activity was inhibited, migration rate had a tendency to increase.

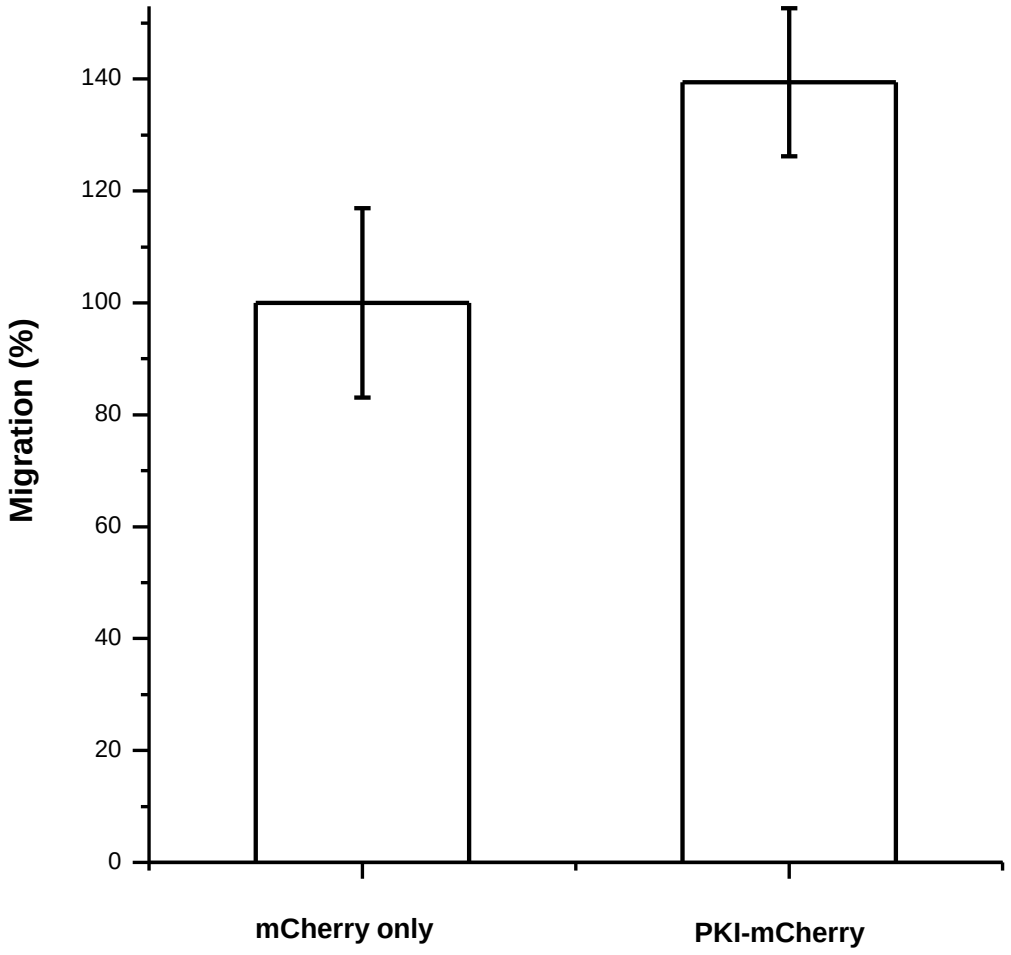

Figure 5.22. The effect of PKI-mCherry expression on cell migration. Cell migration was investigated using Boyden chambers supplemented with DMEM + 1% FBS in both top and bottom wells. Cells were allowed to migrate from top to bottom wells for 6h post seeding. PANC-1 cells were either transfected with PKI-mCherry, or mCherry only (n=6 Boyden chambers for each condition. At least 3 independent experiments were performed. These results were not statistically significant).

5.7.2. Uncoupling PKA from signalling microdomains by disrupting its binding to AKAPs enhances cellular migration rate.

Intrigued by the previous finding, I wanted to further investigate the role of PKA in migration, specifically with respect to compartmentalised PKA signalling. As described previously, the majority, if not all of PKA is targeted to various compartments of the cell through association with AKAP's (Pidoux & Tasken, 2010). This helps regulate the rather broad substrate specificity that PKA has, and produce spatially and temporally restricted signalling complexes. To see what would happen if PKA was uncoupled from such signalling domains, I utilised a peptide named st-Ht31. This cell-permeable compound is able to inhibit the interaction between PKA regulatory subunits and AKAP's (Rosenmund *et al.*, 1994; Pidoux & Tasken, 2010). Cell migration was investigated using standard Boyden chambers as described previously. Cells were treated with either control inactive peptide st-Ht31P (2µM) or the active peptide st-Ht31 (2µM). Following 6 hours of migration cells were quantified. These experiments revealed a remarkable result: cells treated with active AKAP binding disruptor peptide migrated much faster than control cells. Migration rate increased to 240% of the control condition (Figure 5.23). These results indicated that PKA signalling is important in modulating cell migration, and that disruption of compartmentalised PKA signalling could lead to large increase in cell migration. It can also be speculated that the induction of migration induced by PKA uncoupling could be due to the remaining unaffected and unopposed EPAC signalling. This is consistent with our results indicating that selective EPAC activation can lead to the potentiation of migration (see Chapter 4, Figure 5.3).

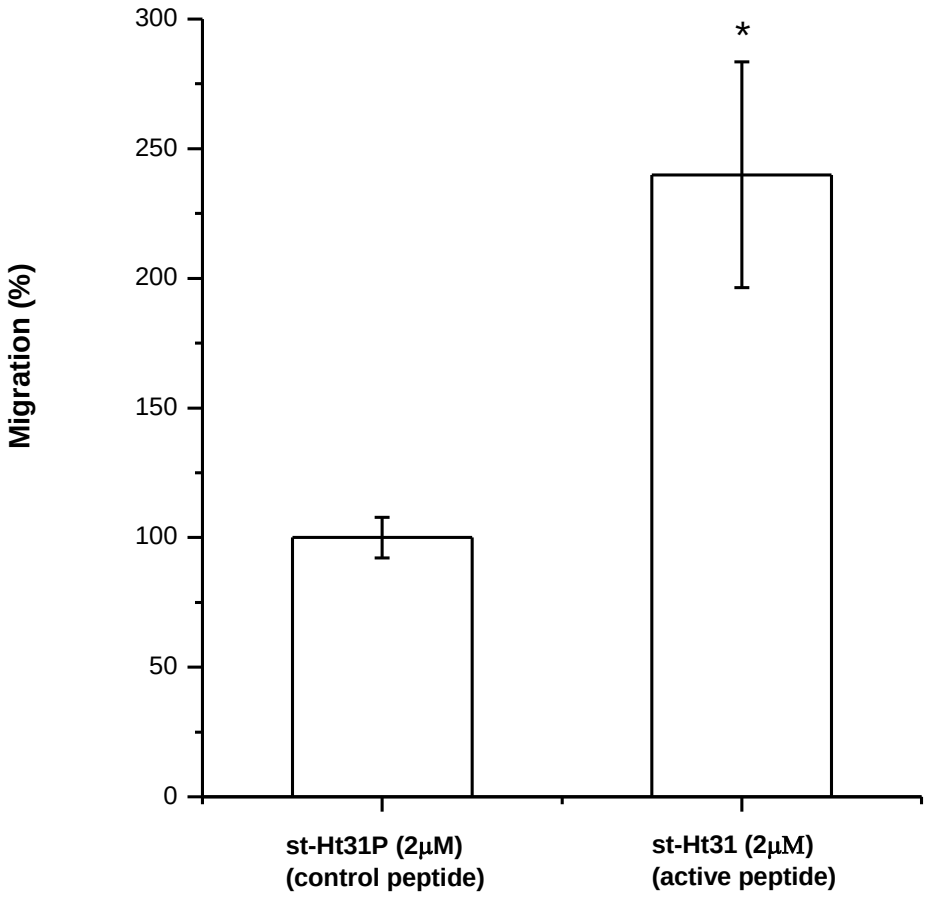

Figure 5.23. Disrupting compartmentalised PKA signalling with st-Ht31 potentiated PANC-1 migration. Cell migration was investigated using Boyden chambers supplemented with DMEM + 1% FBS in both top and bottom wells. Cells were allowed to migrate from top to bottom wells for 6h post seeding. Results were normalized relative to control inactive peptide and displayed as a percentage. Treatment with st-Ht31 (2μM) resulted in strong potentiation of PANC-1 migration (n=6 Boyden chambers for each condition. At least 3 independent experiments were performed. All results were statistically significant to $p<0.05$ and indicated by * symbol).

Summary of the key results in Chapter 5.

In this chapter I utilised selective inhibitor of PKA and selective activators of PKA and EPAC. The selectivity of these compounds was confirmed using EPAC based sensor and AKAR4. The results of experiments involving selective inhibition of PKA suggested that the observed cAMP-induced inhibition of PANC-1 migration (and processes associated with migration) is mediated by PKA. This conclusion was strengthened by observation that a PKA activator induced significant inhibition of migration. Interestingly, selective activation of EPAC potentiated the migration, highlighting the opposing actions of two primary cAMP sensors on the motility in this type of cancer cells.

CHAPTER 6 – DISCUSSION

6.1. cAMP inhibits migration in 5 diverse PDAC cell lines.

Pancreatic ductal adenocarcinoma (PDAC) is characterised by a very high mortality rate (Siegel *et al.*, 2012). The disease initially develops asymptomatically and at the time of diagnosis patients usually have multiple metastases (Rhim *et al.*, 2012). Cellular migration is important for the development of metastasis. Therefore, our studies of the mechanism involved in the regulation of this process (in our case cAMP-dependednt mechanisms) are important for the understanding of the disease. The development of pancreatic adenocarcinoma occurs through accumulation of various mutations and genetic alterations leading to the activation of oncogenes (e.g. activation of KRAS) as well as inactivation of tumour suppressor genes (e.g. SMAD4) (Iacobuzio-Donahue *et al.*, 2012). Due to the random nature of acquiring multiple mutations, this can lead to the development of different sub-classes of the same disease (Jones *et al.*, 2008). It is therefore important to consider that differential development of the disease amongst patients can be due to involvement of different cellular mechanisms; and so it is important to test the role of specific signalling processes on as many diverse forms of pancreatic adenocarcinoma as practical. For this reason, I decided to focus on using 5 diverse pancreatic adenocarcinoma cell lines which encompass different gene mutations and tumorigenicity potential (Moore *et al.*, 2001; Deer *et al.*, 2010). The following pancreatic adenocarcinoma cell lines were studied in our investigation: PANC-1, SUIT-2, BxPC-3, Capan-2, and MIA PaCa-2. PANC-1 cell lines were originally cultured from the primary tumour of a 56 year old male with adenocarcinoma being present in the head of the pancreas (Lieber *et al.*, 1975). Invasion of the carcinoma was found in the duodenal wall of the patient. SUIT-2 was derived from a metastatic liver tumour with pancreatic carcinoma origin (Iwamura *et al.*, 1987). BxPC-3 was obtained from a 61 year old woman from an adenocarcinoma in the body of the pancreas (Tan *et al.*, 1986). Despite chemotherapy and radiation treatments the patient died within 6 months. Capan-2 originated from a 56 year old male diagnosed with

pancreatic adenocarcinoma (Kyriazis *et al.*, 1986). The cell line was derived from the primary tumour. MIA PaCa-2 cell line was derived from a 65 year old man with the pancreatic adenocarcinoma (Yunis *et al.*, 1977). No information is available whether metastasis had occurred within the patient; cell line was established from the primary tumour.

Four most common genetic alterations which occur within pancreatic cancers include v-Ki-ras2 Kirsten rat sarcoma viral oncogenes homolog (KRAS); the mutation leads to constitutively active form of KRAS (Malumbres & Barbacid, 2003). Alterations in the TP53 tumour suppressor gene, encoding for the protein p53, is also commonly muted in many pancreatic cancer cell lines, resulting in a non-functional protein (Scarpa *et al.*, 1993). Tumour suppressor protein SMAD4 (also known as DPC4) is also commonly inhibited though mutations or is deleted in approximately 50% of pancreatic adenocarcinoma cell lines (Kim *et al.*, 1996). Similarly, tumour suppressor CDKN2Aα (also known as p16) is also inhibited through genetic mutations or is fully deleted in many pancreatic adenocarcinoma cell lines studied (Caldas *et al.*, 1994). The cell lines used in this study all have different mutations which between them cover the four most common genetic alterations. Mutated KRAS was found in Capan-2 (Berrozpe *et al.*, 1994; Aoki *et al.*, 2000; Moore *et al.*, 2001; Loukopoulos *et al.*, 2004), MIA PaCa-2 (Durodola, 1975; Berrozpe *et al.*, 1994; Kita *et al.*, 1999; Moore *et al.*, 2001; Sun *et al.*, 2001), and PANC-1 cells (Berrozpe *et al.*, 1994; Kita *et al.*, 1999; Yang *et al.*, 1999; Sun *et al.*, 2001; Loukopoulos *et al.*, 2004). However, wild type KRAS was present in BxPC-3 cells (Berrozpe *et al.*, 1994; Aoki *et al.*, 2000; Sun *et al.*, 2001; Loukopoulos *et al.*, 2004). In contrast, mutated TP53 was found in BxPC-3 (Berrozpe *et al.*, 1994; Caldas *et al.*, 1994; Sun *et al.*, 2001; Loukopoulos *et al.*, 2004), MIA PaCa-2 (Berrozpe *et al.*, 1994; Caldas *et al.*, 1994; Moore *et al.*, 2001; Sun *et al.*, 2001) and PANC-1 (Berrozpe

et al., 1994; Caldas *et al.*, 1994; Yang *et al.*, 1999; Moore *et al.*, 2001; Sun *et al.*, 2001; Loukopoulos *et al.*, 2004). However discrepancy was found which indicated that Capan-2 cells either had wild type TP53 (Caldas *et al.*, 1994; Loukopoulos *et al.*, 2004) or a mutation at intron 4, which resulted in a 200 base pair deletion (Berrozpe *et al.*, 1994). SMAD4 was found to be wild type in Capan-2 (Loukopoulos *et al.*, 2004), MIA PaCa-2 (Moore *et al.*, 2001; Sun *et al.*, 2001) and PANC-1 (Moore *et al.*, 2001; Sun *et al.*, 2001; Loukopoulos *et al.*, 2004) cell lines. BxPC-3 on the other hand displayed a homozygous deletion of SMAD4 (Hahn *et al.*, 1996; Aoki *et al.*, 2000; Sun *et al.*, 2001; Loukopoulos *et al.*, 2004). Finally, PANC-1 (Caldas *et al.*, 1994; Huang *et al.*, 1996; Moore *et al.*, 2001; Sun *et al.*, 2001; Loukopoulos *et al.*, 2004) and MIA PaCa-2 (Caldas *et al.*, 1994; Huang *et al.*, 1996; Moore *et al.*, 2001; Sun *et al.*, 2001) both display homozygous deletion of CDKN2Aα tumour suppressor. However, discrepancy was found with both BxPC-3 and Capan-2 cell lines. Both wild type (Loukopoulos *et al.*, 2004) and homozygous deletion (Caldas *et al.*, 1994; Huang *et al.*, 1996; Sun *et al.*, 2001) were found in BxPC-3 cells. Capan-2 cells displayed either wild type (Loukopoulos *et al.*, 2004), or have a mutation which resulted in a 6 base pair insertion (Caldas *et al.*, 1994) or 7 (Huang *et al.*, 1996). It is interesting to note that different results have been found for mutations of the genes in several cell lines. A possible explanation for such findings is that additional gene mutations could have developed over time during routine cell culture. Also it is noted that the original tumour sample used to establish a particular cell line could its self have had a heterogeneous population of cells (Sun *et al.*, 2001). The known mutations in the SUIT-2 cell line, are the activating KRAS mutation, inactivation of p53, and homozygous deletion of CDKN2Aα (Moore *et al.*, 2001).

After completing experiments with five different cell lines used in this study, I have found that elevation of cAMP inhibited migration in all of cell lines tested, regardless of their

genetic background. This would strongly indicate that the mechanism responsible for the effects of cAMP on migration is common to all cell lines used, and was not specific to a particular cell line. Furthermore, this finding would suggest that cAMP elevation can be used to suppress migration in a broad range of pancreatic adenocarcinoma genetic subtypes.

6.2. cAMP inhibits migration and invasion in different modes of migration.

As mentioned previously, basic mechanisms which govern cell motility have been well documented and are thought to be well understood. In general, cells acquire polarised morphology and have a leading and trailing edge. Intracellular signalling ensures active protrusion / retraction cycles at the leading edge. The protruding area of the cell can bind to the extracellular matrix via integrin mediated adhesion. Contractile forces generated within the cell can pull the cell towards the leading edge, while controlled detachment at the trailing edge ensures effective migration (Lauffenburger & Horwitz, 1996; Ridley *et al.*, 2003). This sequence of steps is seen in large variety of epithelial and mesenchymal cells, and is a process known as 'the cell motility cycle'. What is less well defined is intracellular polarised signalling which specifically leads to the formation and maintenance of polarised morphology (and therefore results in directional migration).

Non-directional migration can occur in response to uniform application of stimulatory chemoattractant signals, such as platelet derived growth factor (PDGF) and FBS (Seppa *et al.*, 1982; Muinonen-Martin *et al.*, 2010). The resulting migration can be fast, however it usually lacks specific directionality, as the net movement of the cells would be much smaller than the total distance travelled. Upon application of a gradient of

chemoattractant, the cells acquire a steering mechanism which is coupled to the cell's migratory machinery. The resulting movement is a lot more coordinated with a higher intrinsic directionality; ratio of net movement relative to total movement is much higher in chemotactic migration (Martin & Martin, 2000; Arrieumerlou & Meyer, 2005). Interestingly, there is not always a correlation between chemoattractant application and migration, as chemoattractants which increase random migration often result in decreased directional migration (Bosgraaf *et al.*, 2005; Pankov *et al.*, 2005). It was therefore important to test the ability of cells to migrate both in non-directional and directional fashion, as the differences between the intracellular signalling networks which are used by the cells for different types of migration can lead to altered responses to inhibitory agents. Thus, after performing experiments which utilised non-directional mode of migration and observed that cAMP elevation resulted in the inhibition of PANC-1 migration, I then proceeded to investigate directional mode of migration which was induced by a 0-10% gradient of FBS across the Boyden chambers. I found that cAMP increase also resulted in a strong inhibition of PANC-1 directional migration, indicating that cAMP elevation was affecting signalling mechanisms common to both types of migration modes.

Invasion is another key process which leads to the formation of cancer metastasis (Takada *et al.*, 2002). This highlights the importance of investigating not only migration, but also the ability of cell to invade. I used matrigel coated Boyden chambers which had a homogenously coated surface and occluded pores. Matrigel is a solubilised basement membrane extracted from Engelberth-Holm-Swarm (EHS) mouse tumour, and consists mainly of laminin, type IV collagen, heparin sulphate, and entactin (Hughes *et al.*, 2010). Matrigel is one of the most commonly used extracellular matrix, and is often used in cell invasion studies (Albini *et al.*, 1987). First I tested invasion in conditions of equal FBS

concentration in upper and lower chambers, and found that elevation of cAMP strongly inhibited this process in PANC-1 cells. I proceeded to test directional invasion induced by asymmetric FBS, and also found that invasion of PANC-1 cells displayed was strongly inhibited by cAMP elevating agents. Thus, I have found that elevation of cAMP can strongly inhibit both non-directional and directional modes of invasion. I can therefore conclude that cAMP elevation can inhibit both migration and invasion, and furthermore that this inhibition can be observed in the presence and absence of FBS gradient (indicating there was a common mechanism involved which cAMP elevation effected to abrogate cell motility).

6.3. Elevation of cAMP inhibits ruffling.

Ruffles are small, actin-rich, sheet-like membrane protrusions. Currently there are two clear groups of ruffle formations both of which are formed primarily from polymerised actin. Dorsal ruffles are formed on the dorsal surface of cells, and form circular structures before disappearing. It is thought that dorsal ruffles are responsible for receptor internalization and macropinocytosis (Buccione *et al.*, 2004). Another form believed to be distinct from dorsal ruffles (Suetsugu *et al.*, 2003), are the peripheral ruffles which assemble at the leading edge of migrating cells (Abercrombie *et al.*, 1970). It is the peripheral ruffles at the leading edge of cells that are associated with cell motility. These structures arise from thin lamellipodia extensions which typically extend 1-3µm past the cell lamellum (Ponti *et al.*, 2004). Upon extension the lamellipodium can form focal complexes with the underlying extracellular substratum. If however insufficient adhesion is made or adhesions complexes become detached, the lamellipodium is withdrawn, causing it to move backwards and change its position upwards. At this stage, the withdrawn lamellipodial protrusion structure is classified as a peripheral ruffle (Abercrombie *et al.*, 1970; Giannone *et al.*, 2007). During

the lifetime progression of a peripheral ruffle, it moves backwards (with respect to the direction of cell membrane protrusion) before disappearing closely behind the leading edge of the cell, which is around the boundary between cell lamellum and lamellipodium. Continuous cycle of lamellipodial membrane protrusion and subsequent retraction gives rise to formation of membrane ruffles (Chhabra & Higgs, 2007). As mentioned previously, the principal mediators which control the membrane protrusions are the Rho GTPases (such as RhoA, Rac1, and Cdc42). Important downstream effectors which control actin polymerisation events include the Arp2/3 complex which enables branched actin polymerisation to take place (Suetsugu *et al.*, 2003; Svitkina, 2007). In our studies performed with PANC-1 cells, I found that cAMP elevation led to inhibition of peripheral ruffles, which was accompanied by decreased actin localisation within the ruffle structures. Our data therefore demonstrated that elevation of cAMP can not only inhibit migration (measured using Boyden chambers with 6 hour time interval), but also suppress relatively quick events associated with migration, such as ruffling. Following these observations, it became clearer that cAMP induced inhibition of migration was unlikely to occur due to long-term signalling changes as a result of altered gene expression, but was more likely to develop as a result of immediate signalling events such as phosphorylation of proteins involved in migratory machinery induced by cAMP.

6.4. cAMP elevation causes paxillin to dissociate from focal adhesions.

To enable efficient motility, cells first need to attach to the extracellular matrix. This occurs though specialised areas on the membrane that contain transmembrane integrin receptor proteins, which are capable of directly binding to the extracellular matrix components (Burridge *et al.*, 1988; Jockusch *et al.*, 1995; Schwartz *et al.*, 1995; Hynes, 2002). Cell-matrix adhesions also play vital roles in biological processes such as cell survival, proliferation,

regulation of gene expression, and cell differentiation (Burridge *et al.*, 1988). The assemblies of integrins are accompanied by a large number of specialized scaffolding molecules, kinases, phosphatases, lipases, GTPases and proteases (Schwartz *et al.*, 1995; Dedhar, 2000; Geiger *et al.*, 2001; Zamir & Geiger, 2001b; Hynes, 2002; Brakebusch & Fassler, 2003; DeMali *et al.*, 2003). The arrangement of these molecules is termed in general as focal adhesions, which serve many functions, one of which includes binding to actin cytoskeleton to enable tractional forces and subsequent cell movement. Over 50 focal adhesion associated proteins have already been identified (Zamir & Geiger, 2001a, 2001b), and the number of proteins which participate in the diverse formation of focal adhesions continues to grow. Although one could speculate that all of the proteins which participate in focal adhesion formation are important, some proteins have so far been found to play more important roles than others. These include proteins such as β1 integrin (Brakebusch & Fassler, 2005), Src kinase (Frame, 2004), FAK (Avraham *et al.*, 2000; Parsons, 2003; Mitra *et al.*, 2005), paxillin (Schaller, 2001; Brown & Turner, 2004), talin (Campbell & Ginsberg, 2004; Critchley, 2005), vinculin (Critchley, 2004; Ziegler *et al.*, 2006), GIT (Hoefen & Berk, 2006), α-actinin (Otey & Carpen, 2004), profilin (Witke, 2004), and PTP1B (Bourdeau *et al.*, 2005).

Paxillin is a very important focal adhesion associated protein that localises to newly forming focal complexes and well established focal adhesions (Laukaitis *et al.*, 2001). The main function of paxillin is to integrate signals from integrins and growth factor stimulated receptors, which can subsequently result in efficient cell migration (Brown & Turner, 2004). Paxillin does not possess any kinase activity, and as a result its functions depend on the ability to act as a large adaptor protein forming many associations with other regulatory proteins (Brown & Turner, 2004). The associations are often controlled by phosphorylation state of both paxillin and its associated proteins (Turner *et al.*, 1989; Turner, 2000b; Turner

et al., 2001). Paxillin is important in migration and cell adhesion as was demonstrated by the finding that tyrosine phosphorylation of paxillin on residues 31 and 118 resulted in subsequent association with CrkII adaptor protein through its SH2 domain; mutation of these sites resulted in the inhibition of migration (Petit *et al.*, 2000). The interaction of paxillin with CrkII has also been implicated in epithelial to mesenchymal transition (EMT), which is an important step in cancer progression (Lamorte *et al.*, 2003). Furthermore, the formation of the paxillin-Crk complex at focal adhesions can lead to activation of Rac1 through the action of Crk-DOCK180 complex (Kiyokawa *et al.*, 1998). Another important function of paxillin has been shown to control activation of extracellular signal-regulated kinase (ERK) at focal adhesions (Hagel *et al.*, 2002). Phosphorylation of tyrosine 118 on paxillin by Src kinase creates a docking site for ERK, causing it to be sequestered into focal adhesions (Ishibe *et al.*, 2003). Interestingly, ERK can then phosphorylate paxillin causing recruitment of FAK, resulting in increased cell migration rates (Liu *et al.*, 2002b). Paxillin can also interact with GIT proteins, which causes recruitment of MEK, resulting in ERK activation at focal adhesions (Yin *et al.*, 2004).

FAK is an important focal adhesion associated protein that binds to paxillin (Turner, 2000a; Schaller, 2001). It was discovered through independent studies in the early 1990's as a highly tyrosine phosphorylated protein that localised within focal adhesions; and that its tyrosine phosphorylation was linked with its association with focal adhesions (Parsons, 2003). FAK function was found to be important in embryonic morphogenesis (Ilic *et al.*, 1995). Although in contrast to initial expectations, active FAK seems to increase the turnover of focal adhesion structures, while knockout results in excessive formation (Webb *et al.*, 2004). Loss of FAK function has also been reported to alter microtubule polarization (Palazzo *et al.*, 2004), which is important for establishment of cell polarity during migration.

FAK has also been implicated in regulating activity of Rho GTPases (Ren *et al.*, 2000) and therefore is important for the remodelling of actin cytoskeleton (again highlighting its importance for migration). Interestingly, FAK genes has been found to be amplified in a number of human cancer cell lines (Agochiya *et al.*, 1999). There have also been reports indicating FAK was over expressed in many highly malignant cancers (Cance *et al.*, 2000), and was associated with formation of invadopodia structures (Hauck *et al.*, 2002). Targeting of FAK to focal adhesions occurs through the C-terminal focal-adhesion targeting (FAT) domain (Mitra *et al.*, 2005). Association of FAK however does not occur directly with integrins, but rather through association with other integrin binding proteins such as talin and paxillin (Schlaepfer *et al.*, 2004). The FAT domain can also bind and activate p190 RhoGEF which can lead to RhoA activation (Zhai *et al.*, 2003). Another focal adhesion associated kinase, Src, binds to and phosphorylates FAK resulting in its maximal activation. FAK associated Src kinase however is able to phosphorylate other target proteins such as paxillin and p130Cas (Turner, 2000a; Hanks *et al.*, 2003; Chodniewicz & Klemke, 2004). Tyrosine phosphorylation of p130Cas, results in downstream activation of Rac1 causing increased lamellipodial protrusion and ruffle formation leading to increased invasion and migration rates (Cho & Klemke, 2002; Hsia *et al.*, 2003; Brabek *et al.*, 2004). Thus it can be seen that FAK functions are diverse and important in controlling migration and invasion of cancer cells, and that FAK associated with paxillin is important for its function.

Vinculin is another important focal contact associated protein that binds paxillin. Vinculin structure comprises of a head and tail domain which are separated by a flexible linker (Bakolitsa *et al.*, 2004). The protein has binding sites on all three of these domains (Critchley, 2000), and one of the best characterised binding partners is talin. Binding of vinculin's head domain to talin, results in vinculin recruitment to focal adhesions. On the

other end of the protein, vinculin's tail section can bind paxillin and F-actin (Ziegler *et al.*, 2008). What is also interesting about vinculin is its involvement in focal adhesion mechanosensitivity. Vinculin incorporation into focal adhesions appears to depend on external and internal mechanical forces (Riveline *et al.*, 2001; Galbraith *et al.*, 2002). Knockout of vinculin results in reduced cellular tractional forces, and also impairs cell spreading and the ability to migrate (Xu *et al.*, 1998; Alenghat *et al.*, 2000; Mierke *et al.*, 2008). Recent findings have revealed vinculin plays important role in focal adhesion assembly which depends on its ability to sense tension. Highest tension detected by vinculin correlates with adhesion assembly and enlargement, whereas low tension results in dismantling and sliding of focal adhesions (Grashoff *et al.*, 2010). Thus correct function of this paxillin-binding protein is also very important in the regulation of focal adhesion assembly and cell migration.

The GPCR-Kinase-interacting proteins 1 and 2 (GIT1 and GIT2) are paxillin-binding proteins located in cytoplasmic complexes, on the cell periphery, and within focal adhesions. They interact with various proteins such as MAPK/ERK kinase 1 (MEK1) kinase, phospholipase Cγ (PLCγ), p21-activated kinase (PAK), PAK-interacting exchange factor (PIX), Rac1, CDC42, and paxillin (Hoefen & Berk, 2006). Considering its binding partners, it is not surprising to find that GIT proteins have important functions in controlling cytoskeletal dynamics. Both GIT-1 and GIT-2 localise into focal adhesion through the interaction with paxillin; this is mediated through LD4 motif on paxillin and a 'paxillin binding site' on GIT (Turner *et al.*, 1999; Di Cesare *et al.*, 2000; Zhao *et al.*, 2000; Matafora *et al.*, 2001; Mazaki *et al.*, 2001; Brown *et al.*, 2002; Lamorte *et al.*, 2003).

It is quite clear that the deregulation of the correct function of paxillin can impact the ability of cell to achieve efficient migration. The numerous functions of paxillin and its important associated binding partners was the motivation for our studies of paxillin trafficking (in and out of focal adhesions). Paxillin has been found to efficiently traffic out of focal adhesions in response to cAMP elevation, which could be the process that results in the inhibition of cell migration and invasion. Furthermore, the relatively quick loss of paxillin in response to cAMP elevation suggests that the observed phenomenon develops as a result of rapid signalling events and is unlikely to be mediated by cAMP-dependent changes in gene expression.

6.5. cAMP elevation causes the breakdown of actin stress fibres.

Composition of stress fibres consists of bundles of actin which are typically made of 10 to 30 filaments (Cramer *et al.*, 1997). The major protein that has been found to crosslink the filaments has been α-actinin (Lazarides & Burridge, 1975). Stress fibres are also rich in non-muscle myosin II protein which enables the contraction and shortening of the fibres to exert pulling forces (Svitkina *et al.*, 1997; Small *et al.*, 1998). There are three main subclasses of stress fibres which have been identified which are based on their localisation within the cell. Transverse arc stress fibres form at the ventral surface of cell and are attached to focal adhesions. Only one end of the fibre is attached to the focal adhesion, while the rest of fibre grows away from it into the dorsal part of the cell, where it often terminates at the nucleus (Heath, 1983). Second type are the dorsal stress fibres which are also only attached at one end to focal adhesions, while the rest of the fibre rises up towards the dorsal side of the cell (Heath & Dunn, 1978). Finally, ventral stress fibres are located at the base of cells and are the most commonly observed stress fibres. Unlike the previous two types, ventral stress fibres are attached to focal adhesions at both ends of the

fibre (Small *et al.*, 1998). For imaging stress fibres I utilised confocal microscopy which allowed us to image a very thin section of the cell; in our experiments I visualised the section close to the coverslip, and thus majority of the stress fibres observed were ventral fibres. However, since all three classes of fibres are associated with focal adhesions, which are located on the ventral part of the cell, some of the stress fibres observed could also have been dorsal or transverse arc fibres.

The exact role of stress fibres in cell motility is not fully known, and literature exists to both support and reject the idea that stress fibre formation promotes migration (Couchman & Rees, 1979; Kreis & Birchmeier, 1980; Burridge, 1981). Following observation that stress fibres have contractile properties, it was suggested that they were involved in promoting migration (Kreis & Birchmeier, 1980). Although other studies have found that stress fibres were in greater abundance in stationary cells, suggesting they function to stabilise cells and inhibit their migration (Couchman & Rees, 1979; Burridge, 1981). There does appear to be more agreement on the participation of myosin IIA in the tail retraction within migrating cells (Even-Ram *et al.*, 2007; Vicente-Manzanares *et al.*, 2007). In migrating fibroblasts the ventral stress fibres are positioned in parallel to the direction of motility (Oliver *et al.*, 1994; Cramer *et al.*, 1997), and the contractile force generated by the fibres appears to be important for motility (Cox & Huttenlocher, 1998; Kirfel *et al.*, 2004). Another study conducted on migrating fibroblasts has found that upon disassembly of a posterior focal adhesions, the ventral stress fibres detach from them and bind to a new adhesions within the cell's tail (Rid *et al.*, 2005). This can result in stress fibre reorientation and alignment with the new direction of migration; and thus the stress fibres could be acting to steer cell motility. Taken together, stress fibre formation appears to play a role in cell migration in a range of cell types. It is therefore likely that stress fibre disassembly induced through cAMP

elevation contributed towards the inhibition of PANC-1 migration. It is also interesting to note that like with ruffling and paxillin, stress fibre disassembly was very rapid and reversible; again indicating that short-term signalling cascades are likely to be responsible for this phenomenon.

6.6. PKA and EPAC have opposing roles in PANC-1 migration.

Many publications have investigated the effects of the specific downstream effectors of cAMP on the migration rate in various cell types and animal models. Rather than finding that the effectors have the same role regardless of cell type, it was found that they can cause both inhibition and activation of migration, which was dependent on the cell type. To give a few examples, it was found that activation of PKA accelerated bovine bronchial cell migration (Spurzem *et al.*, 2002). Similarly it was found that PKA activity was required to promote neuronal progenitor cell motility (Toriyama *et al.*, 2012). In another example, PKA activation was recently found to play an essential role in hypoxia-mediated EMT transition in lung cancer cells, resulting in increased migration and invasion (Shaikh *et al.*, 2012). On the other hand, migration of endothelial cells was inhibited following activation of PKA (Jin *et al.*, 2010). Similarly it was found that migration of mouse embryonic fibroblasts (MEFs) and mouse 4T1 breast tumour cells was inhibited as a result of selective PKA activation (Chen *et al.*, 2008). Similar diversity in results was found with selective EPAC modulation, both inhibition and activation of migration was seen in different cell types. To give a few examples, it was found that EPAC activation promoted migration of vascular smooth muscle cells (Yokoyama *et al.*, 2008a; Yokoyama *et al.*, 2008b). In another study, it was found that EPAC activation induced migration in several melanoma cell lines (Baljinnyam *et al.*, 2009; Baljinnyam *et al.*, 2010). Similarly, it was found that endothelial cell migration was stimulated by selective EPAC or PKA activation, which interestingly worked through

independent but complementary mechanisms (Lorenowicz *et al.*, 2008). Other contrasting studies have found opposing actions of selective EPAC activation. For example, selective activation of EPAC inhibited epithelial cell migration by modulating focal adhesions and leading edge dynamics (Lyle *et al.*, 2008). Similarly EPAC was found to inhibit proliferation and migration of human prostate carcinoma cells (Grandoch *et al.*, 2009).

It is very interesting that activation of the same cAMP effectors can lead to opposing effects in different cell types; there are however many explanations why such differences can occur. Focusing on PKA, it is known that this kinase has a broad substrate specificity with hundreds of direct intracellular targets which have been identified so far (Shabb, 2001). PKA however, is not simply homogenously distributed within the cell, but is rather sequestered into specific regions of the cell through interactions with AKAPs (Pidoux & Tasken, 2010). As mentioned previously, this is a structurally diverse family of proteins that currently includes over 50 members which all share a common function of binding PKA (Pidoux & Tasken, 2010). The interaction occurs between the regulatory subunit of PKA and an amphipathic helix consisting of a stretch of 14-18 amino acids situated on the AKAP (Carr *et al.*, 1991). Each AKAP also contains a unique targeting domain which facilitates PKA targeting to specific regions within the cell. Furthermore, some AKAPs are able to form signal transduction complexes by also binding to other proteins such as phosphodiesterases, phosphoprotein phosphatases, and other kinases(Coghlan *et al.*, 1995; Schillace & Scott, 1999; Feliciello *et al.*, 2001; Tasken *et al.*, 2001). One example of this is the muscle specific AKAP, mAKAP, which has a role of coordinating two cAMP effector pathways. mAKAP binds both PKA and phosphodiesterase 4D3 (PDE4D3) to create a negative feedback loop. This occurs through PKA phosphorylation of the PDE4D3 which increases its activity. Increased degradation of cAMP therefore results in the suppression of

PKA activity (Tasken *et al.*, 2001). Interestingly, PDE4D3 also serves to bind EPAC and extracellular signal-regulated kinase 5 (ERK5) (Dodge-Kafka *et al.*, 2005). ERK5 phosphorylation of PDE4D3 leads to inhibition of phosphodiesterase activity and thus increases the cAMP concentration (Hoffmann *et al.*, 1999). This causes an increase in both PKA and EPAC activity. Through activation of the downstream GTPase Rap1, EPAC is able to inhibit MAPK/ERK kinase kinase (MEKK); this leads to suppression ERK5 activity, and thus reduces the ERK5 induced PDE4D3 activation. Thus mAKAP does not just simply bind and target PKA to specific subcellular regions, but is able to integrate and control multiple signalling pathways. It is therefore conceivable that with different expression of AKAPs within different cell types, can lead to diverse and even opposing effects on migration in response to global cAMP activation.

Global cAMP elevation results in global activation of PKA and EPAC, rather than local activation within individual signalling microdomains. This means that all the individual PKA-AKAP complexes will be activated, and the migration rate seen will be determined by the net summation of each microdomain contribution (if any) towards migration. Again, differential expression of AKAPs between two cell types could result in opposing effects on migration, despite using the same agents to activate PKA. For these reasons, it becomes obvious that characterisation of migration in response to global PKA activation is useful at providing initial insight and is good as a starting point to research, however in future studies it is going to be even more important to modulate PKA activity within individual signalling microdomains. This will enable much more accurate characterisation of the different roles of PKA within each microdomain and the diverse downstream functions.

A number of AKAPs that have been discovered so far and were found to directly interact with important cell structures or signalling proteins associated with cell motility, and have provided new insight into possible roles played by cAMP/PKA signalling. The following AKAPs have been found to directly bind or co-localize with the actin cytoskeleton: ezrin (Dransfield *et al.*, 1997; Bretscher, 1999; Bretscher *et al.*, 2002; Gautreau *et al.*, 2002), gravin (Nauert *et al.*, 1997; Gelman, 2002), AKAP-KL (Dong *et al.*, 1998a; Diviani & Scott, 2001), WASP and WAVE complex (Miki *et al.*, 1998; Westphal *et al.*, 2000; Takenawa & Miki, 2001). AKAP-Lbc has also been implicated in the association with the cytoskeleton by its ability to interact with RhoA GTPase (Diviani *et al.*, 2001; Klussmann *et al.*, 2001). AKAP ezrin is found to localise within membrane ruffles and filopodia projections (Amieva *et al.*, 1999; Menager *et al.*, 1999; Nakamura *et al.*, 2000). This AKAP has been shown to play an important role in linking actin cytoskeleton to the cell membrane (Bretscher *et al.*, 1997; Bretscher *et al.*, 2002). It has also been implemented in controlling RhoA and Rac1 GTPase activities (Mackay *et al.*, 1997; Louvet-Vallee, 2000). WAVE-1 localises to the lamellipodia and plays very important roles in controlling Rac1 and Cdc42 GTPases, which enables actin filament formation (Takenawa & Miki, 2001; Pollard & Borisy, 2003). AKAP-Lbc is associated with stress fibres and has been found to tether PKA together with RhoA at these sites (Diviani *et al.*, 2001; Klussmann *et al.*, 2001). It is very interesting to note that PKA can directly phosphorylate RhoA on serine 188, which leads to the enhanced association with RhoGDI, causing translocation of RhoA away from the membrane into the cytoplasm and resulting in the inhibition of RhoA activity (Lang *et al.*, 1996; Ellerbroek *et al.*, 2003). In support of the above findings, the effects of cAMP elevation and/or selective PKA activation was found to cause stress fibre disassembly; this could be effectively reversed through expression of constitutively active RhoA (Kreisberg *et al.*, 1997), non-phosphorylatable RhoA carrying a S188A mutation (Ellerbroek *et al.*, 2003), and overexpression of RhoA effector ROCK (Dong *et al.*, 1998b). Interestingly, a recent publication has shown that

sequential PKA phosphorylation of RhoA on serine 188 is the main pacemaker driving membrane protrusion and retraction cycles within cells (Tkachenko *et al.*, 2011). It is interesting to speculate that the inhibition of ruffling I observed could be as a result of RhoA phosphorylation by PKA. Continuous global activation of PKA would effectively hyper-phosphorylate RhoA at Ser188, thus inhibiting its function. With continuous RhoA suppression, the protrusion-retraction cycle would be inhibited, and subsequently ruffling structures would also be inhibited. Lowering global cAMP would decrease PKA activity and restore the fine balance of RhoA activation required to maintain the protrusion-retraction cycle, and thus ruffling structures would once again start forming at the cell periphery. These considerations provide possible explanation of the results of our experiments.

Other migration associated proteins found to be directly phosphorylated by PKA include actin; this phosphorylation of actin has been shown to decreases its ability to polymerise *in vitro* (Ohta *et al.*, 1987). Another interesting direct target of PKA is α4 integrin, phosphorylation of which causes inhibition of α4 integrin-paxillin interaction (Gendrel *et al.*, 1992; Han *et al.*, 2001). The interaction between paxillin and α4 integrin has been shown to be of importance in modulating cell migration (Liu *et al.*, 1999; Han *et al.*, 2001; Liu *et al.*, 2002a). Phosphorylation of α4 integrin by PKA appears to occur mostly in protrusive lamellipodial structures and was found to be of great importance for α4β1-dependent migration (Gendrel *et al.*, 1992). Interestingly, it has been found that α4 integrin is a type I AKAP which directly binds PKA (Lim *et al.*, 2007). Other PKA phosphorylatable proteins involved in migration include tyrosine phosphatase PTP-PEST, Src, PAK1, VASP, LASP, myosin light chain (MLC) and others, see review (Howe, 2004). Interestingly, the majority of the PKA targets appear to be negatively regulated by phosphorylation events, suggesting that PKA usually inhibits migration. These reported results are consistent with our finding

that global activation of PKA leads to net inhibition of migration, while suppression of PKA tends to potentiate it.

Several AKAPs have been observed to be associated with cancer progression. For example, AKAP3 mRNA levels have been found elevated in patients with epithelial ovarian cancer (Sharma *et al.*, 2005). In all patients studied, it was found that AKAP3 mRNA levels were significantly elevated when compared with normal tissue. Furthermore, high level of expression was also associated with decreased survival rate of the patients (Sharma *et al.*, 2005). Another AKAP which has been associated with familial breast cancer is AKAP-Lbc. Polymorphic variation of this protein have been suggested to increase the associated RhoA GTPase function and possibly be responsible for the progression of the malignancy (Wirtenberger *et al.*, 2006). Another study investigated the mitochondrial targeted AKAP10, which is a dual specificity AKAP that binds both type-I and type-II PKA. It was found that polymorphism in AKAP10 favoured the binding of RIα subunits, and was associated with familial breast cancer (Wirtenberger *et al.*, 2007). This is an interesting finding, as it is known that malignant transformation is associated with increased PKA-RI expression, and/or with an increase in the PKA-RI : PKA-RII ratio (Bossis & Stratakis, 2004; Neary *et al.*, 2004). Interestingly, earlier studies with cAMP analogue 8-Chloroadenosine 3’5’-cyclic monophosphate (8Cl-cAMP) displayed inhibition of proliferation across a wide variety of human cancers both *in vitro* and *in vivo* (Tagliaferri *et al.*, 1985; Tagliaferri *et al.*, 1988a; Tagliaferri *et al.*, 1988b; Tortora *et al.*, 1988). It was found that this drug could modulate the ratio of PKA-RI : PKA-RII; causing an increase in the PKA-RII : PKA-RI ratio that is more typically seen in normal healthy tissue (Rohlff *et al.*, 1993; Noguchi *et al.*, 1998). As a result of these findings, 8Cl-cAMP has been extensively tested (including several Phase 1 and Phase 2 drug trials (Tortora & Ciardiello, 2002)). The results of our experiments suggest

that cAMP analogues could be effective in the inhibition of migration/invasion and therefore inhibition of the spread of metastasis.

6.7. Concluding remarks

I have established that cAMP signalling plays an important role in PDAC cellular migration. Interestingly, I found that the downstream effectors PKA and EPAC have opposing roles in control of cell motility. Furthermore I characterised rapid cAMP-induced inhibition of ruffling and observed that cAMP increases also triggered fast trafficking of paxillin out of focal adhesions. These rapid effects suggest that the cAMP action on cellular migratory apparatus is unlikely to be mediated by changes in gene expression. The inhibition of migration probably occurs as a result of the rapid action of the cAMP effectors on the proteins responsible for regulating cell migration. Considering that PKA and EPAC have opposing actions on the rate of migration, treatment with cAMP elevating agents could create a potential problem, as both effectors will be activated. The results of our experiments suggest that selective PKA activation combined with selective EPAC inhibition could result in efficient inhibition of migration/invasion of PDAC cells, and therefore should be considered as a possible strategy for developing treatments that will prevent or reduce metastasis of PDAC.

REFERENCES

Abercrombie M, Heaysman JE & Pegrum SM. (1970). The locomotion of fibroblasts in culture. II. "RRuffling". *Exp Cell Res* **60,** 437-444.

Abercrombie M, Heaysman JE & Pegrum SM. (1971). The locomotion of fibroblasts in culture. IV. Electron microscopy of the leading lamella. *Exp Cell Res* **67,** 359-367.

Agochiya M, Brunton VG, Owens DW, Parkinson EK, Paraskeva C, Keith WN & Frame MC. (1999). Increased dosage and amplification of the focal adhesion kinase gene in human cancer cells. *Oncogene* **18,** 5646-5653.

Albini A, Iwamoto Y, Kleinman HK, Martin GR, Aaronson SA, Kozlowski JM & McEwan RN. (1987). A rapid in vitro assay for quantitating the invasive potential of tumor cells. *Cancer Res* **47,** 3239-3245.

Alenghat FJ, Fabry B, Tsai KY, Goldmann WH & Ingber DE. (2000). Analysis of cell mechanics in single vinculin-deficient cells using a magnetic tweezer. *Biochem Biophys Res Commun* **277,** 93-99.

Alexandrova AY, Arnold K, Schaub S, Vasiliev JM, Meister JJ, Bershadsky AD & Verkhovsky AB. (2008). Comparative dynamics of retrograde actin flow and focal adhesions: formation of nascent adhesions triggers transition from fast to slow flow. *PLoS One* **3,** e3234.

Altenhofen W, Ludwig J, Eismann E, Kraus W, Bonigk W & Kaupp UB. (1991). Control of ligand specificity in cyclic nucleotide-gated channels from rod photoreceptors and olfactory epithelium. *Proc Natl Acad Sci U S A* **88,** 9868-9872.

Amieva MR, Litman P, Huang L, Ichimaru E & Furthmayr H. (1999). Disruption of dynamic cell surface architecture of NIH3T3 fibroblasts by the N-terminal domains of moesin and ezrin: in vivo imaging with GFP fusion proteins. *J Cell Sci* **112 (Pt 1),** 111-125.

Angelo R & Rubin CS. (1998). Molecular characterization of an anchor protein (AKAPCE) that binds the RI subunit (RCE) of type I protein kinase A from Caenorhabditis elegans. *J Biol Chem* **273,** 14633-14643.

Aoki Y, Hosaka S, Tachibana N, Karasawa Y, Kawa S & Kiyosawa K. (2000). Reassessment of K-ras mutations at codon 12 by direct PCR and sequencing from tissue microdissection in human pancreatic adenocarcinomas. *Pancreas* **21,** 152-157.

Arrieumerlou C & Meyer T. (2005). A local coupling model and compass parameter for eukaryotic chemotaxis. *Dev Cell* **8,** 215-227.

Arthur WT, Quilliam LA & Cooper JA. (2004). Rap1 promotes cell spreading by localizing Rac guanine nucleotide exchange factors. *J Cell Biol* **167,** 111-122.

Avraham H, Park SY, Schinkmann K & Avraham S. (2000). RAFTK/Pyk2-mediated cellular signalling. *Cell Signal* **12,** 123-133.

Baillie GS, Scott JD & Houslay MD. (2005). Compartmentalisation of phosphodiesterases and protein kinase A: opposites attract. *FEBS Lett* **579,** 3264-3270.

Bakolitsa C, Cohen DM, Bankston LA, Bobkov AA, Cadwell GW, Jennings L, Critchley DR, Craig SW & Liddington RC. (2004). Structural basis for vinculin activation at sites of cell adhesion. *Nature* **430,** 583-586.

Baljinnyam E, De Lorenzo MS, Xie LH, Iwatsubo M, Chen S, Goydos JS, Nowycky MC & Iwatsubo K. (2010). Exchange protein directly activated by cyclic AMP increases melanoma cell migration by a Ca2+-dependent mechanism. *Cancer Res* **70,** 5607-5617.

Baljinnyam E, Iwatsubo K, Kurotani R, Wang X, Ulucan C, Iwatsubo M, Lagunoff D & Ishikawa Y. (2009). Epac increases melanoma cell migration by a heparan sulfate-related mechanism. *Am J Physiol Cell Physiol* **297,** C802-813.

Baruscotti M, Bucchi A & Difrancesco D. (2005). Physiology and pharmacology of the cardiac pacemaker ("funny") current. *Pharmacol Ther* **107,** 59-79.

Berrozpe G, Schaeffer J, Peinado MA, Real FX & Perucho M. (1994). Comparative analysis of mutations in the p53 and K-ras genes in pancreatic cancer. *Int J Cancer* **58,** 185-191.

Bezuidenhout AJ. (1992). Unusual anomalies of the arteries at the base of the heart in a dog. *J S Afr Vet Assoc* **63,** 32-35.

Biel M. (2009). Cyclic nucleotide-regulated cation channels. *J Biol Chem* **284,** 9017-9021.

Biel M & Michalakis S. (2007). Function and dysfunction of CNG channels: insights from channelopathies and mouse models. *Mol Neurobiol* **35,** 266-277.

Birnbaumer L. (1990). Transduction of receptor signal into modulation of effector activity by G proteins: the first 20 years or so. *Faseb J* **4,** 3178-3188.

Boettner B, Harjes P, Ishimaru S, Heke M, Fan HQ, Qin Y, Van Aelst L & Gaul U. (2003). The AF-6 homolog canoe acts as a Rap1 effector during dorsal closure of the Drosophila embryo. *Genetics* **165,** 159-169.

Bos JL. (2005). Linking Rap to cell adhesion. *Curr Opin Cell Biol* **17,** 123-128.

Bos JL. (2006). Epac proteins: multi-purpose cAMP targets. *Trends Biochem Sci* **31,** 680-686.

Bosgraaf L, Waijer A, Engel R, Visser AJ, Wessels D, Soll D & van Haastert PJ. (2005). RasGEF-containing proteins GbpC and GbpD have differential effects on cell polarity and chemotaxis in Dictyostelium. *J Cell Sci* **118,** 1899-1910.

Bossis I & Stratakis CA. (2004). Minireview: PRKAR1A: normal and abnormal functions. *Endocrinology* **145,** 5452-5458.

Bourdeau A, Dube N & Tremblay ML. (2005). Cytoplasmic protein tyrosine phosphatases, regulation and function: the roles of PTP1B and TC-PTP. *Curr Opin Cell Biol* **17,** 203-209.

Brabek J, Constancio SS, Shin NY, Pozzi A, Weaver AM & Hanks SK. (2004). CAS promotes invasiveness of Src-transformed cells. *Oncogene* **23,** 7406-7415.

Brakebusch C & Fassler R. (2003). The integrin-actin connection, an eternal love affair. *Embo J* **22,** 2324-2333.

Brakebusch C & Fassler R. (2005). beta 1 integrin function in vivo: adhesion, migration and more. *Cancer Metastasis Rev* **24,** 403-411.

Bretscher A. (1999). Regulation of cortical structure by the ezrin-radixin-moesin protein family. *Curr Opin Cell Biol* **11,** 109-116.

Bretscher A, Edwards K & Fehon RG. (2002). ERM proteins and merlin: integrators at the cell cortex. *Nat Rev Mol Cell Biol* **3,** 586-599.

Bretscher A, Reczek D & Berryman M. (1997). Ezrin: a protein requiring conformational activation to link microfilaments to the plasma membrane in the assembly of cell surface structures. *J Cell Sci* **110 (Pt 24),** 3011-3018.

Brown MC & Turner CE. (2004). Paxillin: adapting to change. *Physiol Rev* **84,** 1315-1339.

Brown MC, West KA & Turner CE. (2002). Paxillin-dependent paxillin kinase linker and p21-activated kinase localization to focal adhesions involves a multistep activation pathway. *Mol Biol Cell* **13,** 1550-1565.

Buccione R, Orth JD & McNiven MA. (2004). Foot and mouth: podosomes, invadopodia and circular dorsal ruffles. *Nat Rev Mol Cell Biol* **5,** 647-657.

Burridge K. (1981). Are stress fibres contractile? *Nature* **294,** 691-692.

Burridge K, Fath K, Kelly T, Nuckolls G & Turner C. (1988). Focal adhesions: transmembrane junctions between the extracellular matrix and the cytoskeleton. *Annu Rev Cell Biol* **4,** 487-525.

Cadd G & McKnight GS. (1989). Distinct patterns of cAMP-dependent protein kinase gene expression in mouse brain. *Neuron* **3,** 71-79.

Cadd GG, Uhler MD & McKnight GS. (1990). Holoenzymes of cAMP-dependent protein kinase containing the neural form of type I regulatory subunit have an increased sensitivity to cyclic nucleotides. *J Biol Chem* **265,** 19502-19506.

Cain RJ & Ridley AJ. (2009). Phosphoinositide 3-kinases in cell migration. *Biol Cell* **101,** 13-29.

Caldas C, Hahn SA, da Costa LT, Redston MS, Schutte M, Seymour AB, Weinstein CL, Hruban RH, Yeo CJ & Kern SE. (1994). Frequent somatic mutations and homozygous deletions of the p16 (MTS1) gene in pancreatic adenocarcinoma. *Nat Genet* **8,** 27-32.

Campbell ID & Ginsberg MH. (2004). The talin-tail interaction places integrin activation on FERM ground. *Trends Biochem Sci* **29,** 429-435.

Campbell PJ, Yachida S, Mudie LJ, Stephens PJ, Pleasance ED, Stebbings LA, Morsberger LA, Latimer C, McLaren S, Lin ML, McBride DJ, Varela I, Nik-Zainal SA, Leroy C, Jia M, Menzies A, Butler AP, Teague JW, Griffin CA, Burton J, Swerdlow H, Quail MA, Stratton MR, Iacobuzio-Donahue C & Futreal PA. (2010). The patterns and dynamics of genomic instability in metastatic pancreatic cancer. *Nature* **467,** 1109-1113.

Campellone KG & Welch MD. (2010). A nucleator arms race: cellular control of actin assembly. *Nat Rev Mol Cell Biol* **11,** 237-251.

Canaves JM & Taylor SS. (2002). Classification and phylogenetic analysis of the cAMP-dependent protein kinase regulatory subunit family. *J Mol Evol* **54,** 17-29.

Cance WG, Harris JE, Iacocca MV, Roche E, Yang X, Chang J, Simkins S & Xu L. (2000). Immunohistochemical analyses of focal adhesion kinase expression in benign and malignant human breast and colon tissues: correlation with preinvasive and invasive phenotypes. *Clin Cancer Res* **6,** 2417-2423.

Carpenter AE, Jones TR, Lamprecht MR, Clarke C, Kang IH, Friman O, Guertin DA, Chang JH, Lindquist RA, Moffat J, Golland P & Sabatini DM. (2006). CellProfiler: image analysis software for identifying and quantifying cell phenotypes. *Genome Biol* **7,** R100.

Carr DW, Stofko-Hahn RE, Fraser ID, Bishop SM, Acott TS, Brennan RG & Scott JD. (1991). Interaction of the regulatory subunit (RII) of cAMP-dependent protein kinase with RII-anchoring proteins occurs through an amphipathic helix binding motif. *J Biol Chem* **266,** 14188-14192.

Chan KT, Bennin DA & Huttenlocher A. (2010). Regulation of adhesion dynamics by calpain-mediated proteolysis of focal adhesion kinase (FAK). *J Biol Chem* **285,** 11418-11426.

Chen L, Zhang JJ & Huang XY. (2008). cAMP inhibits cell migration by interfering with Rac-induced lamellipodium formation. *J Biol Chem* **283,** 13799-13805.

Chhabra ES & Higgs HN. (2007). The many faces of actin: matching assembly factors with cellular structures. *Nat Cell Biol* **9,** 1110-1121.

Cho SY & Klemke RL. (2002). Purification of pseudopodia from polarized cells reveals redistribution and activation of Rac through assembly of a CAS/Crk scaffold. *J Cell Biol* **156,** 725-736.

Chodniewicz D & Klemke RL. (2004). Regulation of integrin-mediated cellular responses through assembly of a CAS/Crk scaffold. *Biochim Biophys Acta* **1692,** 63-76.

Christensen AE, Selheim F, de Rooij J, Dremier S, Schwede F, Dao KK, Martinez A, Maenhaut C, Bos JL, Genieser HG & Doskeland SO. (2003). cAMP analog mapping of Epac1 and cAMP kinase. Discriminating analogs demonstrate that Epac and cAMP kinase act synergistically to promote PC-12 cell neurite extension. *J Biol Chem* **278,** 35394-35402.

Clegg CH, Cadd GG & McKnight GS. (1988). Genetic characterization of a brain-specific form of the type I regulatory subunit of cAMP-dependent protein kinase. *Proc Natl Acad Sci U S A* **85,** 3703-3707.

Coghlan VM, Perrino BA, Howard M, Langeberg LK, Hicks JB, Gallatin WM & Scott JD. (1995). Association of protein kinase A and protein phosphatase 2B with a common anchoring protein. *Science* **267,** 108-111.

Colledge M & Scott JD. (1999). AKAPs: from structure to function. *Trends Cell Biol* **9,** 216-221.

Conti M & Beavo J. (2007). Biochemistry and physiology of cyclic nucleotide phosphodiesterases: essential components in cyclic nucleotide signaling. *Annu Rev Biochem* **76,** 481-511.

Cooper DM. (2003). Regulation and organization of adenylyl cyclases and cAMP. *Biochem J* **375,** 517-529.

Cooper DM, Mons N & Karpen JW. (1995). Adenylyl cyclases and the interaction between calcium and cAMP signalling. *Nature* **374,** 421-424.

Corbin JD & Keely SL. (1977). Characterization and regulation of heart adenosine 3':5'-monophosphate-dependent protein kinase isozymes. *J Biol Chem* **252,** 910-918.

Corbin JD, Keely SL & Park CR. (1975). The distribution and dissociation of cyclic adenosine 3':5'-monophosphate-dependent protein kinases in adipose, cardiac, and other tissues. *J Biol Chem* **250,** 218-225.

Corbin JD, Soderling TR & Park CR. (1973). Regulation of adenosine 3',5'-monophosphate-dependent protein kinase. I. Preliminary characterization of the adipose tissue enzyme in crude extracts. *J Biol Chem* **248,** 1813-1821.

Cotton M & Claing A. (2009). G protein-coupled receptors stimulation and the control of cell migration. *Cell Signal* **21,** 1045-1053.

Couchman JR & Rees DA. (1979). The behaviour of fibroblasts migrating from chick heart explants: changes in adhesion, locomotion and growth, and in the distribution of actomyosin and fibronectin. *J Cell Sci* **39,** 149-165.

Cox EA & Huttenlocher A. (1998). Regulation of integrin-mediated adhesion during cell migration. *Microsc Res Tech* **43,** 412-419.

Cramer LP, Siebert M & Mitchison TJ. (1997). Identification of novel graded polarity actin filament bundles in locomoting heart fibroblasts: implications for the generation of motile force. *J Cell Biol* **136,** 1287-1305.

Craven KB & Zagotta WN. (2006). CNG and HCN channels: two peas, one pod. *Annu Rev Physiol* **68,** 375-401.

Critchley DR. (2000). Focal adhesions - the cytoskeletal connection. *Curr Opin Cell Biol* **12,** 133-139.

Critchley DR. (2004). Cytoskeletal proteins talin and vinculin in integrin-mediated adhesion. *Biochem Soc Trans* **32,** 831-836.

Critchley DR. (2005). Genetic, biochemical and structural approaches to talin function. *Biochem Soc Trans* **33,** 1308-1312.

Critchley DR. (2009). Biochemical and structural properties of the integrin-associated cytoskeletal protein talin. *Annu Rev Biophys* **38,** 235-254.

Curtis AS. (1964). The Mechanism of Adhesion of Cells to Glass. a Study by Interference Reflection Microscopy. *J Cell Biol* **20,** 199-215.

de Rooij J, Rehmann H, van Triest M, Cool RH, Wittinghofer A & Bos JL. (2000). Mechanism of regulation of the Epac family of cAMP-dependent RapGEFs. *J Biol Chem* **275,** 20829-20836.

de Rooij J, Zwartkruis FJ, Verheijen MH, Cool RH, Nijman SM, Wittinghofer A & Bos JL. (1998). Epac is a Rap1 guanine-nucleotide-exchange factor directly activated by cyclic AMP. *Nature* **396,** 474-477.

Deakin NO & Turner CE. (2008). Paxillin comes of age. *J Cell Sci* **121,** 2435-2444.

Dedhar S. (2000). Cell-substrate interactions and signaling through ILK. *Curr Opin Cell Biol* **12,** 250-256.

Deer EL, Gonzalez-Hernandez J, Coursen JD, Shea JE, Ngatia J, Scaife CL, Firpo MA & Mulvihill SJ. (2010). Phenotype and genotype of pancreatic cancer cell lines. *Pancreas* **39,** 425-435.

DeMali KA, Wennerberg K & Burridge K. (2003). Integrin signaling to the actin cytoskeleton. *Curr Opin Cell Biol* **15,** 572-582.

Deming PB, Campbell SL, Baldor LC & Howe AK. (2008). Protein kinase A regulates 3-phosphatidylinositide dynamics during platelet-derived growth factor-induced membrane ruffling and chemotaxis. *J Biol Chem* **283,** 35199-35211.

Depry C, Allen MD & Zhang J. (2011). Visualization of PKA activity in plasma membrane microdomains. *Mol Biosyst* **7,** 52-58.

Di Cesare A, Paris S, Albertinazzi C, Dariozzi S, Andersen J, Mann M, Longhi R & de Curtis I. (2000). p95-APP1 links membrane transport to Rac-mediated reorganization of actin. *Nat Cell Biol* **2,** 521-530.

Diviani D & Scott JD. (2001). AKAP signaling complexes at the cytoskeleton. *J Cell Sci* **114,** 1431-1437.

Diviani D, Soderling J & Scott JD. (2001). AKAP-Lbc anchors protein kinase A and nucleates Galpha 12-selective Rho-mediated stress fiber formation. *J Biol Chem* **276,** 44247-44257.

Dodge-Kafka KL, Soughayer J, Pare GC, Carlisle Michel JJ, Langeberg LK, Kapiloff MS & Scott JD. (2005). The protein kinase A anchoring protein mAKAP coordinates two integrated cAMP effector pathways. *Nature* **437,** 574-578.

Dodge K & Scott JD. (2000). AKAP79 and the evolution of the AKAP model. *FEBS Lett* **476,** 58-61.

Dong F, Feldmesser M, Casadevall A & Rubin CS. (1998a). Molecular characterization of a cDNA that encodes six isoforms of a novel murine A kinase anchor protein. *J Biol Chem* **273,** 6533-6541.

Dong JM, Leung T, Manser E & Lim L. (1998b). cAMP-induced morphological changes are counteracted by the activated RhoA small GTPase and the Rho kinase ROKalpha. *J Biol Chem* **273,** 22554-22562.

Dostmann WR & Taylor SS. (1991). Identifying the molecular switches that determine whether (Rp)-cAMPS functions as an antagonist or an agonist in the activation of cAMP-dependent protein kinase I. *Biochemistry* **30,** 8710-8716.

Dransfield DT, Bradford AJ, Smith J, Martin M, Roy C, Mangeat PH & Goldenring JR. (1997). Ezrin is a cyclic AMP-dependent protein kinase anchoring protein. *Embo J* **16,** 35-43.

Durodola JI. (1975). Antitumour effects against sarcoma 180 ascites of fractions of Annona senegalensis. *Planta Med* **28,** 32-36.

Eden S, Rohatgi R, Podtelejnikov AV, Mann M & Kirschner MW. (2002). Mechanism of regulation of WAVE1-induced actin nucleation by Rac1 and Nck. *Nature* **418,** 790-793.

Efimov A & Kaverina I. (2009). Significance of microtubule catastrophes at focal adhesion sites. *Cell Adh Migr* **3,** 285-287.

Ellerbroek SM, Wennerberg K & Burridge K. (2003). Serine phosphorylation negatively regulates RhoA in vivo. *J Biol Chem* **278,** 19023-19031.

Enserink JM, Christensen AE, de Rooij J, van Triest M, Schwede F, Genieser HG, Doskeland SO, Blank JL & Bos JL. (2002). A novel Epac-specific cAMP analogue demonstrates independent regulation of Rap1 and ERK. *Nat Cell Biol* **4,** 901-906.

Etienne-Manneville S. (2004). Cdc42--the centre of polarity. *J Cell Sci* **117,** 1291-1300.

Etienne-Manneville S & Hall A. (2003). Cell polarity: Par6, aPKC and cytoskeletal crosstalk. *Curr Opin Cell Biol* **15,** 67-72.

Even-Ram S, Doyle AD, Conti MA, Matsumoto K, Adelstein RS & Yamada KM. (2007). Myosin IIA regulates cell motility and actomyosin-microtubule crosstalk. *Nat Cell Biol* **9,** 299-309.

Fagan KA, Mahey R & Cooper DM. (1996). Functional co-localization of transfected Ca(2+)-stimulable adenylyl cyclases with capacitative Ca2+ entry sites. *J Biol Chem* **271,** 12438-12444.

Farrell TJ, Barbot DJ & Rosato FE. (1997). Pancreatic resection combined with intraoperative radiation therapy for pancreatic cancer. *Ann Surg* **226,** 66-69.

Feliciello A, Gottesman ME & Avvedimento EV. (2001). The biological functions of A-kinase anchor proteins. *J Mol Biol* **308,** 99-114.

Ferlay J, Parkin DM & Steliarova-Foucher E. (2010). Estimates of cancer incidence and mortality in Europe in 2008. *Eur J Cancer* **46,** 765-781.

Frame MC. (2004). Newest findings on the oldest oncogene; how activated src does it. *J Cell Sci* **117,** 989-998.

Franco SJ, Rodgers MA, Perrin BJ, Han J, Bennin DA, Critchley DR & Huttenlocher A. (2004). Calpain-mediated proteolysis of talin regulates adhesion dynamics. *Nat Cell Biol* **6,** 977-983.

Galbraith CG, Yamada KM & Sheetz MP. (2002). The relationship between force and focal complex development. *J Cell Biol* **159,** 695-705.

Gamm DM, Baude EJ & Uhler MD. (1996). The major catalytic subunit isoforms of cAMP-dependent protein kinase have distinct biochemical properties in vitro and in vivo. *J Biol Chem* **271,** 15736-15742.

Gautreau A, Louvard D & Arpin M. (2002). ERM proteins and NF2 tumor suppressor: the Yin and Yang of cortical actin organization and cell growth signaling. *Curr Opin Cell Biol* **14,** 104-109.

Geiger B, Bershadsky A, Pankov R & Yamada KM. (2001). Transmembrane crosstalk between the extracellular matrix--cytoskeleton crosstalk. *Nat Rev Mol Cell Biol* **2,** 793-805.

Gelman IH. (2002). The role of SSeCKS/gravin/AKAP12 scaffolding proteins in the spaciotemporal control of signaling pathways in oncogenesis and development. *Front Biosci* **7,** d1782-1797.

Gendrel D, Chemillier-Truong M, Rodrique D, Raymond J, Bosco O, Saliou P & Lebon P. (1992). Underestimation of the incidence of measles in a population of French children. *Eur J Clin Microbiol Infect Dis* **11,** 1156-1157.

Giannone G, Dubin-Thaler BJ, Rossier O, Cai Y, Chaga O, Jiang G, Beaver W, Dobereiner HG, Freund Y, Borisy G & Sheetz MP. (2007). Lamellipodial actin mechanically links myosin activity with adhesion-site formation. *Cell* **128,** 561-575.

Gilman AG. (1990). Regulation of adenylyl cyclase by G proteins. *Adv Second Messenger Phosphoprotein Res* **24,** 51-57.

Glass DB, Cheng HC, Kemp BE & Walsh DA. (1986). Differential and common recognition of the catalytic sites of the cGMP-dependent and cAMP-dependent protein kinases by inhibitory peptides derived from the heat-stable inhibitor protein. *J Biol Chem* **261,** 12166-12171.

Gold MG, Lygren B, Dokurno P, Hoshi N, McConnachie G, Tasken K, Carlson CR, Scott JD & Barford D. (2006). Molecular basis of AKAP specificity for PKA regulatory subunits. *Mol Cell* **24,** 383-395.

Grandoch M, Rose A, ter Braak M, Jendrossek V, Rubben H, Fischer JW, Schmidt M & Weber AA. (2009). Epac inhibits migration and proliferation of human prostate carcinoma cells. *Br J Cancer* **101,** 2038-2042.

Grashoff C, Hoffman BD, Brenner MD, Zhou R, Parsons M, Yang MT, McLean MA, Sligar SG, Chen CS, Ha T & Schwartz MA. (2010). Measuring mechanical tension across vinculin reveals regulation of focal adhesion dynamics. *Nature* **466,** 263-266.

Hagel M, George EL, Kim A, Tamimi R, Opitz SL, Turner CE, Imamoto A & Thomas SM. (2002). The adaptor protein paxillin is essential for normal development in the mouse and is a critical transducer of fibronectin signaling. *Mol Cell Biol* **22,** 901-915.

Hahn SA, Schutte M, Hoque AT, Moskaluk CA, da Costa LT, Rozenblum E, Weinstein CL, Fischer A, Yeo CJ, Hruban RH & Kern SE. (1996). DPC4, a candidate tumor suppressor gene at human chromosome 18q21.1. *Science* **271,** 350-353.

Hamuro Y, Burns L, Canaves J, Hoffman R, Taylor S & Woods V. (2002). Domain organization of D-AKAP2 revealed by enhanced deuterium exchange-mass spectrometry (DXMS). *J Mol Biol* **321,** 703-714.

Han J, Liu S, Rose DM, Schlaepfer DD, McDonald H & Ginsberg MH. (2001). Phosphorylation of the integrin alpha 4 cytoplasmic domain regulates paxillin binding. *J Biol Chem* **276,** 40903-40909.

Hanks SK, Ryzhova L, Shin NY & Brabek J. (2003). Focal adhesion kinase signaling activities and their implications in the control of cell survival and motility. *Front Biosci* **8,** d982-996.

Hanoune J & Defer N. (2001). Regulation and role of adenylyl cyclase isoforms. *Annu Rev Pharmacol Toxicol* **41,** 145-174.

Hauck CR, Hsia DA, Ilic D & Schlaepfer DD. (2002). v-Src SH3-enhanced interaction with focal adhesion kinase at beta 1 integrin-containing invadopodia promotes cell invasion. *J Biol Chem* **277,** 12487-12490.

Heath JP. (1983). Behaviour and structure of the leading lamella in moving fibroblasts. I. Occurrence and centripetal movement of arc-shaped microfilament bundles beneath the dorsal cell surface. *J Cell Sci* **60,** 331-354.

Heath JP & Dunn GA. (1978). Cell to substratum contacts of chick fibroblasts and their relation to the microfilament system. A correlated interference-reflexion and high-voltage electron-microscope study. *J Cell Sci* **29,** 197-212.

Heller WT, Vigil D, Brown S, Blumenthal DK, Taylor SS & Trewhella J. (2004). C subunits binding to the protein kinase A RI alpha dimer induce a large conformational change. *J Biol Chem* **279,** 19084-19090.

Herberg FW, Maleszka A, Eide T, Vossebein L & Tasken K. (2000). Analysis of A-kinase anchoring protein (AKAP) interaction with protein kinase A (PKA) regulatory subunits: PKA isoform specificity in AKAP binding. *J Mol Biol* **298,** 329-339.

Hoefen RJ & Berk BC. (2006). The multifunctional GIT family of proteins. *J Cell Sci* **119,** 1469-1475.

Hoffmann R, Baillie GS, MacKenzie SJ, Yarwood SJ & Houslay MD. (1999). The MAP kinase ERK2 inhibits the cyclic AMP-specific phosphodiesterase HSPDE4D3 by phosphorylating it at Ser579. *Embo J* **18,** 893-903.

Hofmann F, Biel M & Kaupp UB. (2005). International Union of Pharmacology. LI. Nomenclature and structure-function relationships of cyclic nucleotide-regulated channels. *Pharmacol Rev* **57,** 455-462.

Holly SP, Larson MK & Parise LV. (2005). The unique N-terminus of R-ras is required for Rac activation and precise regulation of cell migration. *Mol Biol Cell* **16,** 2458-2469.

Howe AK. (2004). Regulation of actin-based cell migration by cAMP/PKA. *Biochim Biophys Acta* **1692,** 159-174.

Hsia DA, Mitra SK, Hauck CR, Streblow DN, Nelson JA, Ilic D, Huang S, Li E, Nemerow GR, Leng J, Spencer KS, Cheresh DA & Schlaepfer DD. (2003). Differential regulation of cell motility and invasion by FAK. *J Cell Biol* **160,** 753-767.

Huang L, Goodrow TL, Zhang SY, Klein-Szanto AJ, Chang H & Ruggeri BA. (1996). Deletion and mutation analyses of the P16/MTS-1 tumor suppressor gene in human ductal pancreatic cancer reveals a higher frequency of abnormalities in tumor-derived cell lines than in primary ductal adenocarcinomas. *Cancer Res* **56,** 1137-1141.

Huang LJ, Durick K, Weiner JA, Chun J & Taylor SS. (1997). Identification of a novel protein kinase A anchoring protein that binds both type I and type II regulatory subunits. *J Biol Chem* **272,** 8057-8064.

Hughes CS, Postovit LM & Lajoie GA. (2010). Matrigel: a complex protein mixture required for optimal growth of cell culture. *Proteomics* **10,** 1886-1890.

Humphries JD, Byron A & Humphries MJ. (2006). Integrin ligands at a glance. *J Cell Sci* **119,** 3901-3903.

Hynes RO. (2002). Integrins: bidirectional, allosteric signaling machines. *Cell* **110,** 673-687.

Iacobuzio-Donahue CA, Velculescu VE, Wolfgang CL & Hruban RH. (2012). Genetic basis of pancreas cancer development and progression: insights from whole-exome and whole-genome sequencing. *Clin Cancer Res* **18,** 4257-4265.

Iglesias PA & Devreotes PN. (2008). Navigating through models of chemotaxis. *Curr Opin Cell Biol* **20,** 35-40.

Ilic D, Furuta Y, Kanazawa S, Takeda N, Sobue K, Nakatsuji N, Nomura S, Fujimoto J, Okada M & Yamamoto T. (1995). Reduced cell motility and enhanced focal adhesion contact formation in cells from FAK-deficient mice. *Nature* **377,** 539-544.

Ishibe S, Joly D, Zhu X & Cantley LG. (2003). Phosphorylation-dependent paxillin-ERK association mediates hepatocyte growth factor-stimulated epithelial morphogenesis. *Mol Cell* **12,** 1275-1285.

Iwamura T, Katsuki T & Ide K. (1987). Establishment and characterization of a human pancreatic cancer cell line (SUIT-2) producing carcinoembryonic antigen and carbohydrate antigen 19-9. *Jpn J Cancer Res* **78,** 54-62.

Jahnsen T, Hedin L, Lohmann SM, Walter U & Richards JS. (1986). The neural type II regulatory subunit of cAMP-dependent protein kinase is present and regulated by hormones in the rat ovary. *J Biol Chem* **261,** 6637-6639.

Jeong HW, Nam JO & Kim IS. (2005). The COOH-terminal end of R-Ras alters the motility and morphology of breast epithelial cells through Rho/Rho-kinase. *Cancer Res* **65,** 507-515.

Jin H, Garmy-Susini B, Avraamides CJ, Stoletov K, Klemke RL & Varner JA. (2010). A PKA-Csk-pp60Src signaling pathway regulates the switch between endothelial cell invasion and cell-cell adhesion during vascular sprouting. *Blood* **116,** 5773-5783.

Jockusch BM, Bubeck P, Giehl K, Kroemker M, Moschner J, Rothkegel M, Rudiger M, Schluter K, Stanke G & Winkler J. (1995). The molecular architecture of focal adhesions. *Annu Rev Cell Dev Biol* **11,** 379-416.

Jones S, Zhang X, Parsons DW, Lin JC, Leary RJ, Angenendt P, Mankoo P, Carter H, Kamiyama H, Jimeno A, Hong SM, Fu B, Lin MT, Calhoun ES, Kamiyama M, Walter K, Nikolskaya T, Nikolsky Y, Hartigan J, Smith DR, Hidalgo M, Leach SD, Klein AP, Jaffee EM, Goggins M, Maitra A, Iacobuzio-Donahue C, Eshleman JR, Kern SE, Hruban RH, Karchin R, Papadopoulos N, Parmigiani G, Vogelstein B, Velculescu VE & Kinzler KW. (2008). Core signaling pathways in human pancreatic cancers revealed by global genomic analyses. *Science* **321,** 1801-1806.

Kamisawa T, Isawa T, Koike M, Tsuruta K & Okamoto A. (1995). Hematogenous metastases of pancreatic ductal carcinoma. *Pancreas* **11,** 345-349.

Kang G, Chepurny OG, Malester B, Rindler MJ, Rehmann H, Bos JL, Schwede F, Coetzee WA & Holz GG. (2006). cAMP sensor Epac as a determinant of ATP-sensitive potassium channel activity in human pancreatic beta cells and rat INS-1 cells. *J Physiol* **573,** 595-609.

Katagiri K, Maeda A, Shimonaka M & Kinashi T. (2003). RAPL, a Rap1-binding molecule that mediates Rap1-induced adhesion through spatial regulation of LFA-1. *Nat Immunol* **4,** 741-748.

Kaupp UB & Seifert R. (2002). Cyclic nucleotide-gated ion channels. *Physiol Rev* **82,** 769-824.

Kaverina I, Krylyshkina O & Small JV. (1999). Microtubule targeting of substrate contacts promotes their relaxation and dissociation. *J Cell Biol* **146,** 1033-1044.

Kawasaki H, Springett GM, Mochizuki N, Toki S, Nakaya M, Matsuda M, Housman DE & Graybiel AM. (1998). A family of cAMP-binding proteins that directly activate Rap1. *Science* **282,** 2275-2279.

Kim SK, Fan Y, Papadimitrakopoulou V, Clayman G, Hittelman WN, Hong WK, Lotan R & Mao L. (1996). DPC4, a candidate tumor suppressor gene, is altered infrequently in head and neck squamous cell carcinoma. *Cancer Res* **56,** 2519-2521.

Kirfel G, Rigort A, Borm B & Herzog V. (2004). Cell migration: mechanisms of rear detachment and the formation of migration tracks. *Eur J Cell Biol* **83,** 717-724.

Kita K, Saito S, Morioka CY & Watanabe A. (1999). Growth inhibition of human pancreatic cancer cell lines by anti-sense oligonucleotides specific to mutated K-ras genes. *Int J Cancer* **80,** 553-558.

Kiyokawa E, Hashimoto Y, Kurata T, Sugimura H & Matsuda M. (1998). Evidence that DOCK180 up-regulates signals from the CrkII-p130(Cas) complex. *J Biol Chem* **273,** 24479-24484.

Klussmann E, Edemir B, Pepperle B, Tamma G, Henn V, Klauschenz E, Hundsrucker C, Maric K & Rosenthal W. (2001). Ht31: the first protein kinase A anchoring protein to integrate protein kinase A and Rho signaling. *FEBS Lett* **507,** 264-268.

Kolsch V, Charest PG & Firtel RA. (2008). The regulation of cell motility and chemotaxis by phospholipid signaling. *J Cell Sci* **121,** 551-559.

Kopperud R, Christensen AE, Kjarland E, Viste K, Kleivdal H & Doskeland SO. (2002). Formation of inactive cAMP-saturated holoenzyme of cAMP-dependent protein kinase under physiological conditions. *J Biol Chem* **277,** 13443-13448.

Korn ED, Carlier MF & Pantaloni D. (1987). Actin polymerization and ATP hydrolysis. *Science* **238,** 638-644.

Kreis TE & Birchmeier W. (1980). Stress fiber sarcomeres of fibroblasts are contractile. *Cell* **22,** 555-561.

Kreisberg JI, Ghosh-Choudhury N, Radnik RA & Schwartz MA. (1997). Role of Rho and myosin phosphorylation in actin stress fiber assembly in mesangial cells. *Am J Physiol* **273,** F283-288.

Krugmann S, Williams R, Stephens L & Hawkins PT. (2004). ARAP3 is a PI3K- and rap-regulated GAP for RhoA. *Curr Biol* **14,** 1380-1384.

Kumar P & Walsh DA. (2002). A dual-specificity isoform of the protein kinase inhibitor PKI produced by alternate gene splicing. *Biochem J* **362,** 533-537.

Kurosaka S & Kashina A. (2008). Cell biology of embryonic migration. *Birth Defects Res C Embryo Today* **84,** 102-122.

Kyriazis AA, Kyriazis AP, Sternberg CN, Sloane NH & Loveless JD. (1986). Morphological, biological, biochemical, and karyotypic characteristics of human pancreatic ductal adenocarcinoma Capan-2 in tissue culture and the nude mouse. *Cancer Res* **46,** 5810-5815.

Lafuente EM, van Puijenbroek AA, Krause M, Carman CV, Freeman GJ, Berezovskaya A, Constantine E, Springer TA, Gertler FB & Boussiotis VA. (2004). RIAM, an Ena/VASP

and Profilin ligand, interacts with Rap1-GTP and mediates Rap1-induced adhesion. *Dev Cell* **7,** 585-595.

Lamorte L, Rodrigues S, Sangwan V, Turner CE & Park M. (2003). Crk associates with a multimolecular Paxillin/GIT2/beta-PIX complex and promotes Rac-dependent relocalization of Paxillin to focal contacts. *Mol Biol Cell* **14,** 2818-2831.

Lang P, Gesbert F, Delespine-Carmagnat M, Stancou R, Pouchelet M & Bertoglio J. (1996). Protein kinase A phosphorylation of RhoA mediates the morphological and functional effects of cyclic AMP in cytotoxic lymphocytes. *Embo J* **15,** 510-519.

Lauffenburger DA & Horwitz AF. (1996). Cell migration: a physically integrated molecular process. *Cell* **84,** 359-369.

Laukaitis CM, Webb DJ, Donais K & Horwitz AF. (2001). Differential dynamics of alpha 5 integrin, paxillin, and alpha-actinin during formation and disassembly of adhesions in migrating cells. *J Cell Biol* **153,** 1427-1440.

Lazarides E & Burridge K. (1975). Alpha-actinin: immunofluorescent localization of a muscle structural protein in nonmuscle cells. *Cell* **6,** 289-298.

Lee DC, Carmichael DF, Krebs EG & McKnight GS. (1983). Isolation of a cDNA clone for the type I regulatory subunit of bovine cAMP-dependent protein kinase. *Proc Natl Acad Sci U S A* **80,** 3608-3612.

Lieber M, Mazzetta J, Nelson-Rees W, Kaplan M & Todaro G. (1975). Establishment of a continuous tumor-cell line (panc-1) from a human carcinoma of the exocrine pancreas. *Int J Cancer* **15,** 741-747.

Lim CJ, Han J, Yousefi N, Ma Y, Amieux PS, McKnight GS, Taylor SS & Ginsberg MH. (2007). Alpha4 integrins are type I cAMP-dependent protein kinase-anchoring proteins. *Nat Cell Biol* **9,** 415-421.

Liu S, Kiosses WB, Rose DM, Slepak M, Salgia R, Griffin JD, Turner CE, Schwartz MA & Ginsberg MH. (2002a). A fragment of paxillin binds the alpha 4 integrin cytoplasmic domain (tail) and selectively inhibits alpha 4-mediated cell migration. *J Biol Chem* **277,** 20887-20894.

Liu S, Thomas SM, Woodside DG, Rose DM, Kiosses WB, Pfaff M & Ginsberg MH. (1999). Binding of paxillin to alpha4 integrins modifies integrin-dependent biological responses. *Nature* **402,** 676-681.

Liu ZX, Yu CF, Nickel C, Thomas S & Cantley LG. (2002b). Hepatocyte growth factor induces ERK-dependent paxillin phosphorylation and regulates paxillin-focal adhesion kinase association. *J Biol Chem* **277,** 10452-10458.

Lochner A & Moolman JA. (2006). The many faces of H89: a review. *Cardiovasc Drug Rev* **24,** 261-274.

Lohmann SM, DeCamilli P, Einig I & Walter U. (1984). High-affinity binding of the regulatory subunit (RII) of cAMP-dependent protein kinase to microtubule-associated and other cellular proteins. *Proc Natl Acad Sci U S A* **81,** 6723-6727.

Lopez De Jesus M, Stope MB, Oude Weernink PA, Mahlke Y, Borgermann C, Ananaba VN, Rimmbach C, Rosskopf D, Michel MC, Jakobs KH & Schmidt M. (2006). Cyclic AMP-dependent and Epac-mediated activation of R-Ras by G protein-coupled receptors leads to phospholipase D stimulation. *J Biol Chem* **281,** 21837-21847.

Lorenowicz MJ, Fernandez-Borja M, Kooistra MR, Bos JL & Hordijk PL. (2008). PKA and Epac1 regulate endothelial integrity and migration through parallel and independent pathways. *Eur J Cell Biol* **87,** 779-792.

Loukopoulos P, Kanetaka K, Takamura M, Shibata T, Sakamoto M & Hirohashi S. (2004). Orthotopic transplantation models of pancreatic adenocarcinoma derived from cell lines and primary tumors and displaying varying metastatic activity. *Pancreas* **29,** 193-203.

Louvet-Vallee S. (2000). ERM proteins: from cellular architecture to cell signaling. *Biol Cell* **92,** 305-316.

Lugnier C. (2006). Cyclic nucleotide phosphodiesterase (PDE) superfamily: a new target for the development of specific therapeutic agents. *Pharmacol Ther* **109,** 366-398.

Luster AD, Alon R & von Andrian UH. (2005). Immune cell migration in inflammation: present and future therapeutic targets. *Nat Immunol* **6,** 1182-1190.

Lyle KS, Raaijmakers JH, Bruinsma W, Bos JL & de Rooij J. (2008). cAMP-induced Epac-Rap activation inhibits epithelial cell migration by modulating focal adhesion and leading edge dynamics. *Cell Signal* **20,** 1104-1116.

Machacek M, Hodgson L, Welch C, Elliott H, Pertz O, Nalbant P, Abell A, Johnson GL, Hahn KM & Danuser G. (2009). Coordination of Rho GTPase activities during cell protrusion. *Nature* **461,** 99-103.

Mackay DJ, Esch F, Furthmayr H & Hall A. (1997). Rho- and rac-dependent assembly of focal adhesion complexes and actin filaments in permeabilized fibroblasts: an essential role for ezrin/radixin/moesin proteins. *J Cell Biol* **138,** 927-938.

Malumbres M & Barbacid M. (2003). RAS oncogenes: the first 30 years. *Nat Rev Cancer* **3,** 459-465.

Manabe R, Kovalenko M, Webb DJ & Horwitz AR. (2002). GIT1 functions in a motile, multi-molecular signaling complex that regulates protrusive activity and cell migration. *J Cell Sci* **115,** 1497-1510.

Marchesi F, Monti P, Leone BE, Zerbi A, Vecchi A, Piemonti L, Mantovani A & Allavena P. (2004). Increased survival, proliferation, and migration in metastatic human pancreatic tumor cells expressing functional CXCR4. *Cancer Res* **64,** 8420-8427.

Martin D & Martin M. (2000). Understanding dysfunctional and functional family behaviors for the at-risk adolescent. *Adolescence* **35,** 785-792.

Matafora V, Paris S, Dariozzi S & de Curtis I. (2001). Molecular mechanisms regulating the subcellular localization of p95-APP1 between the endosomal recycling

compartment and sites of actin organization at the cell surface. *J Cell Sci* **114,** 4509-4520.

Mattila PK & Lappalainen P. (2008). Filopodia: molecular architecture and cellular functions. *Nat Rev Mol Cell Biol* **9,** 446-454.

Mazaki Y, Hashimoto S, Okawa K, Tsubouchi A, Nakamura K, Yagi R, Yano H, Kondo A, Iwamatsu A, Mizoguchi A & Sabe H. (2001). An ADP-ribosylation factor GTPase-activating protein Git2-short/KIAA0148 is involved in subcellular localization of paxillin and actin cytoskeletal organization. *Mol Biol Cell* **12,** 645-662.

Mehats C, Andersen CB, Filopanti M, Jin SL & Conti M. (2002). Cyclic nucleotide phosphodiesterases and their role in endocrine cell signaling. *Trends Endocrinol Metab* **13,** 29-35.

Mejillano MR, Kojima S, Applewhite DA, Gertler FB, Svitkina TM & Borisy GG. (2004). Lamellipodial versus filopodial mode of the actin nanomachinery: pivotal role of the filament barbed end. *Cell* **118,** 363-373.

Menager C, Vassy J, Doliger C, Legrand Y & Karniguian A. (1999). Subcellular localization of RhoA and ezrin at membrane ruffles of human endothelial cells: differential role of collagen and fibronectin. *Exp Cell Res* **249,** 221-230.

Michel JJ & Scott JD. (2002). AKAP mediated signal transduction. *Annu Rev Pharmacol Toxicol* **42,** 235-257.

Mierke CT, Kollmannsberger P, Zitterbart DP, Smith J, Fabry B & Goldmann WH. (2008). Mechano-coupling and regulation of contractility by the vinculin tail domain. *Biophys J* **94,** 661-670.

Miki H, Suetsugu S & Takenawa T. (1998). WAVE, a novel WASP-family protein involved in actin reorganization induced by Rac. *Embo J* **17,** 6932-6941.

Mitra SK, Hanson DA & Schlaepfer DD. (2005). Focal adhesion kinase: in command and control of cell motility. *Nat Rev Mol Cell Biol* **6,** 56-68.

Moore PS, Sipos B, Orlandini S, Sorio C, Real FX, Lemoine NR, Gress T, Bassi C, Kloppel G, Kalthoff H, Ungefroren H, Lohr M & Scarpa A. (2001). Genetic profile of 22 pancreatic carcinoma cell lines. Analysis of K-ras, p53, p16 and DPC4/Smad4. *Virchows Arch* **439,** 798-802.

Muinonen-Martin AJ, Veltman DM, Kalna G & Insall RH. (2010). An improved chamber for direct visualisation of chemotaxis. *PLoS One* **5,** e15309.

Mullins RD, Heuser JA & Pollard TD. (1998). The interaction of Arp2/3 complex with actin: nucleation, high affinity pointed end capping, and formation of branching networks of filaments. *Proc Natl Acad Sci U S A* **95,** 6181-6186.

Nakamura N, Oshiro N, Fukata Y, Amano M, Fukata M, Kuroda S, Matsuura Y, Leung T, Lim L & Kaibuchi K. (2000). Phosphorylation of ERM proteins at filopodia induced by Cdc42. *Genes Cells* **5,** 571-581.

Nauert JB, Klauck TM, Langeberg LK & Scott JD. (1997). Gravin, an autoantigen recognized by serum from myasthenia gravis patients, is a kinase scaffold protein. *Curr Biol* **7,** 52-62.

Neary CL, Nesterova M, Cho YS, Cheadle C, Becker KG & Cho-Chung YS. (2004). Protein kinase A isozyme switching: eliciting differential cAMP signaling and tumor reversion. *Oncogene* **23,** 8847-8856.

Newlon MG, Roy M, Morikis D, Hausken ZE, Coghlan V, Scott JD & Jennings PA. (1999). The molecular basis for protein kinase A anchoring revealed by solution NMR. *Nat Struct Biol* **6,** 222-227.

Noguchi K, Murata T & Cho-Chung YS. (1998). 8-chloroadenosine 3',5'-monophosphate (8-Cl-cAMP) selectively eliminates protein kinase A type I to induce growth inhibition in c-ras-transformed fibroblasts. *Eur J Cancer* **34,** 1260-1267.

Ohta Y, Akiyama T, Nishida E & Sakai H. (1987). Protein kinase C and cAMP-dependent protein kinase induce opposite effects on actin polymerizability. *FEBS Lett* **222,** 305-310.

Oliver T, Lee J & Jacobson K. (1994). Forces exerted by locomoting cells. *Semin Cell Biol* **5,** 139-147.

Otey CA & Carpen O. (2004). Alpha-actinin revisited: a fresh look at an old player. *Cell Motil Cytoskeleton* **58,** 104-111.

Otey CA, Pavalko FM & Burridge K. (1990). An interaction between alpha-actinin and the beta 1 integrin subunit in vitro. *J Cell Biol* **111,** 721-729.

Palazzo AF, Eng CH, Schlaepfer DD, Marcantonio EE & Gundersen GG. (2004). Localized stabilization of microtubules by integrin- and FAK-facilitated Rho signaling. *Science* **303,** 836-839.

Pankov R, Endo Y, Even-Ram S, Araki M, Clark K, Cukierman E, Matsumoto K & Yamada KM. (2005). A Rac switch regulates random versus directionally persistent cell migration. *J Cell Biol* **170,** 793-802.

Pape HC. (1996). Queer current and pacemaker: the hyperpolarization-activated cation current in neurons. *Annu Rev Physiol* **58,** 299-327.

Papusheva E, Mello de Queiroz F, Dalous J, Han Y, Esposito A, Jares-Erijmanxa EA, Jovin TM & Bunt G. (2009). Dynamic conformational changes in the FERM domain of FAK are involved in focal-adhesion behavior during cell spreading and motility. *J Cell Sci* **122,** 656-666.

Parsons JT. (2003). Focal adhesion kinase: the first ten years. *J Cell Sci* **116,** 1409-1416.

Parsons JT, Horwitz AR & Schwartz MA. (2010). Cell adhesion: integrating cytoskeletal dynamics and cellular tension. *Nat Rev Mol Cell Biol* **11,** 633-643.

Petit V, Boyer B, Lentz D, Turner CE, Thiery JP & Valles AM. (2000). Phosphorylation of tyrosine residues 31 and 118 on paxillin regulates cell migration through an association with CRK in NBT-II cells. *J Cell Biol* **148,** 957-970.

Pfaff M, Liu S, Erle DJ & Ginsberg MH. (1998). Integrin beta cytoplasmic domains differentially bind to cytoskeletal proteins. *J Biol Chem* **273,** 6104-6109.

Pidoux G & Tasken K. (2010). Specificity and spatial dynamics of protein kinase A signaling organized by A-kinase-anchoring proteins. *J Mol Endocrinol* **44,** 271-284.

Pollard TD & Borisy GG. (2003). Cellular motility driven by assembly and disassembly of actin filaments. *Cell* **112,** 453-465.

Pollard TD & Cooper JA. (2009). Actin, a central player in cell shape and movement. *Science* **326,** 1208-1212.

Pollitt AY & Insall RH. (2009). WASP and SCAR/WAVE proteins: the drivers of actin assembly. *J Cell Sci* **122,** 2575-2578.

Ponsioen B, Zhao J, Riedl J, Zwartkruis F, van der Krogt G, Zaccolo M, Moolenaar WH, Bos JL & Jalink K. (2004). Detecting cAMP-induced Epac activation by fluorescence resonance energy transfer: Epac as a novel cAMP indicator. *EMBO Rep* **5,** 1176-1180.

Ponti A, Machacek M, Gupton SL, Waterman-Storer CM & Danuser G. (2004). Two distinct actin networks drive the protrusion of migrating cells. *Science* **305,** 1782-1786.

Rehmann H, Das J, Knipscheer P, Wittinghofer A & Bos JL. (2006). Structure of the cyclic-AMP-responsive exchange factor Epac2 in its auto-inhibited state. *Nature* **439,** 625-628.

Rehmann H, Prakash B, Wolf E, Rueppel A, de Rooij J, Bos JL & Wittinghofer A. (2003). Structure and regulation of the cAMP-binding domains of Epac2. *Nat Struct Biol* **10,** 26-32.

Reimann EM, Walsh DA & Krebs EG. (1971). Purification and properties of rabbit skeletal muscle adenosine 3',5'-monophosphate-dependent protein kinases. *J Biol Chem* **246,** 1986-1995.

Reinton N, Collas P, Haugen TB, Skalhegg BS, Hansson V, Jahnsen T & Tasken K. (2000). Localization of a novel human A-kinase-anchoring protein, hAKAP220, during spermatogenesis. *Dev Biol* **223,** 194-204.

Ren XD, Kiosses WB, Sieg DJ, Otey CA, Schlaepfer DD & Schwartz MA. (2000). Focal adhesion kinase suppresses Rho activity to promote focal adhesion turnover. *J Cell Sci* **113 (Pt 20),** 3673-3678.

Rhim AD, Mirek ET, Aiello NM, Maitra A, Bailey JM, McAllister F, Reichert M, Beatty GL, Rustgi AK, Vonderheide RH, Leach SD & Stanger BZ. (2012). EMT and dissemination precede pancreatic tumor formation. *Cell* **148,** 349-361.

Rid R, Schiefermeier N, Grigoriev I, Small JV & Kaverina I. (2005). The last but not the least: the origin and significance of trailing adhesions in fibroblastic cells. *Cell Motil Cytoskeleton* **61,** 161-171.

Ridley AJ, Schwartz MA, Burridge K, Firtel RA, Ginsberg MH, Borisy G, Parsons JT & Horwitz AR. (2003). Cell migration: integrating signals from front to back. *Science* **302,** 1704-1709.

Riveline D, Zamir E, Balaban NQ, Schwarz US, Ishizaki T, Narumiya S, Kam Z, Geiger B & Bershadsky AD. (2001). Focal contacts as mechanosensors: externally applied local mechanical force induces growth of focal contacts by an mDia1-dependent and ROCK-independent mechanism. *J Cell Biol* **153,** 1175-1186.

Rohlff C, Clair T & Cho-Chung YS. (1993). 8-Cl-cAMP induces truncation and down-regulation of the RI alpha subunit and up-regulation of the RII beta subunit of cAMP-dependent protein kinase leading to type II holoenzyme-dependent growth inhibition and differentiation of HL-60 leukemia cells. *J Biol Chem* **268,** 5774-5782.

Rosenmund C, Carr DW, Bergeson SE, Nilaver G, Scott JD & Westbrook GL. (1994). Anchoring of protein kinase A is required for modulation of AMPA/kainate receptors on hippocampal neurons. *Nature* **368,** 853-856.

Rottner K, Hall A & Small JV. (1999). Interplay between Rac and Rho in the control of substrate contact dynamics. *Curr Biol* **9,** 640-648.

Sarkar D, Erlichman J & Rubin CS. (1984). Identification of a calmodulin-binding protein that co-purifies with the regulatory subunit of brain protein kinase II. *J Biol Chem* **259,** 9840-9846.

Savai R, Pullamsetti SS, Banat GA, Weissmann N, Ghofrani HA, Grimminger F & Schermuly RT. (2010). Targeting cancer with phosphodiesterase inhibitors. *Expert Opin Investig Drugs* **19,** 117-131.

Scarpa A, Capelli P, Mukai K, Zamboni G, Oda T, Iacono C & Hirohashi S. (1993). Pancreatic adenocarcinomas frequently show p53 gene mutations. *Am J Pathol* **142,** 1534-1543.

Schaller MD. (2001). Paxillin: a focal adhesion-associated adaptor protein. *Oncogene* **20,** 6459-6472.

Schillace RV & Scott JD. (1999). Association of the type 1 protein phosphatase PP1 with the A-kinase anchoring protein AKAP220. *Curr Biol* **9,** 321-324.

Schlaepfer DD, Mitra SK & Ilic D. (2004). Control of motile and invasive cell phenotypes by focal adhesion kinase. *Biochim Biophys Acta* **1692,** 77-102.

Schneider CA, Rasband WS & Eliceiri KW. (2012). NIH Image to ImageJ: 25 years of image analysis. *Nat Methods* **9,** 671-675.

Schwartz MA, Schaller MD & Ginsberg MH. (1995). Integrins: emerging paradigms of signal transduction. *Annu Rev Cell Dev Biol* **11,** 549-599.

Schweiger H. (1991). Investigations on the biochemical characteristics of chronically underperfused muscle. *Angiology* **42,** 239-250.

Schwencke C, Yamamoto M, Okumura S, Toya Y, Kim SJ & Ishikawa Y. (1999). Compartmentation of cyclic adenosine 3',5'-monophosphate signaling in caveolae. *Mol Endocrinol* **13,** 1061-1070.

Scott JD. (1991). Cyclic nucleotide-dependent protein kinases. *Pharmacol Ther* **50,** 123-145.

Scott JD, Glaccum MB, Zoller MJ, Uhler MD, Helfman DM, McKnight GS & Krebs EG. (1987). The molecular cloning of a type II regulatory subunit of the cAMP-dependent protein kinase from rat skeletal muscle and mouse brain. *Proc Natl Acad Sci U S A* **84,** 5192-5196.

Seppa H, Grotendorst G, Seppa S, Schiffmann E & Martin GR. (1982). Platelet-derived growth factor in chemotactic for fibroblasts. *J Cell Biol* **92,** 584-588.

Shabb JB. (2001). Physiological substrates of cAMP-dependent protein kinase. *Chem Rev* **101,** 2381-2411.

Shaikh D, Zhou Q, Chen T, Ibe JC, Raj JU & Zhou G. (2012). cAMP-dependent protein kinase is essential for hypoxia-mediated epithelial-mesenchymal transition, migration, and invasion in lung cancer cells. *Cell Signal* **24,** 2396-2406.

Sharma S, Qian F, Keitz B, Driscoll D, Scanlan MJ, Skipper J, Rodabaugh K, Lele S, Old LJ & Odunsi K. (2005). A-kinase anchoring protein 3 messenger RNA expression correlates with poor prognosis in epithelial ovarian cancer. *Gynecol Oncol* **99,** 183-188.

Shattil SJ, Kim C & Ginsberg MH. (2010). The final steps of integrin activation: the end game. *Nat Rev Mol Cell Biol* **11,** 288-300.

Siegel R, Naishadham D & Jemal A. (2012). Cancer statistics, 2012. *CA Cancer J Clin* **62,** 10-29.

Skalhegg BS & Tasken K. (2000). Specificity in the cAMP/PKA signaling pathway. Differential expression,regulation, and subcellular localization of subunits of PKA. *Front Biosci* **5,** D678-693.

Small JV, Rottner K, Kaverina I & Anderson KI. (1998). Assembling an actin cytoskeleton for cell attachment and movement. *Biochim Biophys Acta* **1404,** 271-281.

Soderling SH & Beavo JA. (2000). Regulation of cAMP and cGMP signaling: new phosphodiesterases and new functions. *Curr Opin Cell Biol* **12,** 174-179.

Spurzem JR, Gupta J, Veys T, Kneifl KR, Rennard SI & Wyatt TA. (2002). Activation of protein kinase A accelerates bovine bronchial epithelial cell migration. *Am J Physiol Lung Cell Mol Physiol* **282,** L1108-1116.

Subach OM, Patterson GH, Ting LM, Wang Y, Condeelis JS & Verkhusha VV. (2011). A photoswitchable orange-to-far-red fluorescent protein, PSmOrange. *Nat Methods* **8,** 771-777.

Suetsugu S, Yamazaki D, Kurisu S & Takenawa T. (2003). Differential roles of WAVE1 and WAVE2 in dorsal and peripheral ruffle formation for fibroblast cell migration. *Dev Cell* **5,** 595-609.

Sun C, Yamato T, Furukawa T, Ohnishi Y, Kijima H & Horii A. (2001). Characterization of the mutations of the K-ras, p53, p16, and SMAD4 genes in 15 human pancreatic cancer cell lines. *Oncol Rep* **8,** 89-92.

Sunahara RK, Dessauer CW & Gilman AG. (1996). Complexity and diversity of mammalian adenylyl cyclases. *Annu Rev Pharmacol Toxicol* **36,** 461-480.

Svitkina T. (2007). Electron microscopic analysis of the leading edge in migrating cells. *Methods Cell Biol* **79,** 295-319.

Svitkina TM & Borisy GG. (1999). Arp2/3 complex and actin depolymerizing factor/cofilin in dendritic organization and treadmilling of actin filament array in lamellipodia. *J Cell Biol* **145,** 1009-1026.

Svitkina TM, Verkhovsky AB, McQuade KM & Borisy GG. (1997). Analysis of the actin-myosin II system in fish epidermal keratocytes: mechanism of cell body translocation. *J Cell Biol* **139,** 397-415.

Swaney KF, Huang CH & Devreotes PN. (2010). Eukaryotic chemotaxis: a network of signaling pathways controls motility, directional sensing, and polarity. *Annu Rev Biophys* **39,** 265-289.

Tagliaferri P, Clair T, DeBortoli ME & Cho-Chung YS. (1985). Two classes of cAMP analogs synergistically inhibit p21 ras protein synthesis and phenotypic transformation of NIH/3T3 cells transfected with Ha-MuSV DNA. *Biochem Biophys Res Commun* **130,** 1193-1200.

Tagliaferri P, Katsaros D, Clair T, Ally S, Tortora G, Neckers L, Rubalcava B, Parandoosh Z, Chang YA, Revankar GR & et al. (1988a). Synergistic inhibition of growth of breast and colon human cancer cell lines by site-selective cyclic AMP analogues. *Cancer Res* **48,** 1642-1650.

Tagliaferri P, Katsaros D, Clair T, Neckers L, Robins RK & Cho-Chung YS. (1988b). Reverse transformation of Harvey murine sarcoma virus-transformed NIH/3T3 cells by site-selective cyclic AMP analogs. *J Biol Chem* **263,** 409-416.

Takada M, Nakamura Y, Koizumi T, Toyama H, Kamigaki T, Suzuki Y, Takeyama Y & Kuroda Y. (2002). Suppression of human pancreatic carcinoma cell growth and invasion by epigallocatechin-3-gallate. *Pancreas* **25,** 45-48.

Takenawa T & Miki H. (2001). WASP and WAVE family proteins: key molecules for rapid rearrangement of cortical actin filaments and cell movement. *J Cell Sci* **114,** 1801-1809.

Tan MH, Nowak NJ, Loor R, Ochi H, Sandberg AA, Lopez C, Pickren JW, Berjian R, Douglass HO, Jr. & Chu TM. (1986). Characterization of a new primary human pancreatic tumor line. *Cancer Invest* **4,** 15-23.

Tasken K & Aandahl EM. (2004). Localized effects of cAMP mediated by distinct routes of protein kinase A. *Physiol Rev* **84,** 137-167.

Tasken K, Skalhegg BS, Solberg R, Andersson KB, Taylor SS, Lea T, Blomhoff HK, Jahnsen T & Hansson V. (1993). Novel isozymes of cAMP-dependent protein kinase exist in human cells due to formation of RI alpha-RI beta heterodimeric complexes. *J Biol Chem* **268,** 21276-21283.

Tasken KA, Collas P, Kemmner WA, Witczak O, Conti M & Tasken K. (2001). Phosphodiesterase 4D and protein kinase a type II constitute a signaling unit in the centrosomal area. *J Biol Chem* **276,** 21999-22002.

Theurkauf I & Vallee RB. (1982). Molecular characterization of the cAMP-dependent protein kinase bound to microtubule-associated protein 2. *J Biol Chem* **257,** 3284-3290.

Tkachenko E, Sabouri-Ghomi M, Pertz O, Kim C, Gutierrez E, Machacek M, Groisman A, Danuser G & Ginsberg MH. (2011). Protein kinase A governs a RhoA-RhoGDI protrusion-retraction pacemaker in migrating cells. *Nat Cell Biol* **13,** 660-667.

Tomar A & Schlaepfer DD. (2009). Focal adhesion kinase: switching between GAPs and GEFs in the regulation of cell motility. *Curr Opin Cell Biol* **21,** 676-683.

Toriyama M, Mizuno N, Fukami T, Iguchi T, Toriyama M, Tago K & Itoh H. (2012). Phosphorylation of doublecortin by protein kinase A orchestrates microtubule and actin dynamics to promote neuronal progenitor cell migration. *J Biol Chem* **287,** 12691-12702.

Tortora G & Ciardiello F. (2002). Protein kinase A as target for novel integrated strategies of cancer therapy. *Ann N Y Acad Sci* **968,** 139-147.

Tortora G, Tagliaferri P, Clair T, Colamonici O, Neckers LM, Robins RK & Cho-Chung YS. (1988). Site-selective cAMP analogs at micromolar concentrations induce growth arrest and differentiation of acute promyelocytic, chronic myelocytic, and acute lymphocytic human leukemia cell lines. *Blood* **71,** 230-233.

Turner CE. (2000a). Paxillin and focal adhesion signalling. *Nat Cell Biol* **2,** E231-236.

Turner CE. (2000b). Paxillin interactions. *J Cell Sci* **113 Pt 23,** 4139-4140.

Turner CE, Brown MC, Perrotta JA, Riedy MC, Nikolopoulos SN, McDonald AR, Bagrodia S, Thomas S & Leventhal PS. (1999). Paxillin LD4 motif binds PAK and PIX through a novel 95-kD ankyrin repeat, ARF-GAP protein: A role in cytoskeletal remodeling. *J Cell Biol* **145,** 851-863.

Turner CE, Pavalko FM & Burridge K. (1989). The role of phosphorylation and limited proteolytic cleavage of talin and vinculin in the disruption of focal adhesion integrity. *J Biol Chem* **264,** 11938-11944.

Turner CE, West KA & Brown MC. (2001). Paxillin-ARF GAP signaling and the cytoskeleton. *Curr Opin Cell Biol* **13,** 593-599.

Ungar AR & Moon RT. (1996). Inhibition of protein kinase A phenocopies ectopic expression of hedgehog in the CNS of wild-type and cyclops mutant embryos. *Dev Biol* **178,** 186-191.

van der Krogt GN, Ogink J, Ponsioen B & Jalink K. (2008). A comparison of donor-acceptor pairs for genetically encoded FRET sensors: application to the Epac cAMP sensor as an example. *PLoS One* **3,** e1916.

Van Haastert PJ & Devreotes PN. (2004). Chemotaxis: signalling the way forward. *Nat Rev Mol Cell Biol* **5,** 626-634.

Varnum MD, Black KD & Zagotta WN. (1995). Molecular mechanism for ligand discrimination of cyclic nucleotide-gated channels. *Neuron* **15,** 619-625.

Verkhovsky AB, Svitkina TM & Borisy GG. (1999). Self-polarization and directional motility of cytoplasm. *Curr Biol* **9,** 11-20.

Vicente-Manzanares M, Zareno J, Whitmore L, Choi CK & Horwitz AF. (2007). Regulation of protrusion, adhesion dynamics, and polarity by myosins IIA and IIB in migrating cells. *J Cell Biol* **176,** 573-580.

Vigil D, Blumenthal DK, Heller WT, Brown S, Canaves JM, Taylor SS & Trewhella J. (2004). Conformational differences among solution structures of the type Ialpha, IIalpha and IIbeta protein kinase A regulatory subunit homodimers: role of the linker regions. *J Mol Biol* **337,** 1183-1194.

Walsh DA, Perkins JP & Krebs EG. (1968). An adenosine 3',5'-monophosphate-dependant protein kinase from rabbit skeletal muscle. *J Biol Chem* **243,** 3763-3765.

Wang W, Goswami S, Sahai E, Wyckoff JB, Segall JE & Condeelis JS. (2005). Tumor cells caught in the act of invading: their strategy for enhanced cell motility. *Trends Cell Biol* **15,** 138-145.

Webb DJ, Donais K, Whitmore LA, Thomas SM, Turner CE, Parsons JT & Horwitz AF. (2004). FAK-Src signalling through paxillin, ERK and MLCK regulates adhesion disassembly. *Nat Cell Biol* **6,** 154-161.

Wedlich-Soldner R & Li R. (2003). Spontaneous cell polarization: undermining determinism. *Nat Cell Biol* **5,** 267-270.

Westphal RS, Soderling SH, Alto NM, Langeberg LK & Scott JD. (2000). Scar/WAVE-1, a Wiskott-Aldrich syndrome protein, assembles an actin-associated multi-kinase scaffold. *Embo J* **19,** 4589-4600.

Wirtenberger M, Schmutzhard J, Hemminki K, Meindl A, Sutter C, Schmutzler RK, Wappenschmidt B, Kiechle M, Arnold N, Weber BH, Niederacher D, Bartram CR & Burwinkel B. (2007). The functional genetic variant Ile646Val located in the kinase binding domain of the A-kinase anchoring protein 10 is associated with familial breast cancer. *Carcinogenesis* **28,** 423-426.

Wirtenberger M, Tchatchou S, Hemminki K, Klaes R, Schmutzler RK, Bermejo JL, Chen B, Wappenschmidt B, Meindl A, Bartram CR & Burwinkel B. (2006). Association of

genetic variants in the Rho guanine nucleotide exchange factor AKAP13 with familial breast cancer. *Carcinogenesis* **27,** 593-598.

Witke W. (2004). The role of profilin complexes in cell motility and other cellular processes. *Trends Cell Biol* **14,** 461-469.

Worthylake RA, Lemoine S, Watson JM & Burridge K. (2001). RhoA is required for monocyte tail retraction during transendothelial migration. *J Cell Biol* **154,** 147-160.

Wozniak MA, Kwong L, Chodniewicz D, Klemke RL & Keely PJ. (2005). R-Ras controls membrane protrusion and cell migration through the spatial regulation of Rac and Rho. *Mol Biol Cell* **16,** 84-96.

Xu W, Baribault H & Adamson ED. (1998). Vinculin knockout results in heart and brain defects during embryonic development. *Development* **125,** 327-337.

Yachida S, Jones S, Bozic I, Antal T, Leary R, Fu B, Kamiyama M, Hruban RH, Eshleman JR, Nowak MA, Velculescu VE, Kinzler KW, Vogelstein B & Iacobuzio-Donahue CA. (2010). Distant metastasis occurs late during the genetic evolution of pancreatic cancer. *Nature* **467,** 1114-1117.

Yagura TS & Miller JP. (1981). Mapping adenosine cyclic 3',5'-phosphate binding sites on type I and type II adenosine cyclic 3',5'-phosphate dependent protein kinases using ribose ring and cyclic phosphate ring analogues of adenosine cyclic 3',5'-phosphate. *Biochemistry* **20,** 879-887.

Yang J, Zhang J & Lu S. (1999). [Acquirement and identification of a novel intron 1 of human Na(+)-K(+)-exchanging ATPase alpha 1 subunit gene]. *Zhongguo Yi Xue Ke Xue Yuan Xue Bao* **21,** 159-165.

Yin G, Haendeler J, Yan C & Berk BC. (2004). GIT1 functions as a scaffold for MEK1-extracellular signal-regulated kinase 1 and 2 activation by angiotensin II and epidermal growth factor. *Mol Cell Biol* **24,** 875-885.

Yokoyama U, Minamisawa S, Quan H, Akaike T, Jin M, Otsu K, Ulucan C, Wang X, Baljinnyam E, Takaoka M, Sata M & Ishikawa Y. (2008a). Epac1 is upregulated during neointima formation and promotes vascular smooth muscle cell migration. *Am J Physiol Heart Circ Physiol* **295,** H1547-1555.

Yokoyama U, Minamisawa S, Quan H, Akaike T, Suzuki S, Jin M, Jiao Q, Watanabe M, Otsu K, Iwasaki S, Nishimaki S, Sato M & Ishikawa Y. (2008b). Prostaglandin E2-activated Epac promotes neointimal formation of the rat ductus arteriosus by a process distinct from that of cAMP-dependent protein kinase A. *J Biol Chem* **283,** 28702-28709.

Yu FH, Yarov-Yarovoy V, Gutman GA & Catterall WA. (2005). Overview of molecular relationships in the voltage-gated ion channel superfamily. *Pharmacol Rev* **57,** 387-395.

Yunis AA, Arimura GK & Russin DJ. (1977). Human pancreatic carcinoma (MIA PaCa-2) in continuous culture: sensitivity to asparaginase. *Int J Cancer* **19,** 128-135.

Zaccolo M, De Giorgi F, Cho CY, Feng L, Knapp T, Negulescu PA, Taylor SS, Tsien RY & Pozzan T. (2000). A genetically encoded, fluorescent indicator for cyclic AMP in living cells. *Nat Cell Biol* **2,** 25-29.

Zaidel-Bar R, Cohen M, Addadi L & Geiger B. (2004). Hierarchical assembly of cell-matrix adhesion complexes. *Biochem Soc Trans* **32,** 416-420.

Zamir E & Geiger B. (2001a). Components of cell-matrix adhesions. *J Cell Sci* **114,** 3577-3579.

Zamir E & Geiger B. (2001b). Molecular complexity and dynamics of cell-matrix adhesions. *J Cell Sci* **114,** 3583-3590.

Zhai J, Lin H, Nie Z, Wu J, Canete-Soler R, Schlaepfer WW & Schlaepfer DD. (2003). Direct interaction of focal adhesion kinase with p190RhoGEF. *J Biol Chem* **278,** 24865-24873.

Zhao ZS, Manser E, Loo TH & Lim L. (2000). Coupling of PAK-interacting exchange factor PIX to GIT1 promotes focal complex disassembly. *Mol Cell Biol* **20,** 6354-6363.

Zhou L & Siegelbaum SA. (2007). Gating of HCN channels by cyclic nucleotides: residue contacts that underlie ligand binding, selectivity, and efficacy. *Structure* **15,** 655-670.

Ziegler WH, Gingras AR, Critchley DR & Emsley J. (2008). Integrin connections to the cytoskeleton through talin and vinculin. *Biochem Soc Trans* **36,** 235-239.

Ziegler WH, Liddington RC & Critchley DR. (2006). The structure and regulation of vinculin. *Trends Cell Biol* **16,** 453-460.

Zimmermann B, Chiorini JA, Ma Y, Kotin RM & Herberg FW. (1999). PrKX is a novel catalytic subunit of the cAMP-dependent protein kinase regulated by the regulatory subunit type I. *J Biol Chem* **274,** 5370-5378.